Blood Compatible Membranes through Surface Functionalization

Blutkompatible Membranen durch Oberflächenfunktionalisierung

Von der Fakultät für Maschinenwesen der
Rheinisch-Westfälischen Technischen Hochschule Aachen zur
Erlangung des akademischen Grades einer Doktorin der
Ingenieurwissenschaften genehmigte Dissertation

vorgelegt von

Ilka Isabelle Rose

Berichter:
Univ.-Prof. Dr.-Ing. Matthias Wessling
Prof. Dr. rer. nat. Carsten Werner

Tag der mündlichen Prüfung: 15.09.2022

Diese Dissertation ist auf den Internetseiten der Universitätsbibliothek online verfügbar.

Titel:	Blood Compatible Membranes through Surface Functionalization
Author:	Ilka Isabelle Rose
Reihe:	Aachener Verfahrenstechnik Series AVT.CVT - Chemical Process Engineering Volume 36 (2023)
Herausgeber:	Aachener Verfahrenstechnik Forckenbeckstraße 51 52074 Aachen Tel.: +49 (0)241 8097717 Fax.: +49 (0)241 8092326 E-Mail: secretary.cvt@avt.rwth-aachen.de http://www.avt.rwth-aachen.de/AVT
Volltext verfügbar:	10.18154/RWTH-2023-01363

Danksagung

Fünf ereignisreiche und spannende Jahre am Lehrstuhl für Chemische Verfahrenstechnik und dem DWI-Leibniz - Institut für Interaktive Materialien sind vorbei. Eine Zeit vieler wissenschaftlicher Erkenntnisse, Freude an der Zusammenarbeit eines so starken und verlässlichen Teams, aber auch eine Zeit der persönlichen Reife. Ich möchte mich bei all denjenigen Personen bedanken, die in diesen Jahren auf unterschiedliche Weisen zum Gelingen dieser Arbeit beigetragen haben.

Mein besonderer Dank gilt meinem Doktorvater, Prof. Dr.-Ing. Matthias Wessling. Ich danke ihm sehr für seine motivierende und fördernde Betreuung, seine vielen innovativen Forschungsideen, die immer wieder neue Türen zu spannenden Projekten geöffnet haben. Ich bin froh und stolz, in seinem Team gearbeitet zu haben.

Ebenfalls möchte ich mich bedanken bei Prof. Dr. rer. nat. Carsten Werner, dem Zweitprüfer meiner Dissertationsprüfung und einem Kooperationspartner im Projekt LTBC. Ich danke ihm für die gute und intensive Zusammenarbeit, die Einblicke in seine Forschung und die helfenden Diskussionen über Analyseverfahren. Es hat mir viel Freude bereitet mit ihm und seinem Team, mit Tina und Manfred, zu arbeiten und voneinander zu lernen.

Ich danke dem BMBF für die finanzielle Unterstützung des Projektes *Low Thrombogenic Blood Circuit (LTBC)*, sowie den Projektpartnern, dem IPF Dresden, der HOT Screen GmbH und Baxter International Inc. für die gute Zusammenarbeit und den intensiven Austausch.

Hannah Roth danke ich für ihre Unterstützung während meiner Zeit als wissenschaftliche Mitarbeiterin an der CVT. Ihre Gelassenheit in Problemsituationen, die guten Ideen für weitere Projektanträge sowie ihre offene Art schätze ich sehr.

Ein weiterer großer Dank geht an das Spinning-Team: Hannah, Maik, Stephan, Stefan, Maria, Ang und Lea. Mir hat das Arbeiten und Forschen

mit Euch immer sehr viel Spaß gemacht. Wir waren ein super Team, sind Probleme gemeinsam angegangen und haben diese auch immer gut gelöst, was die Forschung weiter voran gebracht hat. Gerne schaue ich zurück auf spannende Diskussionen, unvergessliche Momente und einen regen Austausch in kleinen Kaffeerunden, insbesondere mit Suzana, Michael A., Georg, Michael K., Alexander, Anna, Kristina, Stefanie, Hanna und Susi. Auch bei den Kolleginnen und Kollegen von der AVT und dem DWI möchte ich mich für das kooperative Arbeitsklima und die herzliche Aufnahme in die Bürogemeinschaften bedanken.

Ein riesiges Dankeschön geht an die Studierenden, die Hiwis, die Azubis sowie die angehenden Maschinenbautechniker, die mit mir zusammengearbeitet haben. Die vielen Polymeransätze, das zunächst verzweifelte Lösen von Additiven in der Polymerlösung, die daraus resultierende Herstellung von Membranen, sowie das Charakterisieren und Analysieren haben wir zusammen gemeistert. Die Zusammenarbeit mit Euch hat mir viel Freude bereitet. Besonders möchte ich mich bei Mukaddes, Hannah, Jingyu, Katharina, Lukas, Ina, Oliver, Philipp, Vivienne und Judith bedanken.

Vielen Dank an das Laborteam, die Werkstatt, die Buchhaltung, den Einkauf und die IT an der AVT und dem DWI für die Unterstützung. Ganz besonders möchte ich mich bei Karin für die großen Mengen an FESEM-Aufnahmen, bei Jürgen und Joachim für die Fertigung der Spinnanlage und bei Timo für die unzähligen Zeta-Potential Messungen bedanken.

Ich danke vor allem meinen Eltern und meinen Schwestern, die mich in jeder erdenklichen Situation ermutigt haben und immer für mich da sind. Auch bedanke ich mich bei meiner Schwiegerfamilie für die herzliche Aufnahme in ihre Familie und ihre Unterstützung während meiner Promotion. Meinen Freundinnen und Freunden, den MuCo-Mädels und den Bachelor-Mädels danke ich für viele tolle gemeinsame Momente, witzige Abende mit leckerem Essen und gutem Wein. Ganz besonders danke ich meinem Mann Mark, der mich immer unterstützt und für mich da ist, und meinen Töchtern, Mila und Ella. Ihr bereitet mir jeden Tag eine große Freude.

Für meine Familie

Contents

Abstract

Membranes in medical technology, for example, hemodialysis, still have limited hemocompatibility. Therefore, large amounts of heparin, a standard anticoagulant, are injected into the patient's bloodstream during dialysis to reduce the likelihood of blood clotting. However, repeated addition of large amounts of heparin can lead to organ failure and other long-term complications. Some specialized products available on the market use heparin immobilized directly on the membrane surface to reduce the amount of heparin injected. However, due to expensive production and complex handling, these products are only used in high-risk patients. Therefore, this work aims to develop methods for the heparinization of standard products. For this purpose, conventional polyethersulfone dialysis membranes are functionalized subsequently or during membrane production for subsequent heparinization without adversely affecting the membrane properties. In particular, cost-effective single-step fabrication processes, such as the chemistry-in-a-spinneret approach or blending of additives into the polymer solution, are in focus for the formation of functionalized membranes.

Both the subsequent coating and the in-situ functionalization with polydopamine allow heparin binding to the membrane surface. The coated membranes exhibit higher permeability while maintaining selectivity for blood components. X-ray photoelectron spectroscopy and thermogravimetric analyses demonstrate the in-situ functionalization with polydopamine. Permeability measurements indicate successful membrane heparinization.

In addition, alternatives to dopamine, the so-called dopamine analogues, have been investigated, which are cost-effective for large-scale applications such as dialysis membrane coating. Cell culture tests show no toxicity, and further studies show no adverse difference from dopamine-coated membrane surfaces. In addition, the dopamine analogues coating has a significant amount of subsequently immobilized active heparin.

Chitosan, both as a coating and as an additive in the membrane structure, offers the possibility to bind heparin ionically. Surface characterizations show effective chitosan immobilization. In addition, hemocompatibility tests with whole blood confirm successful heparinization.

Cross-linking of glutaraldehyde with amino groups during membrane formation allows the production of a positively charged selective layer that can ionically bind heparin. Surface charges, as well as albumin adsorption, show successful cross-linking at the membrane surface. Regardless of the amine sources, both membranes exhibit a significant amount of stably bound active heparin.

The investigated material systems can improve hemocompatibility by heparinization of the membrane surface. Especially the single-step fabrication processes allow an uncomplicated use of already existing hollow fiber spinning lines.

Zusammenfassung

Membranen in der Medizintechnik, beispielsweise der Hämodialyse, haben noch immer eine limitierte Hämokompatibilität. Daher werden während der Dialyse große Mengen an Heparin, einem Standard-Antikoagulans, in den Blutkreislauf des Patienten injiziert, um die Wahrscheinlichkeit einer Blutgerinnung zu reduzieren. Die wiederholte Zugabe großer Mengen Heparin kann zu Organversagen und weiteren Langzeitkomplikationen führen. Einige am Markt verfügbare spezielle Produkte nutzen direkt auf der Membranoberfläche immobilisiertes Heparin zur Reduktion der injizierten Heparinmenge. Aufgrund der teuren Herstellung und aufwendigen Handhabung werden diese Produkte nur bei Hochrisiko-Patienten eingesetzt. Daher zielt diese Arbeit auf die Entwicklung von Verfahren zur Heparinisierung von Standardprodukten ab. Dazu werden herkömmliche Polyethersulfon-Dialysemembranen nachträglich oder während der Membranherstellung für eine anschließende Heparinsierung funktionalisiert, ohne die Membraneigenschaften nachteilig zu beeinflussen. Insbesondere kostengünstige einstufige Herstellungsverfahren, wie das Reaktivspinnen oder das Beimischen von Additiven in die Polymerlösung, liegen zur Bildung von funktionalisierten Membranen im Fokus.

Sowohl das nachträgliche Beschichten als auch das in-situ Funktionalisieren mit Polydopamin ermöglichen die Heparin-Bindung an die Membranoberfläche. Die beschichteten Membranen weisen bei gleichbleibender Selektivität für Blutbestandteile eine höhere Permeabilität auf. Mithilfe der Röntgen-Photoelektronen-Spektroskopie sowie thermogravimetrischer Analysen wird das in-situ Funktionalisieren mit Polydopamin gezeigt. Permeabilitätsmessungen deuten auf eine erfolgreiche Membran-Heparinisierung hin.

Zusätzlich wurden Alternativen zu Dopamin, die sogenannten Dopamin-Analoga, untersucht, die für große Anwendungen wie die Beschichtung von Dialysemembranen kostengünstiger sind. Zellkulturtests weisen keine Toxizität auf und auch weitere Untersuchungen zeigen keinen nachteiligen Unterschied zu den mit Dopamin beschichteten Membranoberflächen. Beide Beschichtungen weisen eine deutliche Menge an nachträglich immobilisiertem, aktiven Heparin auf.

Chitosan, sowohl als Beschichtung als auch als Additiv in der Membranstruktur bietet die Möglichkeit, Heparin ionisch zu binden. Die gemessenen Oberflächenladungen zeigen eine effektive Chitosan-Immobilisierung. Hämokompatibilitätstests mit Vollblut bestätigen die erfolgreiche Heparinisierung.

Das Vernetzen von Glutaraldehyd mit Aminogruppen während der Membranbildung ermöglicht die Herstellung einer positiv geladenen selektiven Schicht, die Heparin ionisch binden kann. Oberflächenladungen sowie die Albumin-Adsorption zeigen eine erfolgreiche Vernetzung an der Membranoberfläche. Unabhängig der Aminquellen weisen beide Membranen einen hohen Anteil an stabil gebundenem, aktiven Heparin auf.

Die untersuchten Stoffsysteme können die Hämokompatibilität durch die Heparinisierung der Membranoberfläche verbessern. Besonders die einstufigen Herstellungsverfahren lassen eine einfache Nutzung bereits bestehender Hohlfaserspinnanlagen zu.

Publications and student theses

Parts of this thesis have been published as a research article listed below. Texts, figures, and tables have been adopted for this thesis and mentioned at the beginning of each respective chapter.

- [Rose2022a]: I.I. Rose*, H. Roth*, J. Xie, F. Hollmann, S. Votteler, M. Storr, B. Krause, M. Wessling, "Chemistry in a spinneret - Polydopamine functionalized hollow fiber membranes", *Journal of Membrane Science, 2022, DOI: 10.1016/j.memsci.2022.120324*
- [Rose2022b]: I.I. Rose, M. Kather, H. Roth, H. Dünkelberg, L. Rein, S.N. Klimosch, M. Schmolz, M. Wessling, "Single-step chitosan functionalized membranes for heparinization", *Journal of Membrane Science, 2022, DOI: 10.1016/j.memsci.2022.120567*

*These authors are contributed equally to this work

Parts of this thesis will be published as patent application listed below. Texts, figures, and tables have been adopted for this thesis and mentioned at the beginning of each respective chapter.

- M. Hornung, M. Storr, J. Swartjes, S. Votteler, A. Krauss, M. Hulko, L. Peters, M. Wessling, I.I. Rose, G. Linz, H. Roth, "Method for increasing the selectivity of a membrane", European patent application Nr. 21216677.1
- M. Wessling, M. Alders, I.I. Rose, M. Kather, R. Menda, B. Krause, M. Storr, M. Rempfer, V.S. Kurbel, "Membrane with immobilized anticoagulant and process for producing same", International patent application Nr. PCT/EP2021/077211

The Chapter 4 and 6 are in preparation for publication as research articles.

- I.I. Rose, M. Kather, H. Roth, J. Hommes, M. Wessling, "A Dopamine Alternative to Immobilize Heparin", *Journal of Membrane Science*
- I.I. Rose, H. Roth, L. Rein, M. Wessling, "Glutaraldehyde Cross-Linked Amine Sources for Heparinization", *Journal of Membrane Science*

Some experiments and work of this thesis are based on the following student theses:

- Hannah Dünkelberg, Bachelor thesis, 2nd July 2018, Immobilization of chitosan in and on at sheet and hollow fiber PES membranes for medical applications.
- Jingyu Xie, Master thesis, 4th December 2018, Polymerization of polydopamine during manufacturing of flat sheet and hollow fiber membranes under the influence of temperature.
- Thomas Josef Maag, Master thesis, 20th Mai 2021, A stable integration of PAH in PES hollow fiber membranes for later heparinization in medical application.
- Lukas Rein, Research internship, 11th August 2021, Characterization in-situ modified chitosan membranes.
- Jerome Hommes, Research internship, 30th November 2021, Influences of dopamine analogue coatings on polyethersulfone membranes.
- Lukas Rein, Master thesis, 31st March 2022, Glutaraldehyde as a cross-linking agent for stable PAH immobilization on membrane surfaces for heparinization.

1 Introduction

1.1 Membrane Science and Technologies

A membrane is a thin interface, a semi-permeable structure that permeates one component while retaining another. Life as we know it would be inconceivable without membranes. Thus, almost every cell, whether human, animal or plant, consists, among other things, of cell walls, i.e., a membrane. The largest human organ, the skin, illustrates a membrane function. [Meli2007] Body-fluids such as plasma are retained, whereas water and salts can permeate through the skin during perspiration.

The systematic study of membrane phenomena by scientists can be traced back to the 18th century [Bake2012]. After more than two centuries of development, membranes and membrane processes now occupy an important position in chemical technologies and are used in many different areas. Different membrane and operating properties are required depending on the membrane's application. This has led to the development of a wide range of membrane materials and structures, arrangements, and operation methods [Meli2007].

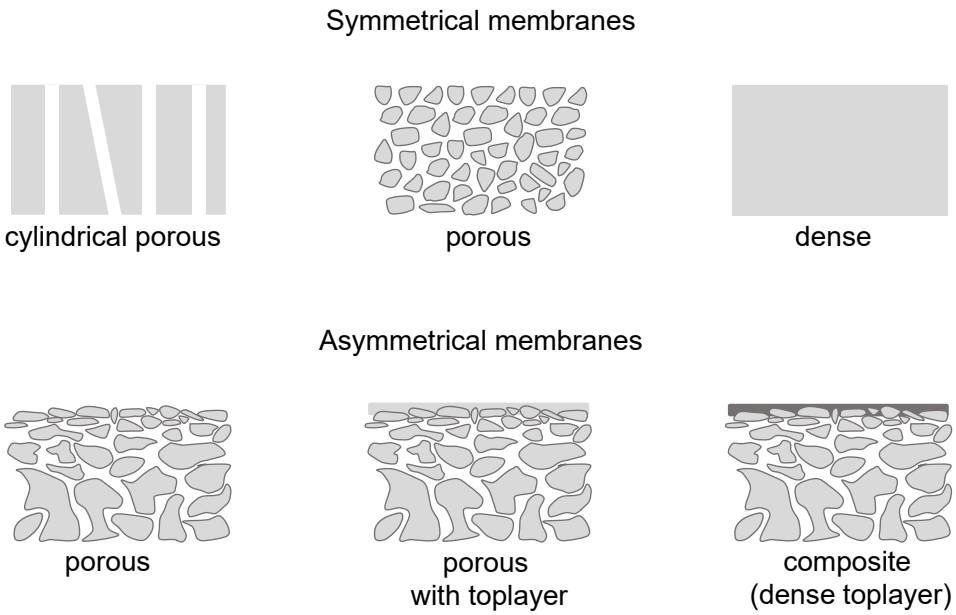

Figure 1.1: Classification of membrane structure (adapted from Melin et al. [Meli2007] and Mulder et al. [Muld1996]).

Organic polymer membranes, in particular, have become increasingly important in recent decades. These membranes are divided into sym-

metric and asymmetric membranes. This subdivision can, in turn, be divided into three membrane structures. The symmetric ones are cylindrical porous, porous, and dense, while the asymmetric ones are porous, porous with a toplayer, and composite membranes (cf. Figure 1.1) [Meli2007]; [Muld1996].

The subdivisions of membrane structures are closely related to the separation mechanisms of the respective membrane. The separation mechanisms are divided into two basic models: the pore-flow model and the solution-diffusion model (cf. Figure 1.2).

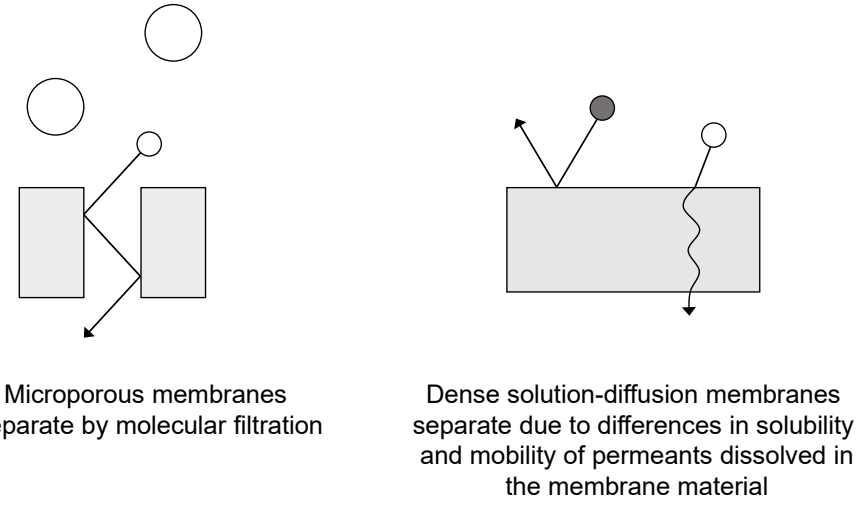

Figure 1.2: Basic modules of separation mechanisms, left: the pore-flow model; right: the solution-diffusion model (adapted from Baker et al. [Bake2012]).

The pore-flow model (cf. Figure 1.2 left) is based on a pressure-driven convective flow that transports permeants through small pores. This type of transport can be described by Darcy's law, depicted in Equation 1.1. Here, J_i is the flux (g/cm^{2}s) of component i, c_i the concentration of component i in the medium, K' is a coefficient reflecting the nature of the medium, and dp/dx is the pressure gradient existing in the porous medium. [Bake2012]

$$J_i = K' c_i \frac{dp}{dx} \tag{1.1}$$

The separation occurs because of the pores, which allow parts to pass and retain others.

In the solution-diffusion model (cf. Figure 1.2 right) permeants dissolve in the membrane material and diffuse through the membrane along a concentration gradient. The separation is based on difference in solubility in the membrane and different diffusion rates through the membrane. The flux (J_i) of a component i is calculated by using Fick's law (cf. Equation 1.2) of diffusion [Bake2012]:

$$J_i = -D_i \frac{dc_i}{dx} \tag{1.2}$$

where D_i is the diffusion coefficient (cm^2/s), a measure of the mobility of the individual molecules, and dc_i/dx is the concentration gradient (g/cm^3cm) of component i. The direction of diffusion is down the concentration gradient, as shown by the negative sign. [Bake2012]; [Meli2007]

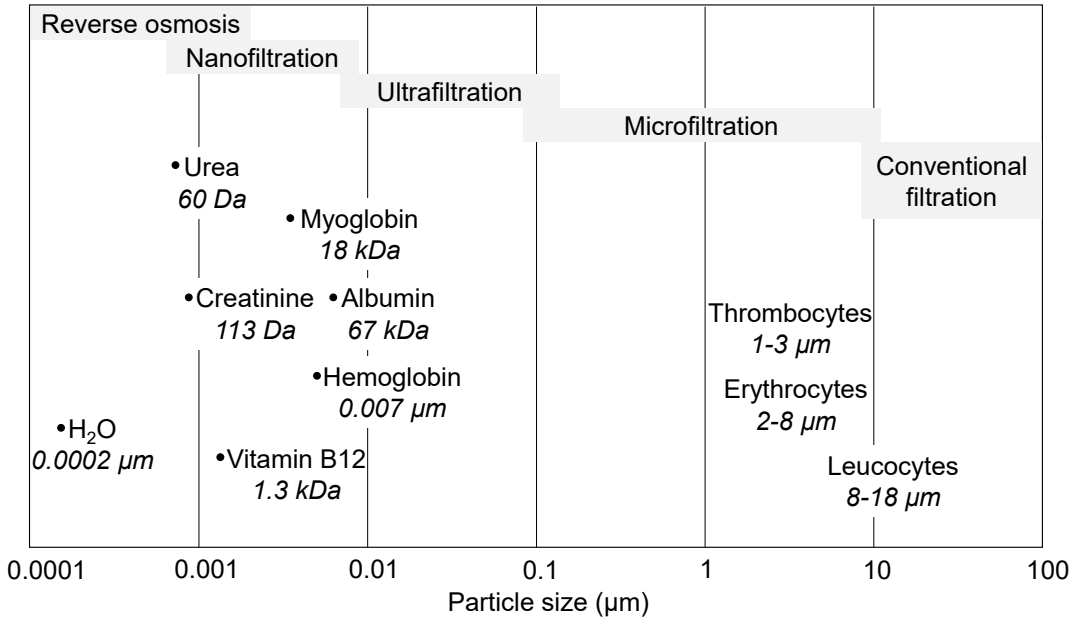

Figure 1.3: Separation processes reverse osmosis, nanofiltration, ultrafiltration, microfiltration, and conventional filtration in relation to their particle size and some molecules or cells of interest in dialysis (adapted from Pino et al. [Pino2017] and Melin et al. [Meli2007]).

A separation mechanism of a membrane is divided according to the size of permeating particles. In Figure 1.3, the separation processes are plotted against the retained components. A distinction is made between reverse

osmosis, nanofiltration, ultrafiltration, microfiltration and conventional filtration. [Meli2007]; [Pino2017]

Reverse osmosis (RO) is used especially in water treatment and desalination technologies for potable water production. Therefore, RO membranes require high water permeability, high salt retention and good chemical, mechanical, and thermal stability. [Hail2020] These membranes consist of a dense selective layer. The separation is based on the solution-diffusion model. According to this transport mechanism, dissolved substances pass through the membrane. In RO membranes, molecules and ions of around 0.1 - 1 nm can pass through the membrane while larger salts and other components (above around 1 nm) are retained [Muld1996]. The driving force of the RO is the transmembrane pressure, and typical process pressures are 10 - 60 bar. [Meli2007]; [Bake2012]

Compared to RO membranes, **nanofiltration** (NF) membranes are two to five times more permeable and thus can operate at lower pressures of 3 - 5 bar. They reject divalent ions and, to a slight extent, also monovalent ions. A typical NF membrane has a pore size of 1 nm and a molecular weight cut-off of 300-500 Da. In terms of the separation performance, NF membranes are between reverse osmosis and ultrafiltration and are used particularly in water and wastewater treatment, pharmaceutical industry and biotechnology, and food processing. The separation mechanism is attributed to a combination of steric, Donnan, dielectric, and transport effects. [Bake2012]; [Tul 2017]; [Moha2015]

The two following filtration processes, **ultrafiltration** (UF) and **microfiltration** (MF), function as a typical porous filter. Particles larger than the pore size of the membrane are completely retained. UF and MF membranes consist of an open microporous substrate with a finely porous surface layer or skin. This surface layer is responsible for the separation, while the microporous substrate provides mechanical strength. Both processes are pressure-driven and differ in pore size. The UF membranes are mainly anisotropic membranes produced by the phase inversion process (cf. Section 1.2.1) and have an average pore diameter of 1 - 100 nm. Whereas MF membranes have a pore size in the range of 0.1 - 10 µm [Bake2012].

[Meli2007]

1.2 Membrane Fabrication

Membranes are classified according to different criteria. One possible classification is the subdivision into membrane materials, another is the subdivision into membrane structures, also called membrane morphologies, which are closely related to the separation mechanism of the membrane [Meli2007].

Membrane fabrication parameters, such as polymer composition, temperature, viscosity, and the complete fabrication parameters, influence the morphology of the membrane. The variation of a single parameter can lead to significant changes in the morphology of the resulting membrane. One reason for this is the highly sensitive process, the phase inversion (cf. Section 1.2.1) applied for the fabrication of asymmetric polymer membranes.

1.2.1 Non-Solvent Induced Phase Separation

The phase inversion technique is one of the most relevant fabrication processes of polymeric membranes consisting of a variety of polymer building blocks [Guil2011]. Loeb and Sourirajan already developed a membrane fabrication technology in the 1960s that used the phase inversion technique to transform a polymer from a liquid dispersion to a solid asymmetric polymer film in a controlled manner [Guil2011]; [Loeb1962]. This phase inversion technique is called non-solvent induced phase separation (NIPS). Commonly used polymers are polyethersulfone (PES), polyvinylidene difluoride (PVDF), polysulfone (PSf), or polyacrylonitrile (PAN). The polymer is dissolved in an organic solvent such as N-methyl-2-pyrrolidone (NMP), N,N-dimethylformamide (DMF), N,N-dimethylacetamide (DMAc), dimethyl sulfoxide (DMSO), or tetrahydrofuran (THF). The resulting homogeneous polymer solution is extruded into a form, for example, for flat sheet membranes casted as free standing layer or on a non-woven (cf. Section 2.2.2), or for hollow fiber membranes by using a spinneret (cf. Section 2.2.4).

The formed polymer solution is immersed in a bath consisting of the non-solvent, typically water. The exchange of the solvent with the non-solvent leads to phase separation. The polymer-rich phase forms the porous polymer matrix, and the polymer-lean phase forms the pores. [Bake2012]

Figure 1.4 shows a typical, simplified ternary phase diagram of the non-solvent phase separation system. Each corner of the diagram represents the pure component: the polymer, the solvent and the non-solvent. Any point inside the diagram indicates a mixture of these three components. The diagram shows two main regions: a one-phase region, in which all components are miscible, and a two-phase region, in which the system separates into a solid (polymer-rich) and a liquid (polymer-lean) phase. [Bake2012]

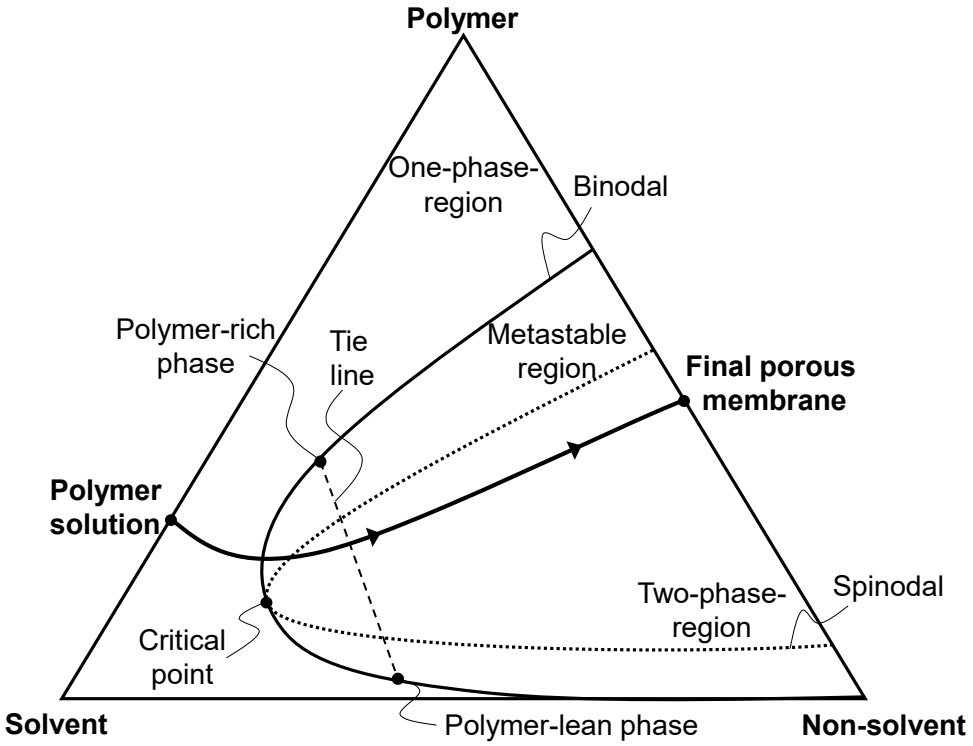

Figure 1.4: Typical ternary phase diagram of the non-solvent phase separation (adapted from Mulder et al. and Baker et al. [Muld1996]; [Bake2012]).

The precipitation process for membrane formation consists of varying the composition of the polymer solution to form the final porous membrane. The pathway of membrane formation in the diagram starts with the polymer solution and ends with the final porous membrane. The polymer solution

consists initially of a homogeneous solvent-polymer mixture in the one-phase region. Up to a certain concentration, the mixture remains in the one-phase by adding the non-solvent. At the point where the path reaches the binodal, a concentration is reached at which the polymer precipitates. Decreasing solvent concentration and increasing non-solvent concentration leads to an increase in viscosity. By reaching a moderate viscosity, the precipitated polymer is considered as solid. At this point, a two-phase region is present. Due to the ongoing precipitation, the polymer finally solidifies, and further movement of the polymer is hindered. [Stra1971]; [Bake2012]; [Chun2021]

However, the polymer solution often consists of a polymer itself and other components such as polyvinylpyrrolidone (PVP), which are added to the polymer solution as a pore-forming agent. Moreover, other components or additives can also be added to the polymer solution. These additives influence the phase inversion process and, thus, the resulting morphology and separation properties of the membrane. These additional components in the polymer solution make the graphical representation of the precipitation behavior much more complicated. As a consequence, a representation in a three-phase diagram is no longer sufficient. Extensive models and simulations have been carried out to better represent the precipitation behavior and the influence of different components [Tang2021]. However, these procedures have not yet been fully completed. Nevertheless, extensive experience in the manufacturing of membranes is of major importance in order to estimate the resulting membrane and particularly its properties. Especially in the fabrication of hollow fiber membranes, the extensive spinning parameters significantly affect the membrane properties [McKe1997].

1.2.2 Dry-Jet Wet Spinning Process

The dry-jet wet spinning process is a common process for hollow fiber fabrication. Hollow fiber membranes are produced on a spinning line, as shown in Figure 1.5. A homogeneous polymer solution, called dope, is extruded into an annular spinneret. To prevent collapsing of the fiber, a liquid, called

bore, is co-extruded into the center of the spinneret. [McKe1997] The outside of the membrane can be affected by another liquid, called shell, which is co-extruded into the outer ring of the spinneret. The phase inversion process (cf. Section 1.2.1) initiates at the first contact between dope and bore (and shell). Below the spinneret is the coagulation bath, which consists of a non-solvent, typically water. Between the spinneret exit and the coagulation bath is an air gap, hence the name dry-jet wet spinning. During the immersion of the polymer solution into the coagulation bath, the phase inversion accelerates. In the coagulation bath, the fiber is deflected and conveyed into a washing bath via a pulling wheel. In the washing bath, the fiber is deflected several times to increase the dwell time of the fiber in the non-solvent. Here, the non-solvent further displaces the solvent. Finally, the fiber exits the washing bath and is collected on a take-up wheel. This dry-jet wet hollow fiber membrane fabrication process is complex, highly sensitive and relies on the adjustment of a variety of spinning parameters (see Figure 1.6). McKelvey et al. [McKe1997] have already published a guide for the fabrication of hollow fiber membranes in 1997. They describe which spinning parameters have to be adjusted and how to obtain the desired membrane.

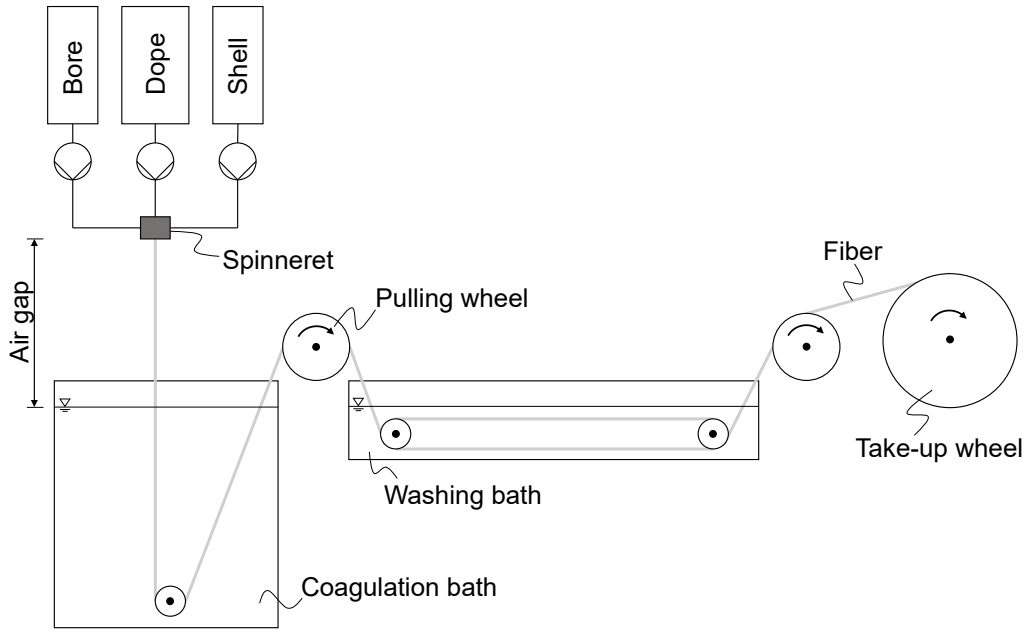

Figure 1.5: Set-up of a general hollow fiber spinning process.

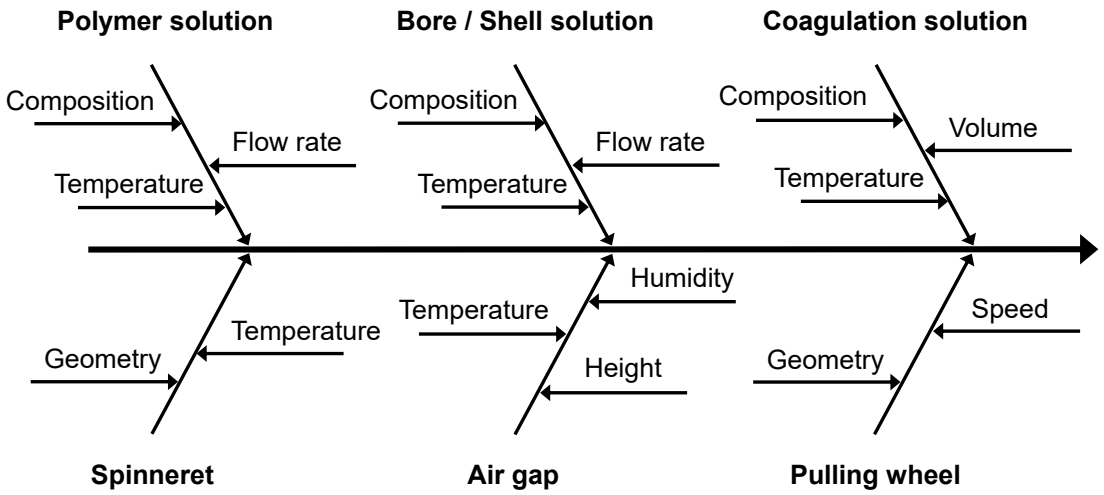

Figure 1.6: Ishikawa diagram of the main spinning parameters during hollow fiber membrane fabrication (adapted from Kopeć et al. [Kope2011a]).

1.3 Membrane Functionalization

The development of high-performance membranes involves selecting suitable membrane material and converting this material to the desired membrane structure. To further improve the overall performance of the membrane, further modifications can be carried out to the material or its structure. Membrane modification generally pursues an increase in flow and/or selectivity, an increase in chemical resistance, or an improvement in surface properties such as fouling or biocompatibility. [Pinn2000] In the following, a distinction is made between post-modification, blending and the chemistry-in-a-spinneret approach for membrane modification.

1.3.1 Post-Modification

The post-modification of membrane surfaces is widely discussed in literature. It improves certain membrane surface properties, for example, the fouling behavior [Zhai2020]; [Zhan2018], to achieve nanofiltration characteristics [Menn2016b]; [Huan2018], or to increase the bio- and hemocompatibility [Sali2016]; [Will2021]; [Sper2006]; [Shan2020]; [Li2020]. The post-modification consists of one or more layers immobilized on the membrane surface. Each layer is chemically or ionically immobilized, or by ad-

sorption. Van der Bruggen [Van 2009] gives an overview of several coating techniques to increase the hydrophilicity of polyethersulfone nanofiltration membranes [Van 2009]. They distinguish between preadsorption, plasma treatment and different types of grafting to modify membrane surfaces [Van 2009].

The layer-by-layer technique is a common and well-established membrane surface modification process for multi-layer functionalization. For example, to obtain nanofiltration properties, the post-treatment with a single layer is often not sufficient. Therefore, multi-layers are needed. [Menn2016a]; [Menn2016b]; [Kamp2021]; [Huan2018] The layer-by-layer technique is applied for further surface functionalizations as well [Li2020]; [Sper2006]; [Dong2010]; [Koch2012]; [Bulw2012]. Based on opposite charges, polyelectrolytes or other charged components are coated in an alternating sequence and adhere to the surface. This process is repeated until the desired membrane property is achieved. [Dech1997]

Methods to influence the membrane properties without subsequent post-modification steps after membrane fabrication are mixing additives into the polymer or the bore solution. A distinction is made between the blending of additives into the polymer or the bore solution and the chemical reaction during membrane fabrication, the so-called chemistry-in-a-spinneret approach.

1.3.2 Blending

In contrast to the post-modification processes, the blending of additives allows both the membrane fabrication and functionalization in a single-step process. Blending requires that an additive, for example, a polymer, is dissolved in the standard polymer solution. The blending eliminates the need for further functionalization steps on the membrane surface. On the other hand, the blended additive may have a significant influence on the membrane fabrication and, thus, on the subsequent membrane properties (cf. Section 1.2.2).

1.3.3 Chemistry-in-a-Spinneret

The chemistry-in-a-spinneret approach combines the membrane fabrication via the phase inversion process with a cross-linking reaction of the membrane material or additives. This approach bases on the research of Kopeć et al. [Kope2011b]. They used polyimide P84 as membrane material and cross-linked it during membrane fabrication with polyethyleneimine, which is dissolved in the bore solution. This approach produces both hollow fiber membranes with a dense, cross-linked thin selective layer for gas separation and solvent-resistant membranes. [Kope2011b] Further applications of the chemistry-in-a-spinneret technique with different material systems demonstrate its versatility (cf. Table 1.1) [Dutc2012]; [Gher2016]; [Roth2018]; [Roth2019]; [Emon2020]; [Gao2020]; [Wang2021]; [Moha2021]; [Emon2022]; [Rose2022a]. Charged additives were cross-linked with the membrane material or with oppositely charged additives [Kope2011b]; [Kope2011c]; [Dutc2012]; [Gher2016]; [Emon2020]. The chemistry-in-a-spinneret approach is further used to cross-link additives from the polymer solution with additives from the bore solution to fabricate nanofiltration membranes in a single step [Roth2018]; [Roth2019].

Table 1.1: Overview of research on the chemistry-in-a-spinneret approach.

Literature	Porous structure forming polymer	Polymer solution active additive	Bore solution active additive	Reached membrane properties
[Kope2011b]	P84		PEI	Gas separation, nano- & ultrafiltration, solvent resistant
[Kope2011c]	P84		SPEEK	Ultrafiltration
[Dutc2012]	P84Kopec2011		PEI	Organic solvent filtration
[Gher2016]	PES	PSS	PEI PDADMAC	Nanofiltration
[Roth2018]	PES	- TMC PEI PEI PEG400	PEI PEI GA - GA	Nanofiltration
[Roth2019]	PES	PEI	GA	Gas separation
[Emon2020]	PES	PEI	Glycerol GA PSS	Nanofiltration
[Roth2022]	PES	-	Precursors of PVCL microgels	Ultrafiltration
[Gao2020]	PES	sPSf	PEI	Nanofiltration
[Wang2021]	PVDF	-	PIP	Nanofiltration
[Moha2021]	Polyimine, sPES	PSS	- PDADMAC	Forward osmosis
[Emon2022]	PES	sPES	PEI PDADMAC	Nanofiltration
[Rose2022a]	PES	Dopamine	- Tris buffer (pH 8.5)	Heparinized hemodialysis

P84: polyimide P84, PEI: polyethylenimine, SPEEK: sulphonated polyetheretherketone, PES: polyethersulfone, PSS: poly(sodium 4-styrenesulfonate), PDADMAC: poly(diallyl dimethylammonium chloride), GA: glutaraldehyde, TMC: trimesoyl chloride, PEG400: polyethylene glycol 400, sPSf: sulfonated polysulfone, PVDF: polyvinylidene fluoride, PIP: piperazine, sPES: sulphonated polyethersulfone.

1.4 Membranes in Medical Applications

One of the most important areas of application for synthetic membranes are medical technologies. Membranes, which are in contact with biological fluids, should avoid any immune reaction, blood clotting, and other biological reactions that affect the properties of the fluid and thus the patient. In addition, properties such as dimension, shape, drug permeability, and porosity have to be adapted for each application. [Stam2008] Especially when the biological fluid is blood, the blood compatibility of the membranes is of crucial importance.

Blood compatibility contains hemocompatibility (cf. Section 1.5), which includes reduced blood coagulation, platelet activation, complement activation, and protein adsorption. In particular, the adsorption of proteins on the membrane surface adversely affects the membrane properties during application. Their adsorption can lead to a decrease in flow rate and lower membrane selectivity. Thus, it is necessary to influence protein adsorption by modifying the membrane surface. A low surface charge, no surface nucleophiles, and a balanced distribution of hydrophilic and hydrophobic domains are advantageous. However, besides the membrane surface, the membrane structure has to be also considered. Some characteristics of membrane structures are pore size and pore size distribution, porosity, tortuosity, and diffusivity. For blood contact, membranes with the following characteristics are used: an asymmetric membrane structure with a thin selective layer and high porosity, narrow pore size distribution, small tortuosity and a high diffusion coefficient. [Stam2008]; [Sun2003]

A lot of research is performed of membranes in medical applications, especially in the field of drug delivery, tissue engineering, and artificial organs such as artificial kidneys and membrane oxygenator, etc. [Stam2008]

Drug Delivery

In an optimal system, the drug delivery ensures the targeted release of a drug at a specific location at a specific time. Drug delivery offers particular advantages in flattening peaks caused by the addition of conventional

drugs in tablet form, injectable solution, or similar. This is a significant challenge in any drug delivery system. Therefore, a lot of research is being done in the efficiency of the drug delivery systems. One field of the research is membrane-based systems: osmotic membrane systems and diffusion-controlled membrane systems. In both systems, the membrane device contains the drug reservoir. [Stam2008]

In the osmotic membrane system, the semi-permeable membrane allows water permeation into the reservoir due to osmotic pressure, but prevents the drug from permeating. The drug solution produced in the reservoir is released through an orifice. [Stam2008]

The diffusion-controlled membrane system works similar to the osmotic membrane system, except the transport of the drug solution which takes place through the membrane. The drug transport is determined by its drug diffusivity and the membrane thickness. [Stam2008]

Tissue Engineering

The goal of tissue engineering is to develop functional substitutes for damaged tissues or organs of the human organism. Tissue engineering research of the past decade can be classified into three components: the engineering of cells, the engineering of materials and the engineering of tissue architecture [Khad2016]. In recent years, three-dimensional (3D) bioprinting technologies, integration of nanotechnologies, stem-cell technologies, among others, have gained particular importance [Lanz2020]. The 3D printing technology, especially, is used to fabricate complex biocompatible structures from natural or synthetic materials, which then can be seeded with cells [Khad2016]. These structures are used to shape the cell layer and supply oxygen and nutrients if they permeate through the respective material. Another somewhat older method is the cultivation of flat sheet or hollow fiber membranes. The semi-permeable membrane allows the supply of nutrients and oxygen. The surface of the membrane further allows the settlement of cells. [Stam2008]

Artificial Internal Organs

There are different applications for artificial internal organs, for example, the artificial liver, the artificial pancreas, the artificial kidney, or especially in times of the Covid-19 pandemic, the artificial lung.

The largest of these applications is the artificial kidney, also known as dialysis. Regularly, every human is born with two kidneys located in the upper abdomen. They are each about 11 cm long and have a weight of about 160 g [Stam2008]. The main functions of the kidneys are the following:

- Regulation of water balance
- Regulation of electrolyte and pH balance
- Regulation of the formation of red blood cells
- Influencing the blood pressure
- Removal of toxins from the blood

However, suppose a person suffers from acute or chronic kidney failure. In that case, kidney function may decline sharply over a period of time to an end-stage where kidney function reaches below 15 % of a healthy kidney. At this point, the patient requires renal replacement therapy. This therapy is based on an efficient and reliable concept, at the heart of which is a dialyzer consisting of membranes. The membrane serves as the separating medium between the patient's blood and the dialysate and typically consists of one of the two main materials: cellulosic materials or synthetic materials [Stam2008]; [Krau2006]. However, a significant market share of dialysis membranes consists of hydrophilic blends, often polyvinylpyrrolidone (PVP) and/or poly-amide (PA), in a synthetic material base such as polysulfone (PSf) or polyethersulfone (PES). [Krau2006]

Basic requirements of dialysis membranes are: the removal of toxins and excess fluid from the body, the restoration of electrolyte balance in the body, a good hemocompatibility, and the thermal, mechanical and chemical stability for the necessary sterilization types or cleaning cycles [Stam2008];

[Krau2006]. The separation is based on a mass transfer through the membrane. In dialysis membranes, this solute transport is both diffusive and convective [Krau2006]; [Lang1994]. The transport mechanism for urinary substances is the diffusion across the membrane caused by the concentration gradient between the blood and dialysate circuits [Krau2006]. Thus, the solute flux (J_S) depends on the diffusion coefficient ($D_{S,M}$) and the convective fluid flux through the membrane (J_V) and can be explained as follows: [Stam2008]

$$J_S = C_{S,M}(1-\sigma)J_V - D_{S,M}\frac{dc}{dx} \tag{1.3}$$

Here, dc/dx is the concentration gradient of the solute across the membrane, and σ is the Staverman reflection coefficient. An accurate description of both diffusion and convection of solutes through the membrane is necessary for the proper application of a dialyzer. [Stam2008] The solvent clearance represents another important parameter in the application of dialysis. It provides information on the effectiveness of the separation of individual components and is determined as follows:

$$\text{Clearance} = \frac{\text{Rate of solute removal}}{\text{Incoming blood concentration}} \tag{1.4}$$

The clearance is influenced not only by the membrane but also by process parameters such as volume flows and pressure differences. Thus, as a consequence, the clearance is determined differently for hemodialysis, hemofiltration, or hemodiafiltration. [Stam2008]; [Krau2006]

1.5 Hemocompatibility

Materials used for medical applications must have special properties in order to minimize the interactions between the material surfaces and the blood components. These interactions can lead to undesirable reactions

such as protein adsorption, complement activation, or platelet adhesion. In particular, the adsorption of proteins to the surface of the foreign material happens within a few milliseconds [Jung2016] and leads to a complex chain reaction leading to the formation of a blood clot.

Blood Coagulation

Blood clotting involves a complex system in which a series of proteolytic reactions occur, culminating in the formation of a fibrin clot. This specific proteolytic reaction activates an enzyme, which in turn activates another enzyme and thus starts the coagulation cascade. This blood coagulation cascade is visualized in Figure 1.7. The coagulation cascade consists of the intrinsic (contact activation) pathway and the extrinsic (tissue factor) pathway, each of which can activate the coagulation cascade on its own.

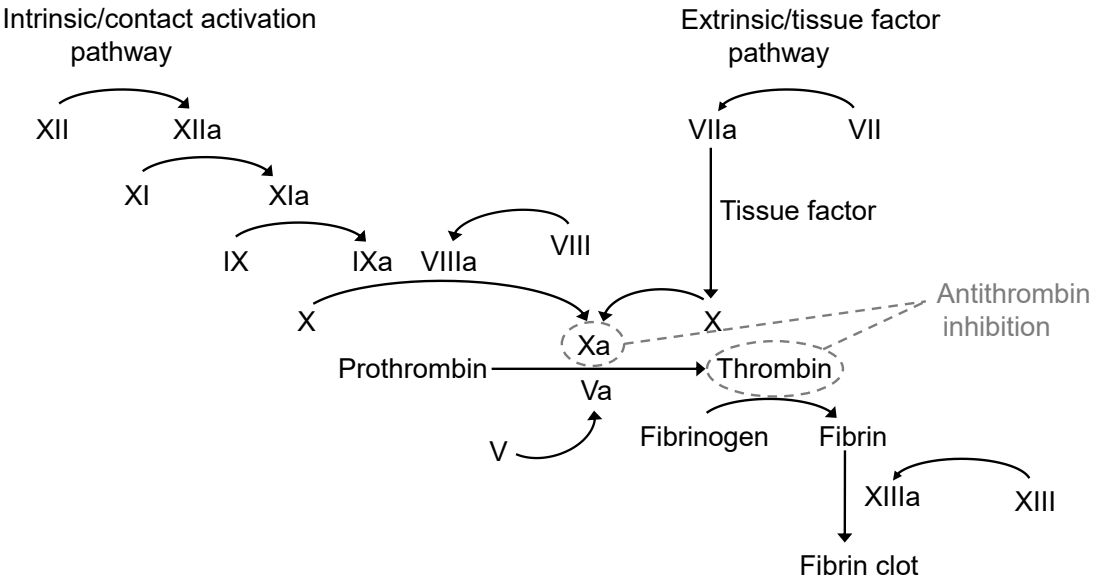

Figure 1.7: A simplified illustration of the coagulation cascade (adapted from Shantsila et al. [Shan2016]). Shown in gray is the main inhibition of antithrombin.

The intrinsic pathway starts, for example, when blood interacts with a foreign surface, with factor XII, also known as Hageman factor. The heavy chain of the enzyme factor XII binds to the foreign surface and thus enables a local increase in concentration, which allows, among others, an action on factor XI to form factor XIa. This factor XIa activates factor IX. The activated

factor IX and the activated factor VIII are required for factor X activation. [Colm2006]

Parallel to the intrinsic pathway is the extrinsic pathway, which involves components from blood and vascular elements and is the principal initiation pathway for *in vivo* blood coagulation. The key component of the extrinsic pathway is the tissue factor. It activates factor VII, which in turn activates factor X in combination with tissue factor. [Colm2006]

Both pathways form factor Xa and merge to the 'final common pathway' in which prothrombin forms thrombin. Interaction of factor Xa, factor V, phospholipid and calcium provides a significantly increased prothrombin activation rate. This resulting active thrombin is of particular importance for blood clotting. Active thrombin is the proteinase for the cleavage of fibrinogen and the resulting fibrin, which is responsible for the formation of a fibrin clot [Thom2017].

Negative feedback also occurs in the coagulation system and the activation of different factors. For example, thrombin activates factors V and VIII, whereas the conversion of protein C to active protein C promoted by thrombin leads to the destruction of factors Va and VIIIa. Furthermore, the tissue factor pathway inhibitor (TFPI) combined with the activated factor X leads to negative feedback in the extrinsic pathway. This combination inhibits the tissue factor-factor VII complex, and thus the activation of factor X. Other inhibitors can interrupt the coagulation cascade, such as C1 inhibitor, which inhibits factor XIIa. A further, widely known inhibitor is antithrombin. Antithrombin is the main inhibitor of factor Xa and thrombin (cf. Figure 1.7 gray). An arginine in the active center of the antithrombin reacts with the catalytic-site serine of the thrombin. A covalent complex is formed. This inhibition of antithrombin is enhanced and accelerated (1000-fold) by heparin [Hetz2005]. [Colm2006]

Heparin is the most common anticoagulant in medical applications, which is a sulfonated polysaccharide with a molecular weight (MW) range of 1,200 to 40,000 Da, with an average MW of around 10,000 Da (cf. Figure 1.8) [Seft2020]; [Hirs2001].

For the anticoagulant effect of heparin, it requires the plasma cofac-

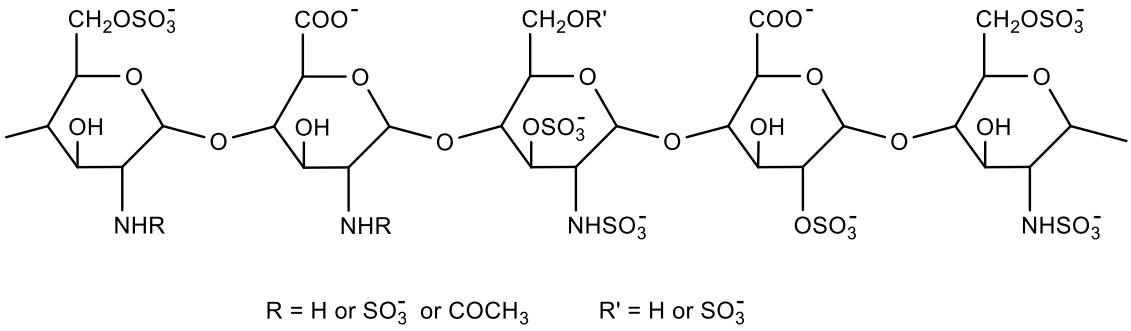

Figure 1.8: Chemical structure of heparin (adapted from He et al. [He2019]).

tor antithrombin [Brin1939]. Heparin binds to the lysine site on the antithrombin molecule and causes a conformational change at the arginine-reactive site. As a result of this binding, antithrombin transforms from a slow, progressive thrombin inhibitor to a very fast inhibitor of thrombin and factor Xa. An arginine-reactive site achieves this on the antithrombin molecule that inhibits due to the covalent binding to the active serine centers of thrombin and further coagulation enzymes, including factor Xa. Thrombin and factor Xa are most sensitive to inhibition by the heparin-antithrombin complex, with thrombin being ten times more sensitive to this inhibition than factor Xa. Subsequently, heparin dissociates from this antithrombin-thrombin/antithrombin-coagulation enzyme complex and can be used again. [Hirs2001]; [Colm2006]

The excellent anticoagulant effect of heparin is the reason for its wide use in medical applications. In dialysis, for example, heparin is injected into the patient to prevent coagulation of the blood during treatment. Over the past years, intensive research has been conducted into various ways of modifying the blood facing artificial surfaces to minimize or even inhibit protein adsorption from blood and thereby the formation of a blood clot. However, so far only a few approaches are already applied in medical products.

Surface Behavior

Whether a surface is susceptible to protein adsorption and adherence of platelets, and thus, for the activation of the coagulation cascade, depends on many different factors such as electrical charge, hydrophilicity/hydropho-

bicity, and surface roughness [Jung2016]. Mechanisms of protein adsorption are still not fully understood, as they are highly complex and dependent on a variety of factors, for example, on the heterogeneous composition of the blood [West2021]. Nevertheless, several studies suggest that protein adsorption or platelet adherence can be reduced through surface modification. This modification is achieved either by surface post-treatments or by blending [Fish2021]; [Mass2005]. For example, hydrophilic surfaces exhibit significantly lower protein adsorption than hydrophobic surfaces [Krau2006]; [Chou2020]. A hydrophilic surface prevents direct contact between membrane surface and proteins by a hydration layer. Thus, less proteins adsorb to the surface, resulting in less platelet activation, which in turn reduces thrombus formation. [He2021] Hydrophilic surfaces are obtained by hydrogel coating or surface grafting, coating or blending of hydrophilic polymers such as PVP, or by immobilizing water-soluble synthetic polymers such as polyethylene glycol (PEG) [Seft2020]. However, in literature it is still not clarified whether a surface should be hydrophilic or hydrophobic to do not react with platelets and coagulation factors [Seft2020].

Another widely used method to increase the hemocompatibility of surfaces and thus reduce the dosage of anticoagulants is the immobilization of heparin directly on the surface. The resulting surface is also referred to as the heparinized surface.

1.6 Heparinized Surface

The immobilization of heparin on artificial surfaces to improve blood compatibility was already of great importance in the mid-20th century. In 1963, Gott et al. [Gott1963] worked on the ionic binding of heparin onto graphite, plastic, and silicone surfaces. The high content of negatively charged sulfonate and carboxylate groups is the reason for the strong negative charge density of heparin [Gott1963]; [Capi2002]; [Bhal2015]. This property allows for ionic binding to various positively charged surfaces. The work of Gott et al. serves as a base for numerous studies on the immobilization of heparin onto surfaces. [Sper2006]; [Shan2020].

In general, heparin immobilization can be carried out either by grafting [Shan2020]; [Akso2008]; [Zhen2016]; [Wang2017]; [Yang2002]; [Yang2003]; [Lin2004c]; [Lin2004a]; [Hou2008]; [Wang2014b]; [Phil2018]; [Kale2021] or by coating heparin onto surfaces [Shan2020]; [Gao2014]; [Li2020]; [Sper2006]; [Dong2010]; [Zhu2009]; [Jian2010]; [Droz2022]; [Zhan2021]; [Mahl2013]; [Xie2016]. Heparin coating onto membrane surfaces is achieved through prior functionalization with heparin anchors. Sperling et al. [Sper2006], for example, used bovine serum albumin (BSA) as a heparin anchor to immobilize heparin onto polyethersulfone (PES) membrane surfaces. As a result of the heparin immobilization, various blood tests revealed an improvement in the blood compatibility of the membrane surface [Sper2006]; [Shan2020].

In addition to BSA, self-polymerized dopamine, also known as polydopamine, is used as a heparin anchor. Several studies have already addressed the immobilization of heparin on polydopamine-modified surfaces [Jian2010]; [Gao2014]; [Xie2016]. Polydopamine adsorbs to almost any surface [Lee2007], allowing for heparinization on these surfaces. The phenolic hydroxyl groups of polydopamine allow a covalent bonding to the amine groups of heparin [Jian2010]; [Gao2014]; [Xie2016]. Gao et al. [Gao2014] discussed an improvement in blood compatibility, particularly hemocompatibility, by heparinizing the polydopamine functionalized surface.

Grafting is another effective method to bind heparin to the surfaces to improve blood compatibility [Akso2008]; [Wang2017]; [Shan2020]; [Lavi2014]; [Yang2002]; [Yang2003]; [Lin2004c]; [Lin2004a]. Covalent binding to heparin is facilitated by plasma-activation of functional groups such as hydroxyl groups [Wang2017]; [Akso2008], which then react with a coupling agent to chemically bind heparin to the surface [Shan2020]. For example, Aksoy et al. [Akso2008] grafted heparin to a polyurethane (PU) film by first performing plasma activation to activate functional groups, which then react with acrylic acid and with the coupling agent N'-3-(dimethyl-aminoproply)-N'-ethylcarbodiimide hydrochloride (EDC) [Akso2008]. Moreover, their research showed improved blood compatibility in the form of cell adhesion for the heparin grafted PU surface [Akso2008]. Furthermore, Wang et

al. [Wang2017] showed improved blood compatibility in terms of platelet adhesion and coagulation time using heparin grafted surfaces. Wang et al. treated polysulfone (PSF) membrane surfaces with plasma to graft polyethylene glycol (PEG) as a coupling agent, which immobilizes heparin [Wang2017]. Figure 1.9 and 1.10 summarize the publications of heparin immobilization used in this work. Most of these immobilization methods of heparin significantly improve blood compatibility, especially hemocompatibility, regardless of the foreign surface. The studies suggested that surface modification with heparin can reduce or eliminate the need for injected anticoagulants during any blood circulation, such as hemodialysis [Kess2013]; [Teli2014]; [Lavi2014]. In hemodialysis, the blood encounters a large area of foreign material. To prevent blood clotting, high amounts of the anticoagulant heparin are injected into the patient when the hemodialysis starts. With the development of a heparinized dialyzer, known as the Evodial Dialyzer from the company Baxter International Inc., this dialysis treatment can be performed with reduced or no anticoagulant injection [Kess2013]; [Lavi2014]. The surface of the Evodial Dialyzer consists of a copolymer of acrylonitrile and sodium methallylsulfonate, post-treated with polyethyleneimine (PEI) and finally grafted with heparin [Thom2011]; [Lavi2014]. This dialyzer is already used for hemodialysis treatments due to its excellent blood- and hemocompatible properties. However, this special dialyzer is only used to treat high-risk patients.

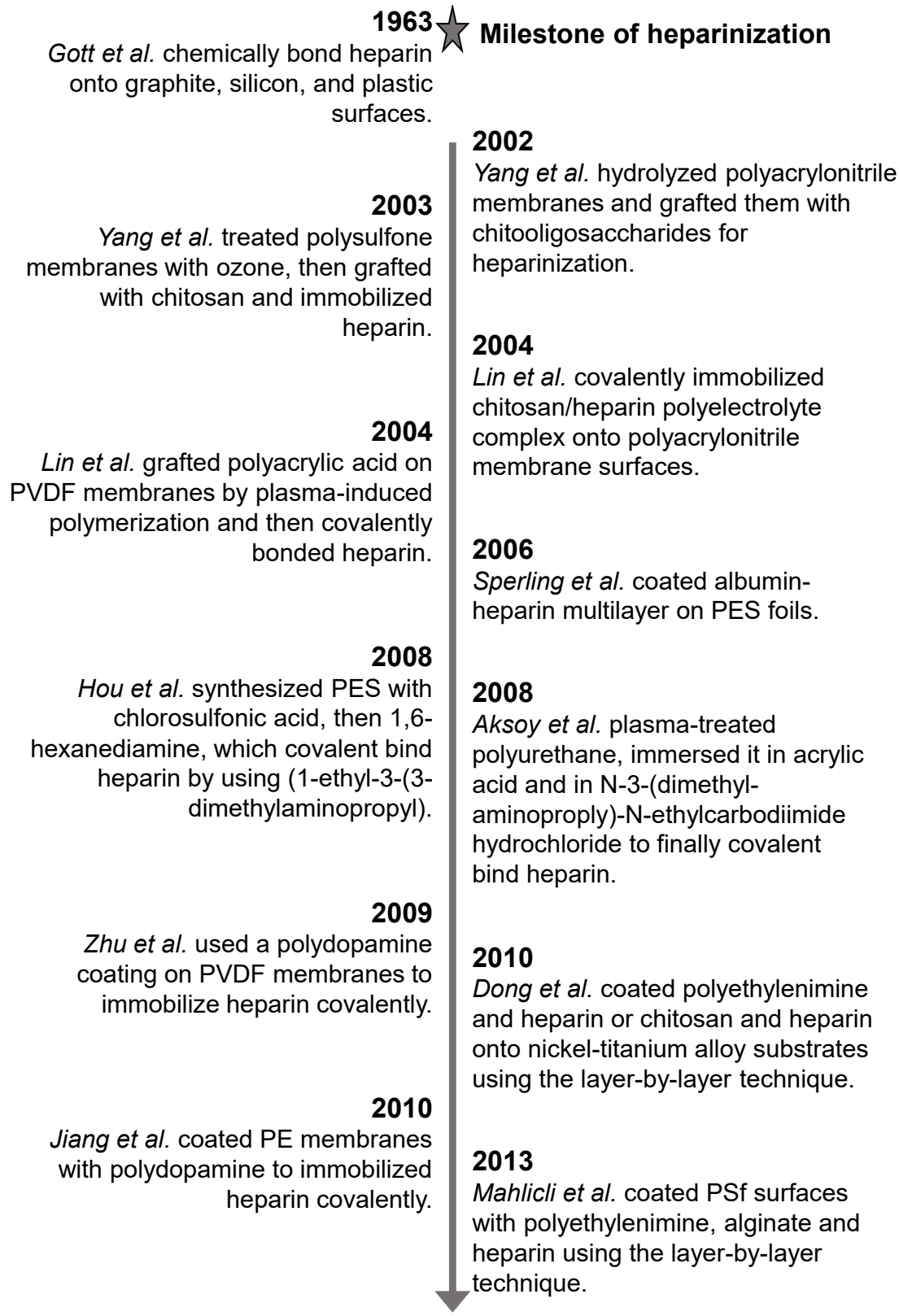

Figure 1.9: Publications dealing with the heparinization from 2002 to 2013 used in this thesis.

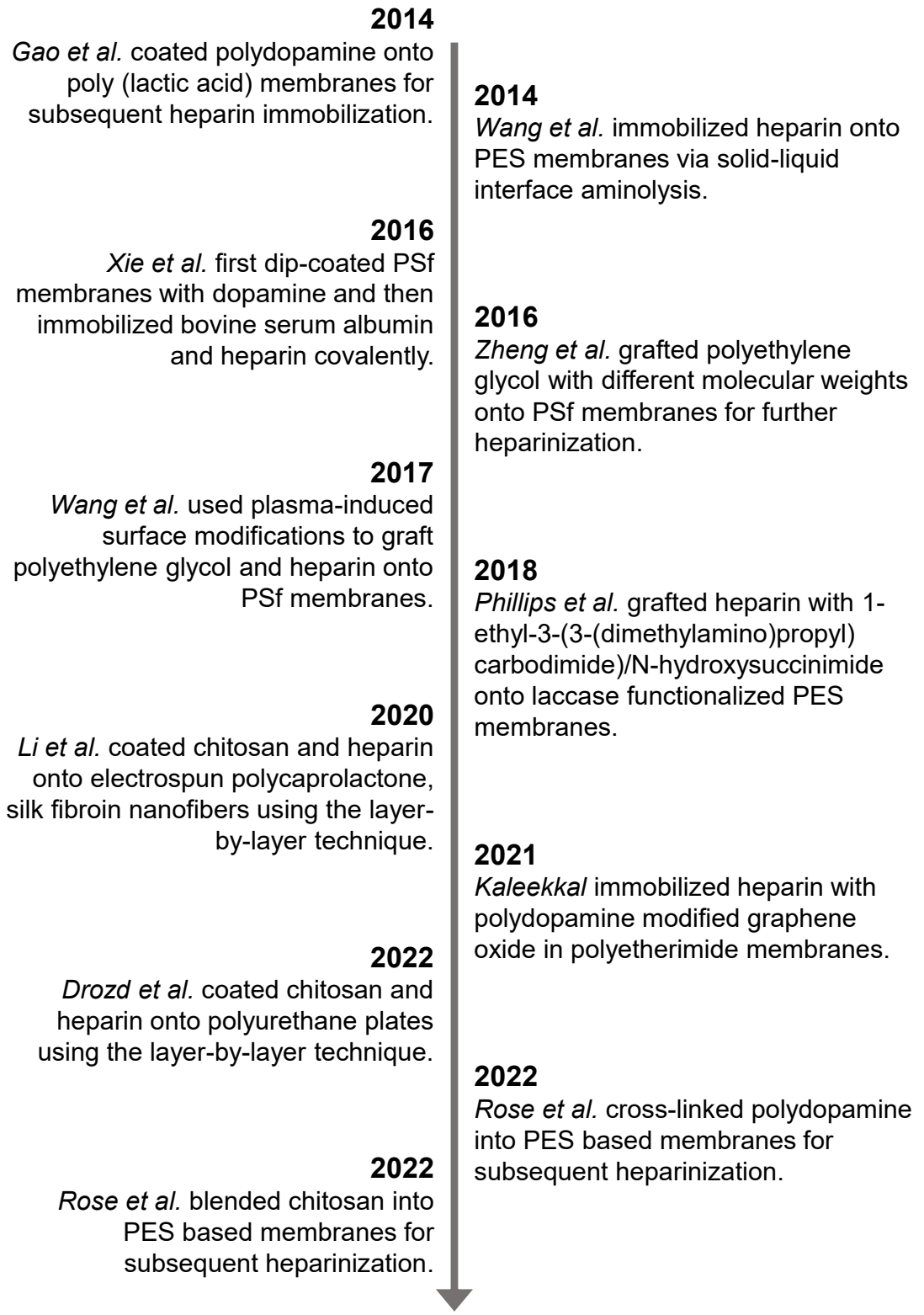

Figure 1.10: Publications dealing with the heparinization from 2014 to 2022 used in this thesis.

1.7 Hypothesis and Outline of the Thesis

In this thesis, the anticoagulant heparin is immobilized on membrane surfaces using various additives to improve the hemocompatibility of membranes surfaces based on polyethersulfone (PES). Four different additives are investigated, allowing heparinization of membrane surfaces. The additives are immobilized on the membrane surface by three different approaches coating, blending, or chemistry-in-a-spinneret. Single-step fabrication processes that simultaneously entail functionalization of the membrane surface are of significant interest. Since they are much more time- and cost-efficient due to the omission of subsequent coating steps. This thesis aims to fabricate a cost-efficient heparinized dialyzer based on PES, making it affordable to any dialysis patient.

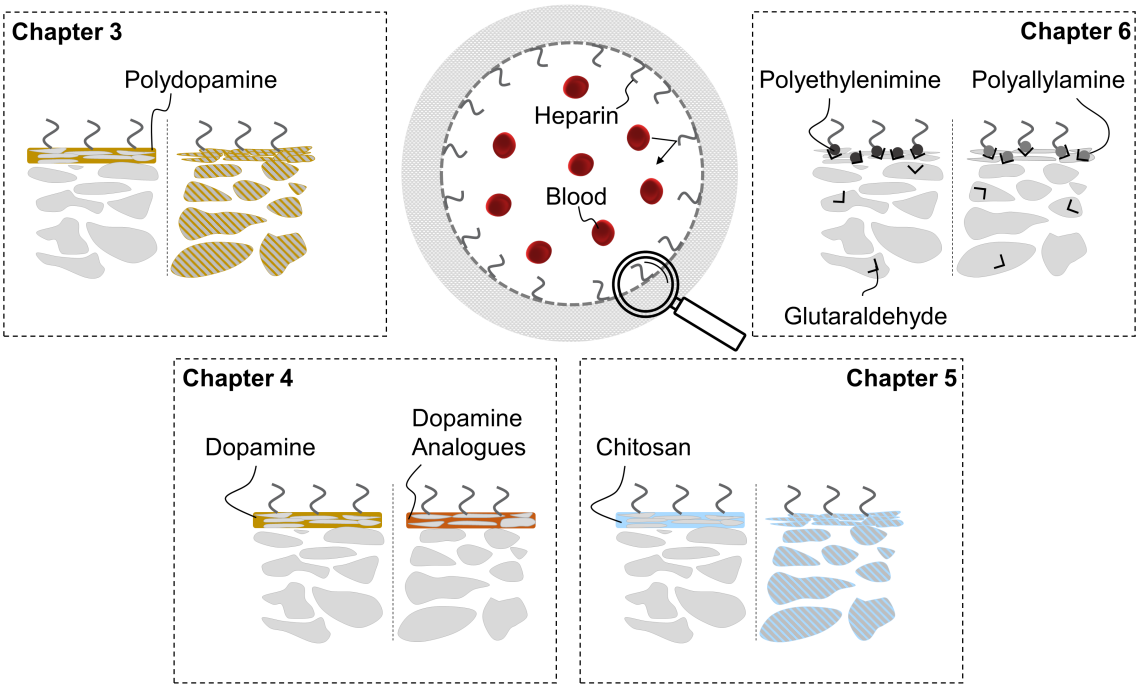

Figure 1.11: Visualization of the functionalization methods performed in this thesis for the heparinization of membrane surfaces.

Chapter 2 describes the main materials, membrane fabrication methods with the associated solution preparations, and various membrane characterization methods. The following chapters focus on four different additives that enable heparinization on the membrane surface and thus improve

hemocompatibility.

Chapter 3 introduces membranes that are functionalized with polydopamine in two different methods. First, post-modification of commercial dialysis hollow fiber membrane modules with polydopamine and subsequently with heparin. The successful immobilization while maintaining their selectivities for proteins present in human blood is highlighted. Further, membranes are in-situ modified with polydopamine using the chemistry-in-a-spinneret technology base. In a single-step process, polydopamine-functionalized membranes are produced by adding polydopamine into the polymer solution.

Chapter 4 presents an alternative to dopamine, the dopamine analogues, consisting of catechol and propylamine. Microtiter plates, flat sheet membranes, and hollow fiber membranes are post-modified with dopamine or dopamine analogues equimolar to dopamine. Membranes modified with dopamine analogues have similar properties as those modified with dopamine. The respective coatings have been shown to immobilize heparin on the surface successfully. Despite additional coatings on the membrane, permeance and molecular weight cut-off are not changed significantly. On the other hand, the anti-fouling properties improve with dopamine or dopamine analogues coatings.

Chapter 5 introduces chitosan as an additive for the immobilization of heparin. First, commercial dialysis hollow fiber membrane modules are post-modified with chitosan and subsequently with heparin. The resulting membranes exhibit significant charge differences and a considerable increase in pure water permeance. To overcome time-consuming and multi-step coating procedures, chitosan functionalized membranes are fabricated in a single step by blending chitosan into the polymer solution. Highlights of these membranes are their significant surface charge differences, strong anti-fouling properties, and excellent hemocompatibility, shown by the thrombin-antithrombin complex, complement and platelet activation measurements. Furthermore, the heparinized surface increases the pure water permeance of the chitosan-blended membranes.

In **Chapter 6**, polyethylenimine and polyallylamine are introduced as ad-

ditives to immobilize heparin on the membrane surfaces. These are immobilized using the chemistry-in-a-spinneret technology base during membrane fabrication. For this purpose, glutaraldehyde is present in the polymer solution and cross-links with the respective amine source in the coagulation bath for flat membranes or in the bore solution for hollow fiber membranes. The cross-linking does not significantly change the membrane properties such as pure water permeance and molecular weight cut-off. All membranes enable a successful heparinization.

Chapter 7 summarizes and reflects the use of the different additives for the immobilization of heparin on the membrane surface and thus an increase in hemocompatibility. Furthermore, an outlook gives a perspective of future work.

2 Material and Methods

Parts of this chapter have been published in:

[Rose2022a]: I.I. Rose*, H. Roth*, J. Xie, F. Hollmann, S. Votteler, M. Storr, B. Krause, M. Wessling, "Chemistry in a spinneret - Polydopamine functionalized hollow fiber membranes", *Journal of Membrane Science, 2022, DOI: 10.1016/j .memsci.2022.120324*

[Rose2022b]: I.I. Rose, M. Kather, H. Roth, H. Dünkelberg, L. Rein, S.N. Klimosch, M. Schmolz, M. Wessling, "Single-step chitosan functionalized membranes for heparinization", *Journal of Membrane Science, 2022, DOI: 10.1016/j .memsci.2022.120567*

*These authors are contributed equally to this work

This chapter first summarizes the materials used and then the methods employed. In addition to the membrane fabrication processes, the post-treatment with heparin is discussed, as well as the subsequent membrane characterization methods. The following sections contain the names and descriptions of special materials and individual methods.

2.1 Materials

The base polymer, polyethersulfone (PES, Ultrason 6020P), is provided as granulate from BASF. Polyvinylpyrrolidone with an average molecular weight of 40 kDa (PVP K30) and 900 - 1,200 kDa (PVP K90) are purchased from Carl Roth, while PVP K85 is provided from Baxter International Inc.. The solvent N-methyl-2-pyrrolidone (NMP) with a purity of 99 % is purchased from Fisher Scientific.

For the post-treatment with heparin, heparin sodium salt with 180 IU/mg purity is purchased from Carl Roth. For buffer solution preparation, sodium acetate with purity above 99 % is purchased from Carl Roth, and acetic acid with purity above 99 % is purchased from Sigma-Aldrich.

To adjust pH values in solutions, sodium chloride (NaCl) with purity above 99 % is purchased from Carl Roth, and hydrochloric acid (HCl) with ACS reagent is purchased from Sigma Aldrich.

For rinsing before each measurement of surface charge, potassium chloride (KCl) with purity above 99.5 % is purchased from Carl Roth.

For fouling measurements, bovine serum albumin (BSA) with purity above 96 % and fluorescent-marked albumin-fluorescein isothiocyanate conjugate (FITC-BSA) with purity above 99 % are purchased from Sigma Aldrich. Phosphate-buffered saline buffer (PBS) tablets (ROTI®Fair PBS 7.4) are purchased from Carl Roth.

For molecular weight cut-off (MWCO) measurements polyethylene glycol (PEG) 600, PEG 2,000, PEG 4,000, PEG 6,000, PEG 10,000, PEG 20,000, PEG 35,000, and polyethylene oxide (PEO) 100,000 are purchased from Carl Roth.

2.2 Membrane Fabrication

2.2.1 Preparation of Polymer Solution

The polymer solutions used in this thesis consist of the base polymer polyethersulfone (PES), various polyvinylpyrrolidones (PVPs) that act as pore-forming agents, a solvent, DI water, and often an additive. Each polymer is dried for at least 24 h at 30 °C in a vacuum oven before being used.

The weight share of the additive is reduced from the weight share of the solvent. Water-soluble additives first dissolve in the DI water, then mixed with the solvent, and stirred with the polymers with a KPG stirrer from Heidolph Instruments GmbH & Co. KG. On the other hand, solvent-soluble additives first dissolve in the solvent and are finally stirred with the polymers. Temperature control of polymer solutions is possible throughout the entire preparation process.

2.2.2 Flat Sheet Membrane Fabrication

Flat sheet membranes are fabricated by a casting process in which a casting knife from BYK-Gardner GmbH creates a uniform 200 μm thick film from a degassed polymer solution on a glass support. This polymer film is then immersed in a coagulation bath, which typically consists of DI water. Figure 2.1 depicts this casting process. As soon as the polymer comes into contact with the water, the phase inversion begins. The resulting porous flat sheet membrane detaches from the glass support and is placed in another water bath with tweezers. With the goal of flushing out as much solvent as possible, the membrane is stored in this water bath for 24 h. Finally, the membranes are air-dried at room temperature overnight.

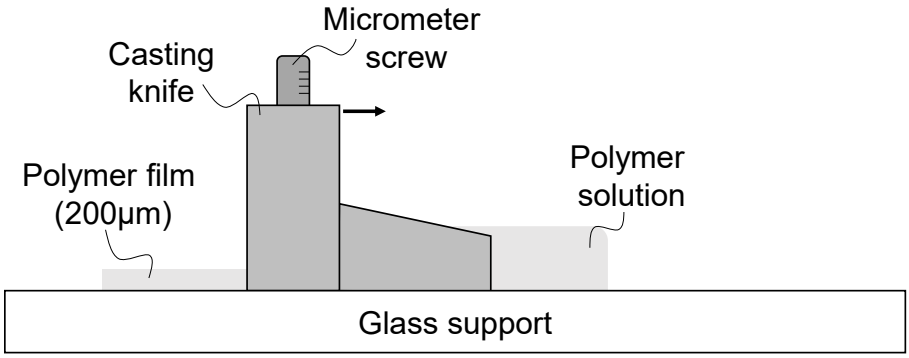

Figure 2.1: Flat sheet membrane casting process.

2.2.3 Preparation of Bore Solution

The bore solution is prepared around 24 h before the fabrication of hollow fiber membranes (cf. Section 2.2.4) starts. Usually, a 50/50 or a 80/20 DI water/NMP mixture is used. Approximately 2 h before the membrane fabrication starts, the bore solution is filled into 60 mL syringes.

2.2.4 Hollow Fiber Membranes Fabrication

Hollow fiber membranes are fabricated in the spinning process. The polymer solution is typically placed for degassing in a polymer vessel 24 h before the spinning process starts. The polymer vessel is double-walled so that the temperature of the polymer solution can be controlled throughout spinning. A piston closes the vessel and enables polymer flow by moving downwards. In addition to the polymer vessel, the spinning line consists of a syringe pump from Harvard Apparatus GmbH, which delivers the bore solution into a switchable orifice spinneret, a coagulation bath, typically consisting of DI water and heatable, a motorized pulling wheel; and a washing bath, also consisting of DI water. The setup of this spinning line is shown in Figure 2.2.

During spinning, both the polymer and the bore solution enter the spinneret. The formed fiber leaves the spinneret, passes through the air gap, and enters the coagulation bath. Here, it is deflected and conveyed into the water bath via the pulling wheel, which controls the take-up speed. Each membrane bath is stored for 24 h in DI water after spinning. Finally, the

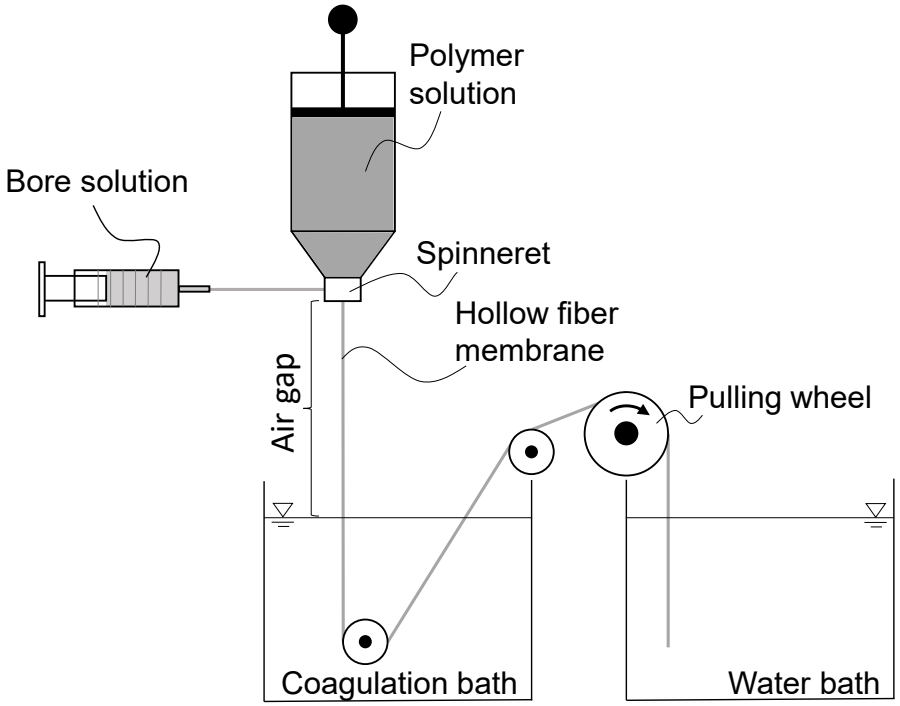

Figure 2.2: Spinning line setup for hollow fiber membrane fabrication.

fibers are air-dried at room temperature overnight.

2.3 Post-Treatment of Heparin

The immobilization of heparin on the membrane surface occurs independently of any previously performed functionalization of the respective membrane. A buffer solution of 50 mM acetic acid and 50 mM sodium acetate in DI water at pH 4.5 and 0.5 mM sodium chloride are prepared. Then, 1 mg/mL heparin is added.

For coating flat sheet membranes, membrane pieces are immersed in the heparin solution for 24 h and then rinsed with DI water.

For coating hollow fiber membranes, membrane fibers are glued into tubes to create membrane modules (cf. Section 2.4.6). The heparin solution is now filled into the lumen side, see Figure 2.3. The shell side is filled with acetate buffer. After a rest period of 24 h, the hollow fiber membranes are flushed with DI water on the lumen and shell side.

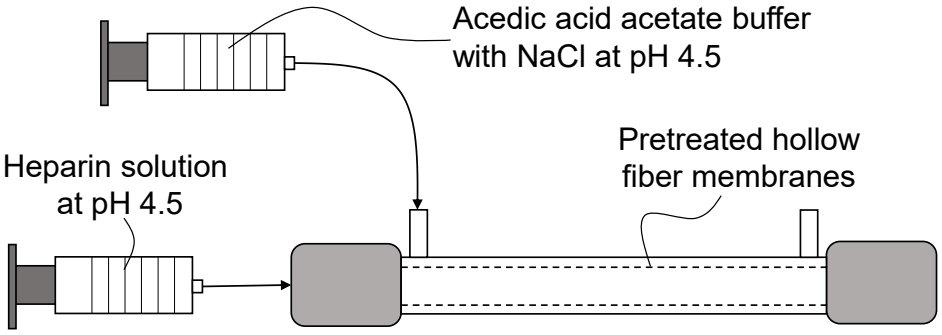

(a) Filling of buffer solution in shell side and heparin solution in lumen channel with syringes.

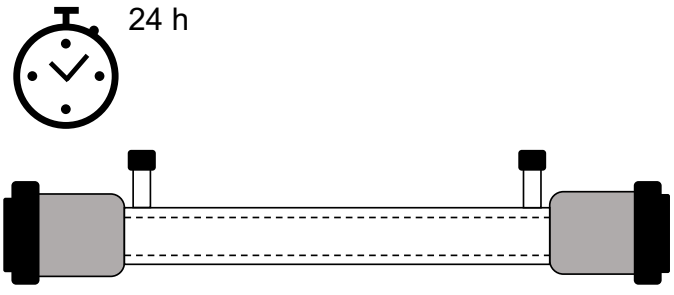

(b) Heparin immobilization carried out for 24 h in closed membrane module.

Figure 2.3: Process of post-modification of hollow fiber membrane modules with heparin on the lumen of the hollow fibers for 24 h.

Throughout this thesis, a heparin-coated membrane is indicated with the

abbreviation '-H'.

2.4 Membrane Characterization

2.4.1 Membrane Morphology

Field emission scanning electron microscopy (FeSEM) is employed to characterize the morphology of the membranes with a Hitachi S-4800 or a Hitachi SU 5000 Scanning Electron Microscope. Top view and cross-section of the membranes are visually recorded. To create a smooth surface for a clear cross-section image, the membranes are fractured in liquid nitrogen. The samples are dried in a vacuum oven and subsequently sputtered with AuPd 80/20 (around 7 nm) before images are taken.

2.4.2 XPS Measurement

Membrane samples are washed multiple times with DI water and dried under vacuum at 30 °C over night before the measurement. X-ray photoelectron spectroscopy (XPS) measurements are recorded using an Ultra Axis™spectrometer (Kratos Analytical, Manchester, UK).

2.4.3 Static BSA Fouling Measurements

Flat sheet membranes are cut into 1 cm^2 pieces to perform the static bovine serum albumin (BSA) fouling measurements. These membrane pieces are placed in a 12-well plate and washed three times with 2 mL PBS buffer solution while placed on a rocking chamber for 1 min at 60 rpm. For protein adsorption, 2 mL of 50 mg/L FITC-BSA in PBS buffer is added to each well and placed on a rocking chamber for 3 h at 60 rpm. To protect the FITC-BSA solution from light, the closed well plate is wrapped in aluminum foil. Afterward, the FITC-BSA solution is removed, and the membrane pieces are washed with DI water three times. Next, each membrane piece is placed on a microscope slide, covered with PBS solution, and finally covered with another glass slide while avoiding the trapping of air bubbles. The

membrane preparation procedure is shown in Figure 2.4. The samples are measured at 2000 ms via an Axiovert 200M epifluorescence microscope.

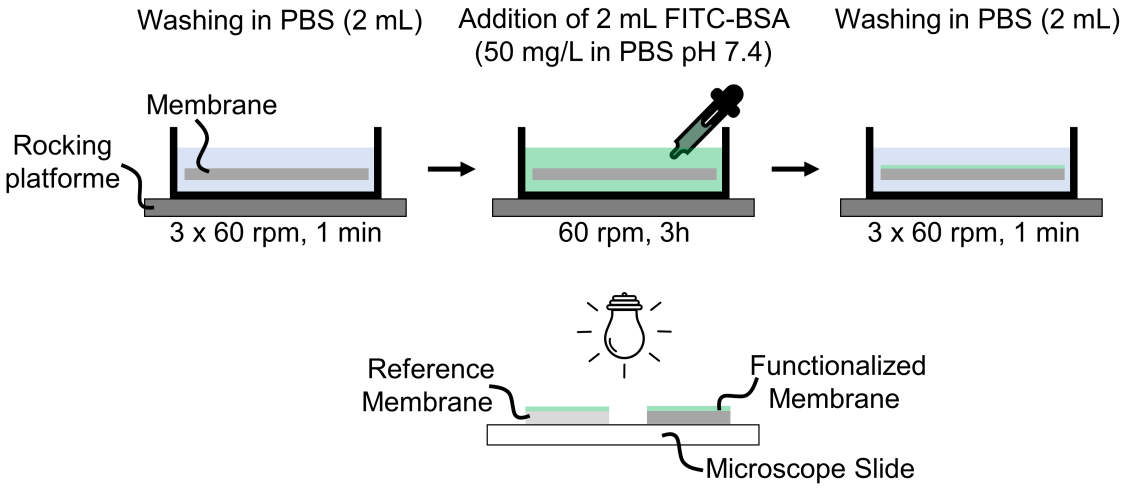

Figure 2.4: Membrane preparation procedure of static BSA fouling measurements.

2.4.4 Membrane Surface Charge

The surface charge of flat sheet membranes or the lumen channel of hollow fibers is analyzed with a SurPASS electrokinetic analyzer (Anton Paar, Austria). The analyzer automatically varies the pH from 3 to 6 by titration of 0.1 M HCl and 0.1 M NaOH. For each pH value, four zeta potentials are measured. The error bars represent the standard deviation from the average zeta potential. Flat sheet membranes are placed directly on the measuring die and analyzed. For the measurements of the hollow fiber membranes, a specific membrane module is required. Therefore, a single hollow fiber is placed into a 7 cm long PE tube, and the permeate side is filled with glue preventing any permeation during the measurement. The membrane module is flushed with 5 L of 1 mM KCl solution before the measurement is started.

2.4.5 Burst Pressure

To obtain information on the membrane stability and thus on the mechanical properties of the membranes, burst pressure measurements are carried

out. A single hollow fiber with 10 cm length is glued on one side in a 8 cm polyethylene (PE) tube. The protruding end of the fiber is closed with a clamp, resulting in a dead-end mode. DI water is pumped by a pump handle in the lumen channel, the pressure increases until the fiber bursts. A manometer saves the maximum pressure value. Three measured fibers represent the average burst pressure.

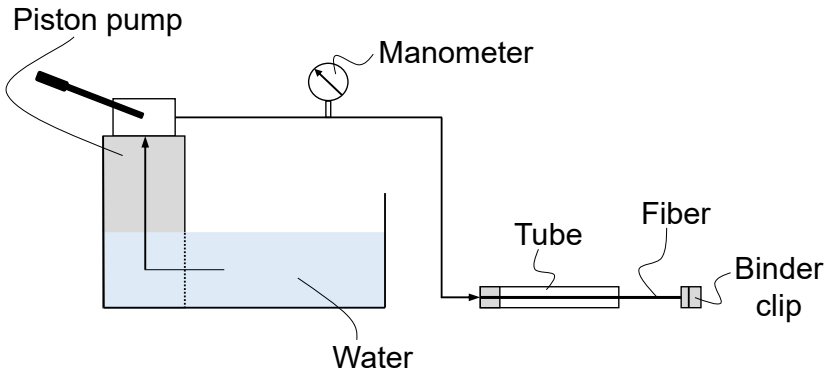

Figure 2.5: Setup of burst pressure measurement.

2.4.6 Membrane Module

For the following characterization methods, hollow fiber membranes are placed in four-end modules. Fibers are glued into a 25 cm polyethylene (PE) tube with two IQS T-connectors with an inlet and outlet on the permeate side (cf. Figure 2.6). After drying and before the first measurement, each module is flushed with a 50 wt.% ethanol and DI water mixture to wet the pores of the fibers.

Figure 2.6: Membrane module for hollow fiber membrane characterization.

2.4.7 Pure Water Permeance

A dead-end filtration with DI water and a transmembrane pressure (TMP) of 1 bar is used for measuring the pure water permeance (PWP). As soon as the continuous permeate flux (J) is reached, the measurement is started. The permeating water mass is translated into the permeance of the membrane in L/(m^2 h bar), short LMH/bar. The permeance is averaged for three measured membrane modules.

2.4.8 Molecular Weight Cut-Off

For the determination of the molecular weight cut-off (MWCO), a cross-flow filtration with an aqueous solution, consisting of different PEGs and DI water, and a TMP of 1 bar is conducted. PEGs with molecular weights between 600 Da to 100 kDa are solved in the mixture with 1 g/L of each PEG size. The feed flow is set to 150 kg/h to ensure a turbulent flow (Re $>$2300) on the lumen side of the fibers. Permeate samples are analyzed by size-exclusion chromatography (SEC) using an Agilent 1200 system to determine the molecular weight and the concentration of each PEG. The retention is calculated with the measured concentration in the feed c_{Feed} and in the permeate c_{Permeate}:

$$\text{Retention} = (1 - \frac{c_{\text{Permeate}}}{c_{\text{Feed}}}) \cdot 100\% \tag{2.1}$$

The MWCO represents the MW of the PEG that is retained by the membrane to 90 %.

3 Polydopamine Functionalization Allows Heparin Immobilization

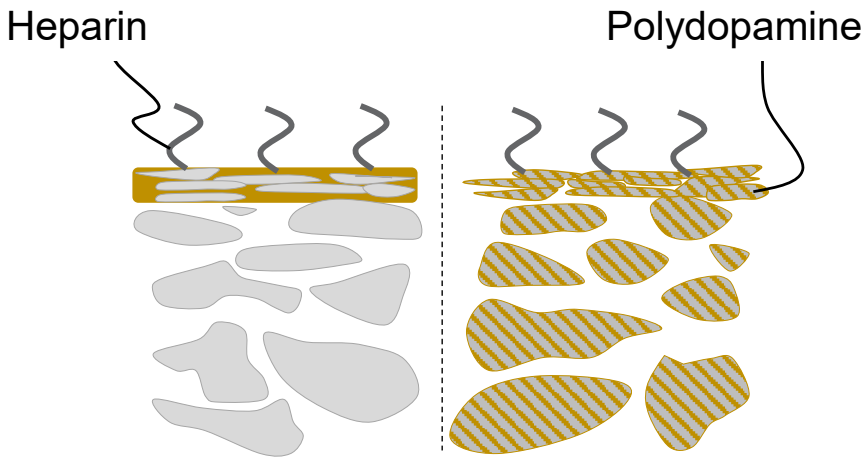

Parts of this chapter have been published and submitted as patent in:
[Rose2022a]: I.I. Rose*, H. Roth*, J. Xie, F. Hollmann, S. Votteler, M. Storr, B. Krause, M. Wessling, "Chemistry in a spinneret - Polydopamine functionalized hollow fiber membranes", *Journal of Membrane Science, 2022, DOI: 10.1016/j.memsci.2022.120324*

M. Hornung, M. Storr, J. Swartjes, S. Votteler, A. Krauss, M. Hulko, L. Peters, M. Wessling, I.I. Rose, G. Linz, H. Roth, "Method for increasing the selectivity of a membrane", European patent application Nr. 21216677.1
*These authors are contributed equally to this work

3.1 Introduction

Polydopamine is widely used in many different applications in literature [Yang2015]; [Shah2021]; [Gao2014]; [Xie2016]; [Zhu2009]. In particular, the characteristic potential of polydopamine-functionalized membrane surfaces to bind heparin opens the application in the field of dialysis [Gao2014]; [Jian2010]; [Kale2021]. However, approaches of polydopamine-functionalized membrane surfaces found in the literature require laborious multiple fabrication steps to achieve the final membrane product.

This Chapter 3 aims to create polydopamine functionalized membranes in a single step by adding dopamine to the polymer solution and coagulation in an alkaline environment. First a post-modification of commercial dialysis membrane modules with polydopamine and heparin as a reference is developed. The coating is intended to immobilize heparin on the membrane surface while improving or at least leaving the separation properties unchanged. Further and most importantly, the chemistry-in-a-spinneret technology base (cf. Section 1.3.3) enables the in-situ modification of membranes with polydopamine, which is assessed by membrane characterizations. These functionalized membranes have the potential for use as hemodialysis membranes and in other membrane processes.

The versatile applications of polydopamine refer to its strong adhesion properties to a wide range of surfaces. Dopamine contains catechol and amine groups, which are responsible for the oxidative polymerization of dopamine to polydopamine to form strong adhesion [Lee2007]. To date, no final conclusion has been drawn of the resulting polydopamine structure. Figure 3.1 depicts one possible polymerized polydopamine structure in a simplified form [Lieb2013]; [Ho2014]. Dopamine is first oxidized to dopamine-quinone and then polymerized to polydopamine. It is further discussed in the literature that the binding of the amine group of the dopamine structure to the various support materials happens via the Michael addition or the Schiff base reaction [Lee2006]; [Sala2016].

Membranes post-modified with polydopamine find use in medical fields because this functionalization improves both the biocompatibility and the

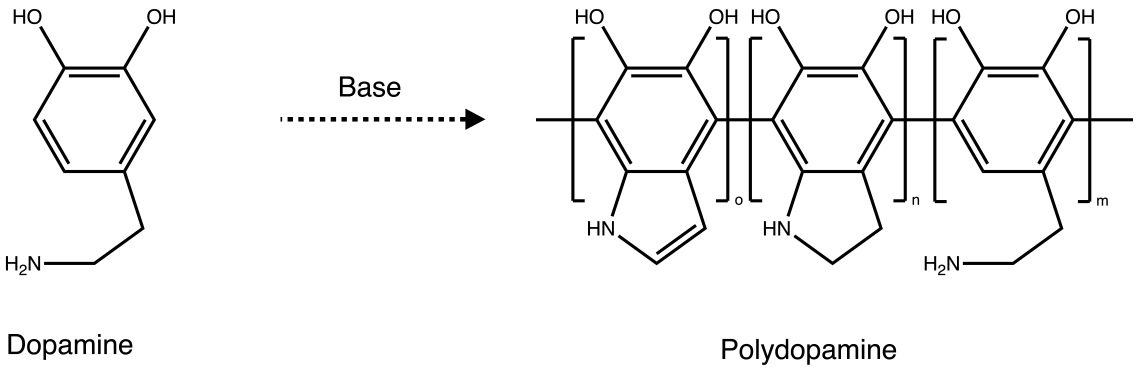

Figure 3.1: Dopamine in an alkaline environment forms polydopamine.

adhesion properties of the membrane material [Lee2007]; [Liu2013]. Additionally, the polydopamine functionalization offers the immobilization of heparin. The binding mechanism of heparin to polydopamine functionalized surfaces is controversially discussed in the literature. On the one hand, Jin et al. [Jin2020] presented a condensation reaction between the amine groups of heparin and the dihydroxyindole/indolequinone groups of polydopamine [Jin2020]. On the other hand, Zhu et al. [Zhu2009] assumed a covalent bond between the quione species of polydopamine and the amine groups of heparin [Zhu2009]. The catechol groups of polydopamine can oxidize into a quinone structure, which binds covalently with active -NH_2(-NH-) of heparin [Lee2006]; [Jian2010]. Nevertheless, the successful immobilization of heparin on membrane surfaces using polydopamine has been reported several times, which results in an increased hemocompatibility of those membrane surfaces. [Gao2014]; [Zhu2009]; [You2011]

Hemodialysis treatment usually requires heparin to be administered intravenously to the patient to prevent blood clotting on the artificial membrane surface [Lavi2014]. Heparin activates antithrombin, which inhibits both factor Xa and thrombin. Hence, the formation of a thrombus in the human blood is prevented due to the influence of heparin on the coagulation cascade. Furthermore, heparin significantly reduced the platelet deposition [Lin2004b]. In clinical treatment, the dosage of heparin is not customized. Therefore, it is administered in large amounts and results in long waiting times until the heparin is degraded in the patients' blood after each treatment procedure. The immobilization of heparin on the membrane surface is

a promising approach to prevent administrating heparin, thus avoiding long-term damages. An intermediate polydopamine layer offers the binding of heparin to commercial dialysis membrane surfaces, which then enables a reduction or even an elimination of the injected heparin during hemodialysis treatment. Zhu et al. [Zhu2009] were the first to combine heparin with polydopamine on poly(vinylidene fluoride) (PVDF) microporous membranes. It was followed by further research in the field. For example, Jiang et al. [Jian2010] coated polyethylene (PE) porous membranes and created a covalent bond during the coating process, while You et al. [You2011] demonstrated a significant reduction in blood clotting by the use of treated poly(urethane) (PU) substrates. Gao et al. [Gao2014] developed poly(lactic acid) (PLA) membranes for hemodialysis and created a covalent bond between the phenolic hydroxyl group of polydopamine and the amino group of heparin [Gao2014]; [Jian2010]. Ma et al. [Ma2014] used dopamine and heparin functionalized PES membranes to decrease plasma protein adsorption and suppress platelet adhesion compared to an untreated membrane.

Besides these fundamental research achievements, the company Baxter International Inc. sells heparinized acrylonitrile/sodium methallyl sulfonate membranes, called Evodial dialyzer, for dialysis treatment. The lumen side of the Evodial dialyzer membrane is treated with polyethylenimine (PEI). In a further step, heparin is grafted to the surface. The heparinization of membrane surfaces allows for heparin reduced or even heparin-free dialysis treatment. [Lavi2014]; [Thom2011]; [Mala2017] However, this special heparinized dialyzer is only used to treat high-risk patients. There is still no cost-effective heparinized dialyzer based on polyethersulfone (PES) that is accessible to every dialysis patient.

In contrast to the cited post-modification processes, the chemistry-in-a-spinneret approach (cf. Section 1.3.3) allows for both the formation and the functionalization of membranes in one step. This approach combines the fabrication of membranes via the phase separation process with a cross-linking reaction of the membrane material or additives. Applications of the concept with different material systems show the versatility of the

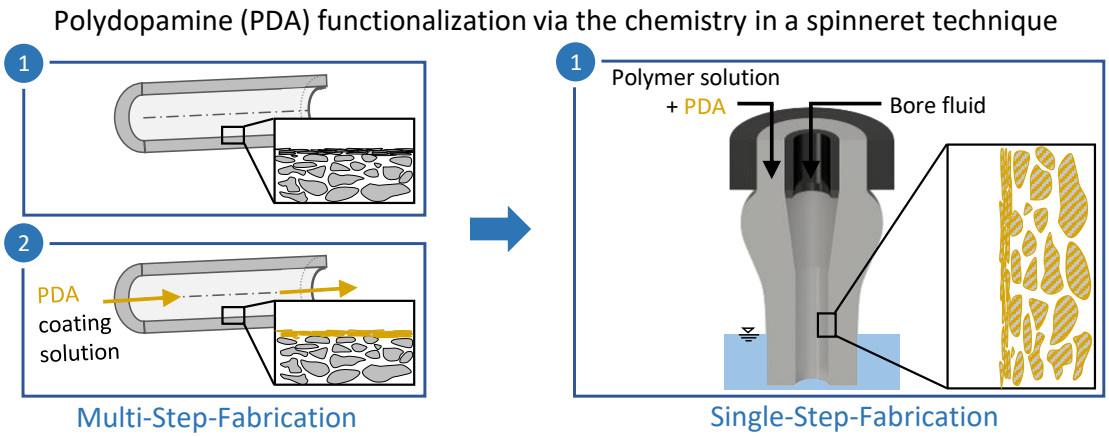

Figure 3.2: Scheme of post-modification and in-situ modification of membranes with polydopamine presented in this chapter.

chemistry-in-a-spinneret approach (cf. Section 1.3.3).

This chapter first presents the post-modification with polydopamine of commercial dialysis hollow fiber membranes (cf. Figure 3.2 left). Further functionalization with heparin is assessed and the characterization focuses on the application in dialysis. In the second part, the findings of the post-modification are transferred to the chemistry-in-a-spinneret technique. With the addition of dopamine in the polymer solution, functionalized membranes evolve directly during membrane fabrication (cf. Figure 3.2 right) and only needs to be further coated with heparin. Therefore, the necessity for laborious post-treatment can be overcome to create heparinized, PES based hollow fiber membranes.

3.2 Experimental

3.2.1 Materials

In addition to the materials described in Section 2.1, the following materials were used. Dopamine hydrochloride (98 %, Sigma Aldrich, Germany) is used as functional ingredient. For the membrane post-treatment, glycerol is purchased at Carl Roth with purity above 99 %. Tris-(hydroxymethyl)-aminomethan (tris) ($\geq$99.9 %, Carl Roth, Germany), sodium acetate ($\geq$99 %, Carl Roth, Germany), and hydrochloric acid (ACS reagent, Sigma Aldrich,

Germany) are used as buffer solutions and to adjust the pH of the different solutions.

For sieving coefficient measurements, myoglobin from horse heart is purchased at Sigma Aldrich.

Baxter International Inc. kindly supplied four-end mini-modules of their Revaclear membranes containing either 177 or 355 PES/PVP fibers.

3.2.2 Preparation of Solutions

For the functionalization of membranes with polydopamine and heparin, solutions are prepared and used in different membrane functionalization procedures to achieve the desired membrane structures.

Polymer Solutions

The used polymer solutions are summarized in Table 3.1.

Table 3.1: Overview of polymer solution compositions for flat sheet casting and hollow fiber spinning.

Polymer solution	PES [wt. %]	NMP [wt. %]	PVP K30 [wt. %]	PVP K90 [wt. %]	Dopamine [wt. %]
P3.1	22.0	78.0	-	-	-
P3.2	21.9	77.6	-	-	0.5
P3.3	15.9	75.6	4	4	0.5
P3.4	14.0	84.0	-	2	-
P3.5	14.0	83.5	-	2	0.5
P3.6	14.0	85.5	-	-	0.5

For the polymer solutions P3.1 to P3.4, all ingredients are prepared as stated in Section 2.2.1.

For the polymer solutions P3.5 and P3.6, all ingredients except dopamine are stirred with a KPG stirrer at 65 °C for at least 24 h until a homogeneous solution is formed. 2 h before transforming the polymer solutions into membranes, dopamine is added into the polymer solution and stirred until a homogeneous solution is formed. Subsequently, the solutions are left degassing.

Polydopamine Coating Solution

The polydopamine coating solution is prepared shortly before starting the coating procedure to synchronize the polymerization of the dopamine and the coating of the membrane surface. If not stated otherwise, the polydopamine coating solution contains 0.5 g/L dopamine in 10 mM tris buffer adjusted to a pH of 8.5 with HCl. Subsequently some membranes are coated with heparin as stated in Section 2.3.

3.2.3 Post-Modification with Polydopamine

Small membrane modules containing commercial hollow fiber dialysis membranes from Baxter International Inc. are functionalized with polydopamine via a post-modification. All polydopamine and heparin immobilization procedures, which are conducted in this work, are summarized visually in Figure 3.3. The post-modification procedures with polydopamine on hollow fiber membranes are depicted in Figure 3.3 A and are described in the following.

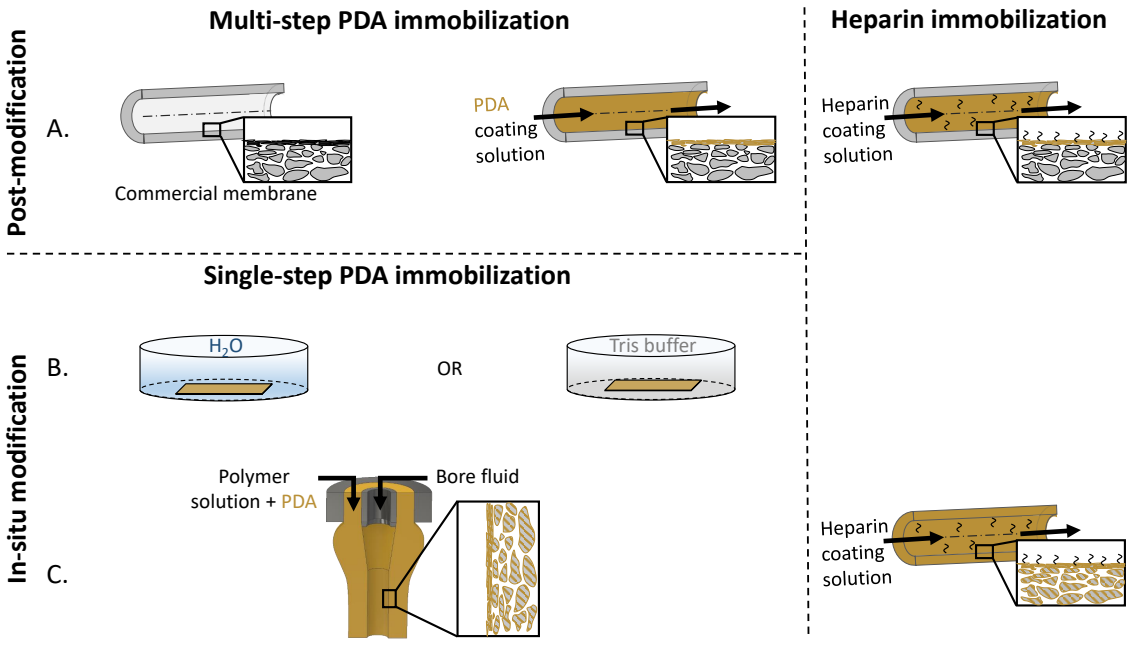

Figure 3.3: Scheme of post-modification and in-situ modification of membranes with polydopamine presented in this thesis.

The post-modification of hollow fiber membranes happens in module

configuration. Specifically, membrane modules from Baxter International Inc. with 177 or 355 fibers receive post-modification with polydopamine. These fibers have an inner diameter of 190 μm and a wall thickness of 35 μm. Figure 3.4a shows the coating procedure. First, the shell side of the module is filled with tris buffer, which is adjusted to pH 8.5 with HCl. The polydopamine coating solution contains 0.5 mg/mL dopamine dissolved in tris buffer at pH 8.5 rinses through the lumen of the fibers. Then, all ports of the module are closed, and the polymerization of polydopamine is carried out for 24 h in the filled membrane module (cf. Figure 3.4b). Finally, the lumen and the shell side are flushed three times with DI water.

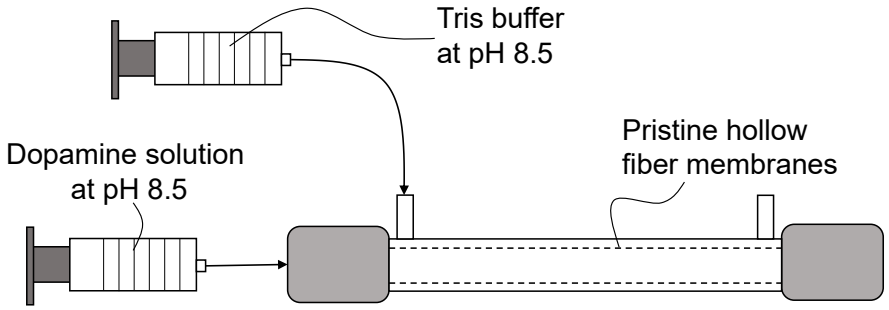

(a) Filling of buffer solution in shell side and dopamine solution in lumen channel with syringes.

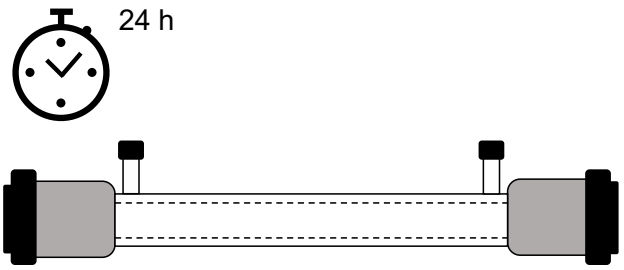

(b) Dopamine polymerization carried out for 24 *h* in closed membrane module.

Figure 3.4: Process of post-modification of hollow fiber membrane modules with dopamine on the lumen of the hollow fibers via alkaline polymerization carried out for 24 *h*.

In a subsequent step, heparin is immobilized on the polydopamine-coated dialysis hollow fiber membranes as stated in Section 2.3.

Table 3.2: Overview of post-modified commercial hollow fiber membranes (HF-PM) and heparin functionalization.

	polydopamine coating composition				
	Polydopamine concentration	Tris buffer	pH (adjusted with HCl)	Coating time	Heparin coating
	[mg/mL]	[mM]	[-]	[h]	[mg/mL]
HF-PM-D0$_L$	-	-	-	-	-
HF-PM-T+D0.5$_L$	0.5	10	8.5	24	-
HF-PM-T+D0.5$_L$-H	0.5	10	8.5	24	1

3.2.4 In-Situ Modification with Polydopamine

By superimposing the membrane fabrication with the polymerization of polydopamine, the modification is occurring in-situ. Polydopamine is included in different ways in the fabrication process, which is described in the following subsections.

Flat Sheet Membranes

Flat sheet membranes are fabricated out of polymer solutions P3.1, P3.2 and P3.6. The composition of the polymer solutions and the coagulation conditions of the flat sheet membranes are summarized in Tables 3.1 and 3.3. The flat sheet casting is conducted as stated in Section 2.2.2. Polymer films are coagulated either in pure DI water or tris buffer. The water bath is exchanged every 24 h. After 72 h, the flat sheet membranes are dried at room temperature.

Table 3.3: Overview of reference and in-situ functionalized flat sheet membranes.

	Polymer solution	Coagulation bath	
		DI water	Tris buffer (10mM)
FS-D0$_P$	P3.1	x	-
FS-D0$_P$-T$_C$	P3.1	-	x
FS-24h-D0.5$_P$	P3.2	x	-
FS-24h-D0.5$_P$-T$_C$	P3.2	-	x
FS-2h-D0.5$_P$	P3.6	x	-
FS-2h-D0.5$_P$-T$_C$	P3.6	-	x

Hollow Fiber Membranes

Polymer solutions P3.4 and P3.5 (cf. Table 3.1) are transformed into hollow fiber membranes. The bore solution is prepared 2 h before spinning and the compositions are summarized in Table 3.5. All spinning parameters are summarized in Table 3.4, and the resulting hollow fiber batches are listed in Table 3.5. A double orifice spinneret with a diameter of 0.4 mm for the bore and 1.12 mm for the polymer solution is used. The spinning of hollow fiber membranes is conducted as stated in Section 2.2.4. The spun

Table 3.4: Overview of spinning parameters of the in-situ modified hollow fiber membranes.

Parameter	Unit	Value
Polymer solution flow rate	g/min	6.8
Polymer solution temperature	°C	65
Bore solution flow rate	mL/min	5.5
Pulling speed	m/min	10.3
Air gap	cm	2
Coagulation bath temperature	°C	65

fibers are stored in DI water for 34 h before storing them for another 24 h in a 5 wt.% glycerol in DI water solution. Finally, the fibers are air-dried at room temperature overnight. Three different batches are presented in this chapter. Two of them, HF-CiS-D0.5$_P$ and HF-CiS-D0.5$_P$-T$_B$ based on the polymer solution P3.5 but are fabricated with different bore solutions, see Table 3.5.

Subsequently, modules of each fiber type (cf. Section 2.4.6) receive a heparin coating using the in Section 2.3 described immobilization technique. The samples are indicated by "-H" in Table 3.4.

Table 3.5: Overview of in-situ modified hollow fiber membranes (HF-CiS) and heparin functionalization.

Membrane type	Polymer solution	Bore solution			Heparin immobilization	
		NMP [50 wt.%]	H_2O [50 wt.%]	Tris buffer (10mM) [50 wt.%]	Concentration [mg/mL]	Time [h]
HF-CiS-D0$_P$	P4	x	x	-	-	
HF-CiS-D0$_P$-H	P4	x	x	-	1	24
HF-CiS-D0.5$_P$	P5	x	x	-	-	
HF-CiS-D0.5$_P$-H	P5	x	x	-	1	24
HF-CiS-D0.5$_P$-T$_B$	P5	x	-	x	-	
HF-CiS-D0.5$_P$-T$_B$-H	P5	x	-	x	1	24

3.2.5 Membrane Characterization

In addition to the characterization methods described in Section 2.4, further characterization methods relevant for this Chapter 3 are described below.

Thermogravimetric Analysis

For the detection of polydopamine, small membrane pieces of around 6 g are analyzed via thermogravimetric analysis (TGA) using a Simultaneous Thermal Analyzer STA 6000 (PerkinElmer, USA). Each membrane sample is heated in nitrogen from 30 °C to 650 °C with a heating rate of 10 °C/min. The results of the TGA measurement are analyzed using the software Pyris (PerkinElmer, USA). Excluding pure dopamine powder, two samples per membrane are examined with TGA.

Fourier Transform Infrared Spectroscopy

Fourier transform infrared spectroscopy (FTIR) spectra are recorded using a FT-IR Spectrum 3 (PerkinElmer, USA). Each membrane sample is tested under ATR mode. For each spectrum, four scans are averaged to enhance the signal-to-noise ratio.

Sieving Coefficient Measurement

Sieving coefficients are measured per the methodology stated in ISO8637 (cf. Figure 3.5) with a re-circulating fluid setup. Before testing, the filters are aspirated with a priming fluid (0.9 % NaCl), typically used for hemodialysis treatments, so no air remains in the circuit. As test solution, 1 L heparin anticoagulated bovine plasma with a total protein concentration of 60 $\pm$ 5 g/L is used. Albumin is already present in native plasma, so no additional dosing is necessary. In contrast, myoglobin is added at a concentration of 100 mg/L. The operating temperature of the solutions is 37 °C. To fill the circuit with plasma, a blood flow rate of 82 mL/min and filtration rate of 10 mL/min is set. The priming fluid is discarded so that the total protein concentration of the plasma remains in the range of 60 $\pm$ 5 g/L. Flow rates

are kept constant throughout the experiment, and the stability of pressure, temperature, and flow rates are verified.

For determination of the albumin sieving coefficient, samples are taken 15 minutes and for the myoglobin sieving coefficient 30 minutes after starting the plasma flow at the blood inlet port, the blood outlet port of the dialyzers and from the filtrate. The albumin concentration is measured with the bromocresol-green based photometric assay with test kit LtAB0103 (Lt Sys Labor und Technik, Berlin, Germany). The myoglobin concentration is measured photometrically at 405 and 450 nm.

Each sieving coefficient is calculated from the measured retention as follows:

$$\text{Sieving coefficient} = (1 - \text{Retention}) \tag{3.1}$$

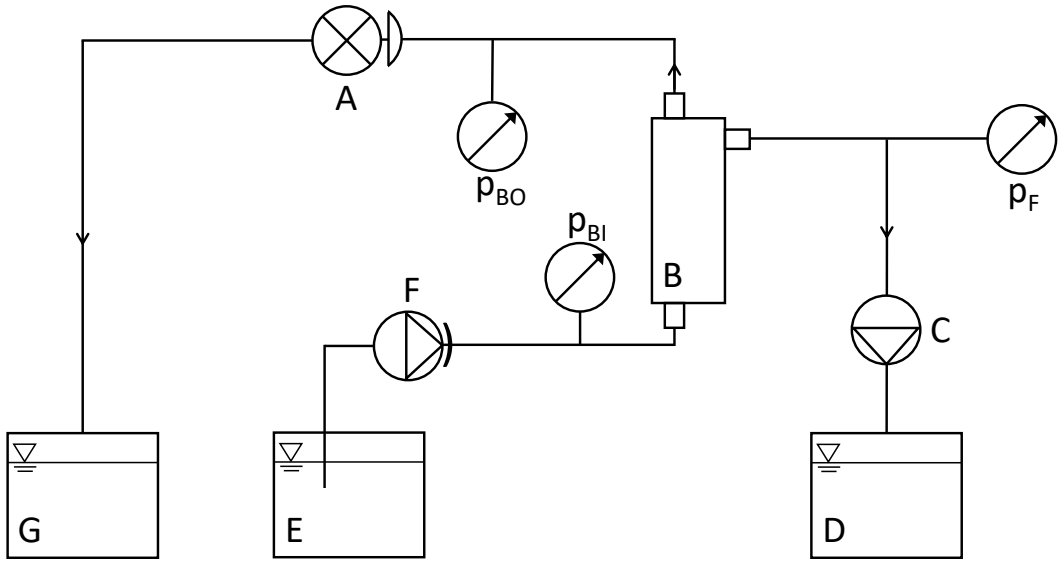

Figure 3.5: Set-up for measuring sieving coefficients as shown in ISO8637. A: pressure control; B: dialyzer; C: filtrate pump; D: filtrate; E: test solution reservoir; F: blood pump; G: waste; p_{BO}: blood pressure, out; p_{BI}: blood pressure, in; p_F: filtrate pressure.

3.3 Results and Discussion

The first part of this section focuses on the post-modification of commercial dialysis hollow fiber modules with subsequent heparin immobilization. The modules are characterized regarding their suitability for dialysis applications. In the second part, the findings of the laborious post-modification are transferred to the chemistry-in-a-spinneret technique in which dopamine is added directly to the polymer solution. Diverse analytical methods characterize the functionalized membranes regarding their composition, surface charge, morphology, and transport properties. Finally, the improved surface chemistry resulting from the polydopamine immobilization may offer possibilities for additional functionalization, such as heparin.

3.3.1 Post-Modification of Hollow Fiber Membranes with Polydopamine and Heparin

Commercial hollow fiber membrane modules supplied by Baxter International Inc. are coated. After 24 hours coating with dopamine, the hollow fiber membranes show a brownish discoloration. Not only the lumen side discolors, but also the shell side turns brownish. This color change suggests that polydopamine diffuses through the pores and coats the surface of the pores and the shell side as well. In contrast, the subsequent heparin coating does not lead to any optical changes of the membranes.

Figure 3.6 shows zeta potential measurements of a reference dialysis membrane module (HF-PM-D0$_L$), a dopamine functionalized module (HF-PM-T+D0.5$_L$), and a module post-treated with dopamine and subsequently with heparin (HF-PM-T+D0.5$_L$-H). HF-PM-D0$_L$ shows a negative zeta potential between pH 3 to 6. This course is typical for fibers fabricated with a PES polymer solution [Ma2014]. The immobilization of polydopamine results in an increase in surface charge of the membrane (cf. HF-PM-T+D0.5$_L$). From the literature, it is known that depending on the polydopamine layer thickness, a shift of the zeta potential can be observed. Li et al. showed a slightly increased surface charge after coating a mem-

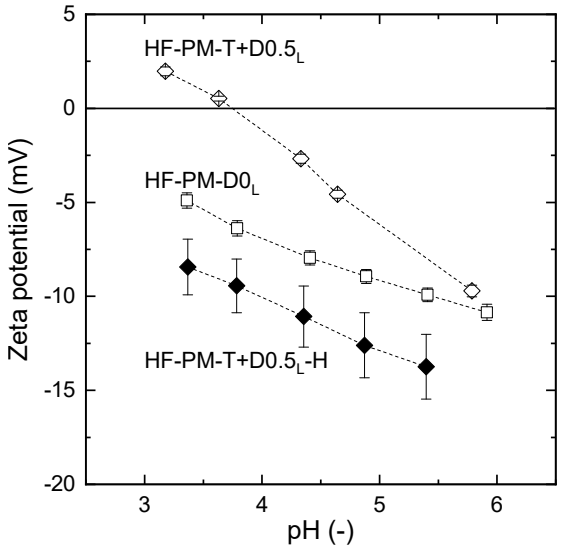

Figure 3.6: Zeta potential of commercial hollow fiber membranes that were coated with 0.5 g/L polydopamine and 1 g/L heparin. The error bars correspond to the standard deviation.

brane surface twice with polydopamine [Li2012]. Azari et al. [Azar2012], on the other hand, observed no change in surface charge and concluded that the polydopamine layer thickness is in the nanometer range. Therefore, it is assumed that the created polydopamine coating on the dialysis membranes has a significant thickness. The subsequent immobilization of heparin induces a shift to a negative surface charge (HF-PM-T+D0.5$_L$-H). This shift is expected since heparin is highly negatively charged due to its sulfate groups in the carbohydrate moiety [Chan2003]. Therefore, the change in the zeta potential after heparin coating proves the successful immobilization of heparin on the membrane. The results are in accordance with the literature. Luxbacher et al. measured zeta potential of approx. -18 mV at pH 5.5 for PES hollow fiber membranes with chemical grafted heparin [Luxb2012] and Ma et al. [Ma2014] showed surface zeta potentials of up to -31 mV due to the coating with heparin [Ma2014].

The plot in Figure 3.7 summarizes the measurement results of the pure water permeance (PWP) and the sieving coefficients of myoglobin as well as albumin at a physiological temperature of 37 °C for the membrane modules HF-PM-D0$_L$, HF-PM-T+D0.5$_L$, and HF-PM-T+D0.5$_L$-H. The reference membrane HF-PM-D0$_L$ has a PWP of around 300 LMH/bar. The sieving co-

efficients of myoglobin and albumin are at 87 % and 2.5 %. In comparison, the polydopamine coated fiber HF-PM-T+D0.5$_L$ features a higher PWP of around 350 LMH/bar. The additional coating with polydopamine further hydrophilizes the PES membrane surface and thus, results in an increased PWP. Similar behavior after a polydopamine coating has been observed by Miller et al. [Mill2017]. The polydopamine layer also influences the sieving coefficients. The sieving coefficient of myoglobin increases with the polydopamine coating to 93 % and the sieving coefficient of albumin increases to 3.5 %. After heparinization, the module HF-PM-T+D0.5$_L$-H shows an even higher PWP of around 420 LMH/bar. The improved hydrophilicity is assigned to the presence of heparin, which leads to the PWP difference. A higher PWP of polydopamine immobilized membranes modified with heparin was already reported by Ma et al. [Ma2014]. To be highlighted are the sieving coefficients of the module HF-PM-T+D0.5$_L$-H. The membrane module with polydopamine and heparin entirely removes myoglobin with a MW of around 17 kDa, while the sieving coefficient for albumin with a MW of around 66.4 kDa stays almost constant around 3.5 %. This translates into a steeper sieving curve resulting in a high molecular weight retention onset. In dialysis application, this allows also larger molecular weight toxins to pass the membrane to a significant extent.

The results show that our coating procedure functionalizes the membrane surface successfully and at the same time improves the PWP and sieving characteristics for dialysis applications, revealing high retention for albumin and better removal of myoglobin. Varying the base membrane for the coating offers the possibility to tailor the permeability and sieving coefficients further.

While only changing the membrane transport properties slightly, the proposed post-modification procedure is a novel way to prepare heparin coatings directly on commercial PES membranes aiming at improving dialysis treatment. Nevertheless, this multi-step modification is time and labor-intensive.

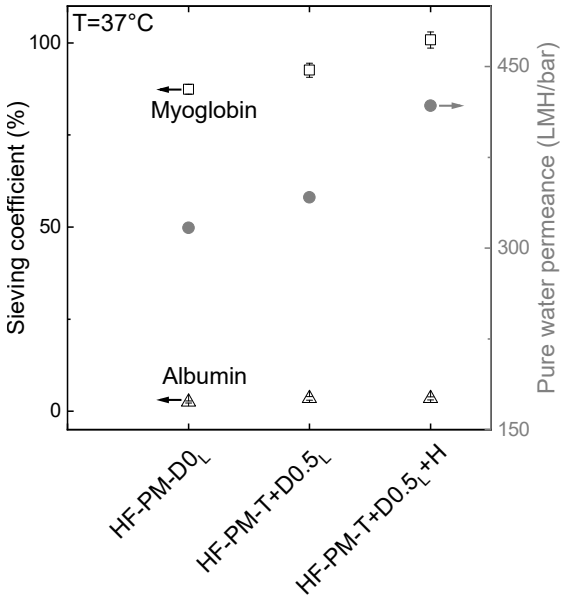

Figure 3.7: Sieving coefficient of myoglobin and albumin in water and pure water permeance at 37 °C of commercial hollow fiber membranes (HF-PM-D0$_L$) coated with 0.5 g/L polydopamine (HF-PM-T+D0.5$_L$) and 1 g/L heparin (HF-PM-T+D0.5$_L$-H).

3.3.2 In-Situ Modification of Membranes with Polydopamine

Combining membrane fabrication and dopamine polymerization in one process step offers the direct fabrication of functionalized flat sheet or hollow fiber membranes. In a single post-treatment step, heparin is then coated on the polydopamine functionalized surface of the membrane. The following sections present the proof-of-concept results and analysis of flat sheet membranes functionalized in-situ with dopamine. Hollow fiber spinning, including dopamine cross-linking and subsequent immobilization of heparin on the spun fibers, is then discussed.

In-Situ Modified Flat Sheet Membranes

Dry dopamine powder can function as an additive in the polymer solution. Polymer solutions with dopamine already begin to change their color during the formulation process indicating self-polymerization (see Figure 3.8. It starts triggered by UV light and present oxidants.

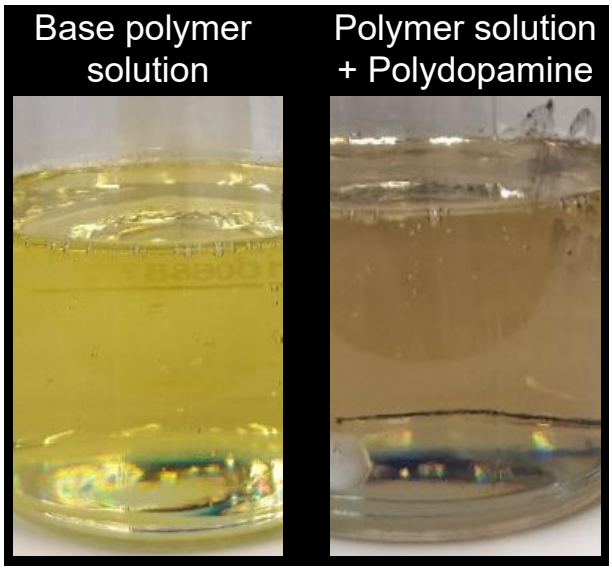

Figure 3.8: Polymer solutions of left: the base polymer solution (PES/NMP) and right: the base polymer solution with polydopamine.

Flat sheet membranes out of a polymer solution containing only PES dissolved in NMP (polymer solution P1) are compared to flat sheet membranes with 0.5 wt.% dopamine in the polymer solution (P2 and P6). Each polymer solution is precipitated in both, water and tris buffer at pH 8.5 (cf. Table 3.3).

TGA provides the amount of incorporated polydopamine into the flat sheet membranes. The plot in Figure 3.9 and the data in Table 3.6 show the results of the TGA measurements. Pure dopamine powder shows a weight loss of -68.0 % between 260 °C and 650 °C. Coagulated membranes out of PES without additives lose an average of -55.9 % of their weight in the same temperature range. The measurements of membranes containing dopamine precipitated in water show a minorly lower weight loss. FS-2h-D0.5$_P$-H_2O_C and FS-24h-D0.5$_P$-H_2O_C have weight losses of -56.1 % and -56.3 %. In contrast, a decreased mass loss is observed for the membranes precipitated in alkaline tris buffer with -53.9 % for FS-2h-D0.5$_P$-T_C and -54.8 % for FS-24h-D0.5$_P$-T_C.

Cross-linking of dopamine increases its temperature stability, and polydopamine is even more temperature stable than pure PES [Buch2017]. Therefore, the decreased weight loss of the membranes fabricated with

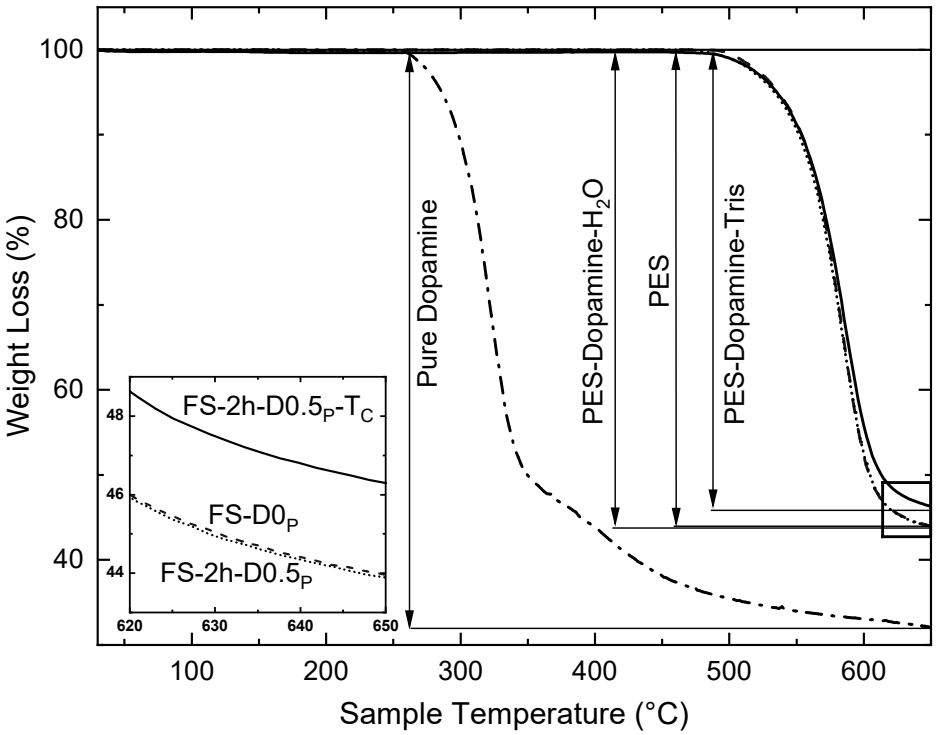

Figure 3.9: Thermogravimetric analysis of the first measurement of pure dopamine (dash dot), PES membrane (FS-D0$_P$ (dash)), PES-Dopamine-H_2O membrane (FS-2h-D0.5$_P$ (dot)) and PES-Dopamine-Tris membrane (FS-2h-D0.5$_P$-T$_C$ (solid)). Arrows indicating average mass loss as shown in Table 3.6.

Table 3.6: Results of TGA measurement of pure dopamine and different PES and polydopamine flat sheet membranes.

Membrane division	Averaged weight loss (%)	Membrane	Weight loss (%)	Measurement	Weight loss (%)
Pure dopamine	-68.0	Dopamine powder	-68.0	1.	-68.0
PES	-55.9	FS-D0$_P$	-56.0	1.	-56.3
				2.	-55.7
		FS-D0$_P$-T$_C$	-55.7	1.	-55.2
				2.	-56.1
PES-Dopamine-H_2O	-56.2	FS-2h-D0.5$_P$	-56.1	1.	-56.6
				2.	-55.6
		FS-24h-D0.5$_P$	-56.3	1.	-54.7
				2.	-57.7
PES-Dopamine-Tris	-54.4	FS-2h-D0.5$_P$-T$_C$	-53.9	1.	-51.2
				2.	-55.0
		FS-24h-D0.5$_P$-T$_C$	-54.8	1.	-54.6
				2.	-55.0

dopamine in the polymer solution and coagulated in tris buffer indicates the successful polydopamine immobilization. Even though the differences in weight loss and, therefore, the amounts of immobilized polydopamine are small, Bucher et al. [Buch2017] showed comparable changes after polydopamine coating of PES membranes. The membranes discussed here evolve from the polymer solutions P2 and P6 (cf. Table 3.1) and can therefore contain a theoretical maximum amount of 2.2 wt.% and 3.4 wt.% polydopamine in the created membrane samples. Dopamine seems to be washed out during the coagulation process in all cases because the changes in mass loss are below the theoretically present polydopamine amounts. However, some cross-linked and not cross-linked dopamine might be trapped in the porous structure as the weight losses cancel out. Nevertheless, the lower mass losses for the membranes precipitated in alkaline tris buffer is addressed to the successfully immobilize cross-linked polydopamine within the membrane structure and on its surface.

Figure 3.10 shows FTIR spectra of the pure PES membrane (FS-D0$_P$) and the polydopamine flat sheet membranes FS-2h-D0.5$_P$ and FS-2h-D-0.5$_P$-T$_C$. The FTIR spectrum of FS-D0$_P$ depicts a typical course of PES surfaces [Li2014]. The in-situ polydopamine immobilization changes the strength of the measured vibrations, but only slightly changes the curve of the FTIR spectrum. One small band between 1730-1770 cm^{-1} (circled) is in correspondence to the N-H deformation vibration and is an indicator for immobilized polydopamine. Furthermore, the peaks of FS-2h-D0.5$_P$-T$_C$ become much weaker compared to FS-D0$_P$. It seems as the higher the polydopamine content in the polymer structure, the flatter is the course of the spectrum.

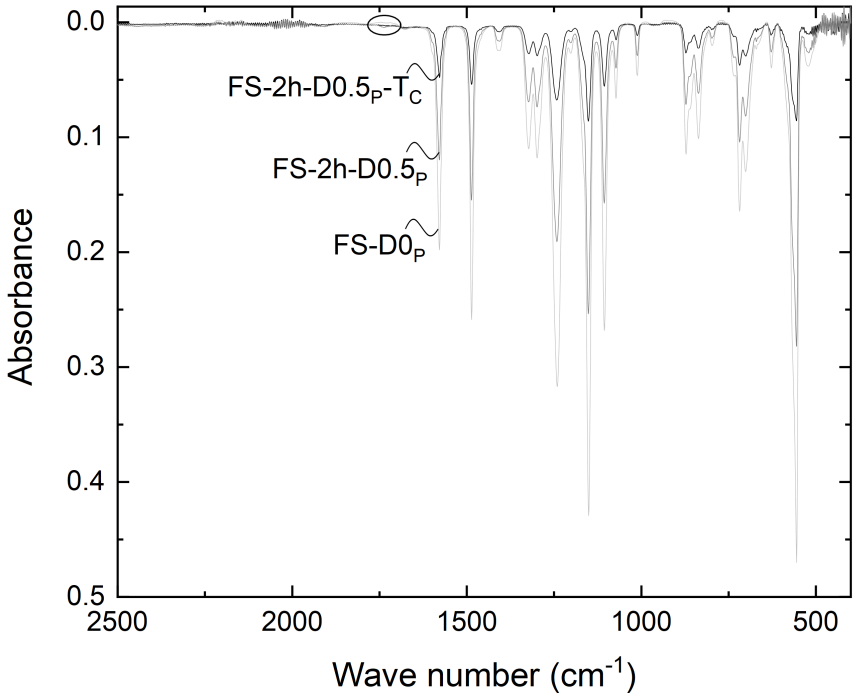

Figure 3.10: FTIR spectra of pure PES membrane FS-D0$_P$ and the in-situ modified flat sheet membranes FS-2h-D0.5$_P$ and FS-2h-D0.5$_P$-T$_C$.

To further verify the presence of in-situ immobilized polydopamine, Table 3.7 demonstrates the elemental composition of the membrane surfaces measured by XPS. Nitrogen content indicates the presence of polydopamine. The membranes with in-situ immobilized polydopamine contain 3.9 % nitrogen after coagulation in DI water (FS-2h-D0.5$_P$) and 6.6 % nitrogen after coagulation in an alkaline coagulation bath (FS-2h-D0.5$_P$-T$_C$). This indicates the deposition of polydopamine on the membrane surface. The value for the nitrogen to carbon ratio is around 0.125 for pure polydopamine [Lee2007]. Lee et al. [Lee2007] showed successful polydopamine coatings with values between 0.10 and 0.13 . The nitrogen to carbon ratio of FS-2h-D0.5$_P$ is 0.07 . In contrast, a ratio of 0.11 is obtained for the sample FS-2h-D0.5$_P$-T$_C$. This is a clear proof that polydopamine is present on the membrane surface by in-situ modification. The pure PES membranes (FS-D0$_P$) on the other hand shows an amount of 2.0 % nitrogen, which is accounted to a low residue of the nitrogen containing solvent NMP.

Table 3.7: Elemental composition of the membrane surface of flat sheet membranes with and without in-situ modified polydopamine coagulated in different bathes measured with XPS.

Element or ratio	Unit	FS-D0$_P$	FS-2h-D0.5$_P$	FS-2h-D0.5$_P$-T$_C$
O	%	23.8	26.1	28.7
N	%	2.0	3.9	6.6
C	%	62.9	60.7	58.3
S	%	11.4	9.3	6.4
N/C	-	0.03	0.07	0.11

Summing up, the brownish appearance of the polymer solution with polydopamine, the TGA, FTIR, and XPS analysis prove the successful in-situ functionalization with polydopamine. In the following, the promising results of the in-situ modification technique are transferred to hollow fiber spinning.

In-Situ Modification of Hollow Fiber Membranes

Three fiber batches, including reference fibers and functionalized fibers, are presented. Additionally, membrane modules containing the fibers received a post-modification with heparin.

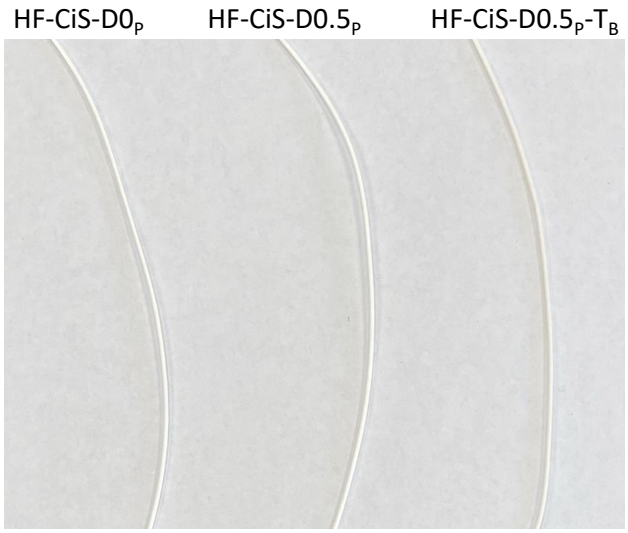

Figure 3.11: Photography of the fibers HF-CiS-D0$_P$, HF-CiS-D0.5$_P$ and HF-CiS-D0.5$_P$-T$_B$ from left to right.

Figure 3.11 shows a photo of the reference fiber HF-CiS-D0$_P$ and the

functionalized fibers HF-CiS-D0.5$_P$ and HF-CiS-D0.5$_P$-T$_B$. These single fibers do not differ significantly in color even though 0.5 wt.% polydopamine was present in the polymer solution of HF-CiS-D0.5$_P$ and HF-CiS-D0.5$_P$-T$_B$. Only a slight brownish discoloration of HF-CiS-D0.5$_P$-T$_B$ suggests the polydopamine in the membrane structure.

FESEM images of the fibers show their morphology. HF-CiS-D0$_P$ and HF-CiS-D0.5$_P$ have an inner diameter of 0.4 mm with a wall thickness of 0.06 mm (cf. Figure 3.12 a) and d)). The walls of the fibers are open porous, and the lumen sides show a skin (cf. Figure 3.12 c) and f), b) and e)). This fits our expectations as the spinning parameters of both fiber batches are the same, and only the composition of the polymer solutions differs. Merely, the surface of the lumen channel of HF-CiS-D0$_P$ appears to be slightly rougher than HF-CiS-D0.5$_P$.

The influence of the polydopamine and heparin on the fiber's surface charge is examined via zeta potential measurements (cf. Figure 3.13). The zeta potential of HF-CiS-D0$_P$ is negatively charged between pH 3 and 6. The addition of polydopamine to the polymer solution spun with a bore solution containing water induces no change in the zeta potential. This means no or only small amounts of polydopamine or dopamine are present on the membrane surface, or the functionalization may not be continuous (cf. Figure 3.13 (a)) [Sagl2009]. However, after heparin coating, a difference in charge can be observed. The higher the charge difference of the membrane surface, the more heparin is present on the surface. Even if there is no charge difference between HF-CiS-D0$_P$ and HF-CiS-D0.5$_P$, the dopamine present in the polymer solution seems to affect the binding of heparin positively. Azari et al. [Azar2012] also did not observe a change of surface charge after polydopamine coating but noted effects of polydopamine in further experiments. For the HF-CiS-D0$_P$ fiber, heparin adsorbs non-specific on the membrane surface.

The presence of tris buffer in the bore solution leads to a different zeta potential course. Between pH 3 and 6, the drop of zeta potential is significantly stronger. Contrary to the expectation, the zeta potential is not shifted towards a positive zeta potential as observed for the polydopamine

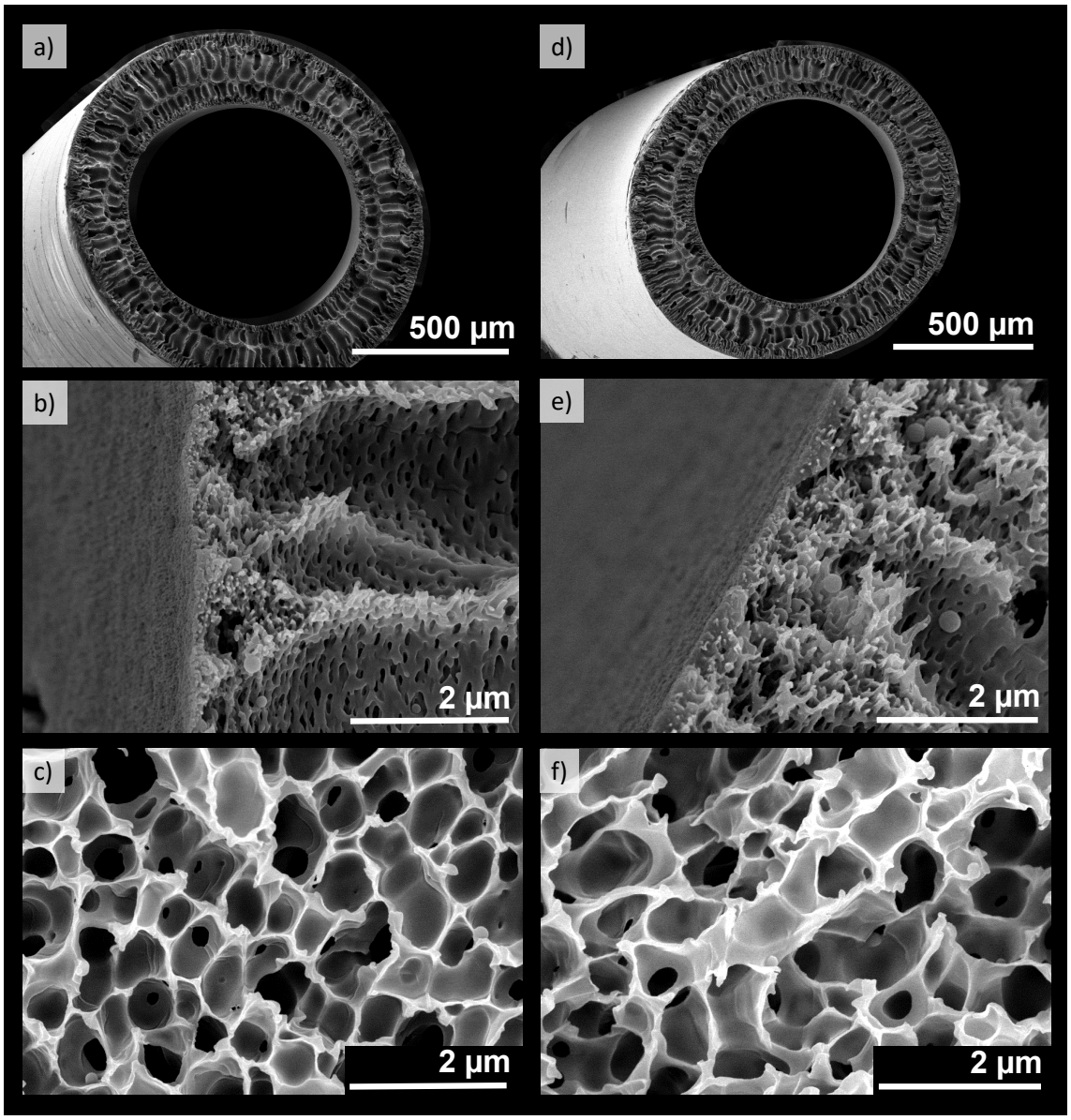

Figure 3.12: Morphology of a)-c) HF-CiS-D0$_P$, d)-f) HF-CiS-D0.5$_P$ fibers: a)+d) cross-section; b)+e) lumen channel of enlarged cross-section; c)+f) pore structure of enlarged cross-section.

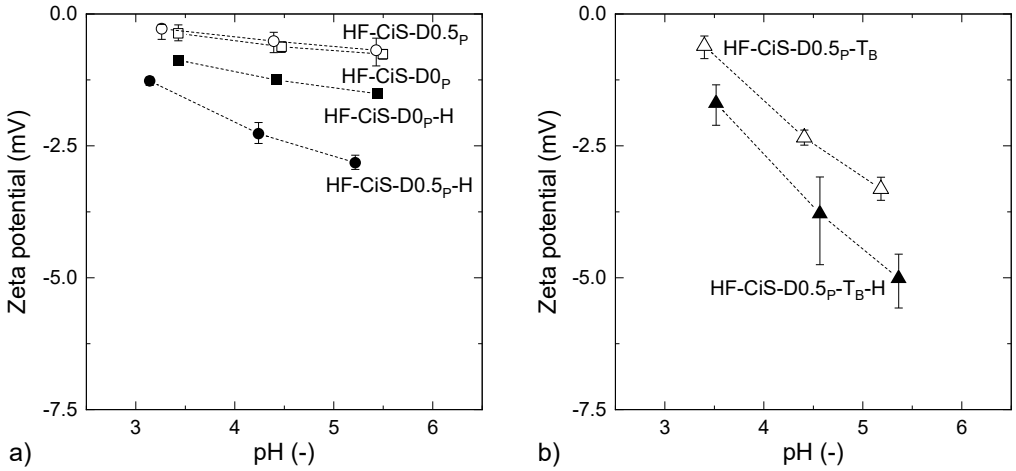

Figure 3.13: Zeta potential measurements for a) HF-CiS-D0$_P$ and HF-CiS-D0.5$_P$ and b) HF-CiS-D0.5$_P$-T$_B$ fibers, all fibers coated with and without heparin.

post-modified commercial dialysis fibers. A difference in zeta potential can also originate from a change in surface morphology, which may result from different phase inversion conditions. Again, the binding of heparin shows a slight change in surface charge towards the negative region, suggesting that heparin has bound on the membrane surface. Concluding, both dopamine and polydopamine in the porous membrane enhance the immobilization of heparin, while due to alkaline conditions, the cross-linking of polydopamine on the surface increases.

Figure 3.14 illustrates the results of pure water permeance (PWP) and molecular weight cut-off (MWCO) measurements of membrane modules with HF-CiS-D0$_P$, HF-CiS-D0.5$_P$, and HF-CiS-D0.5$_P$-T$_B$ fibers, each with and without immobilized heparin. The presented membrane batches have a PWP in a range of 6 to 31 LMH/bar. The MWCO results of the spun fibers are in a range of around 6 to 11 kDa. Overall, the dopamine in the polymer solution only slightly influences the membrane transport properties as all PWP and MWCO results are in a similar range. However, the presence of dopamine and tris buffer at the same time for the fiber HF-CiS-D0.5$_P$-T$_B$ causes a higher MWCO and PWP. Additionally, for the fibers containing dopamine, the PWP increases or stays constant after heparin coating indicating successful immobilization. Compared to the post-modified hollow fiber modules, the in-situ polydopamine functionalization is thinner and

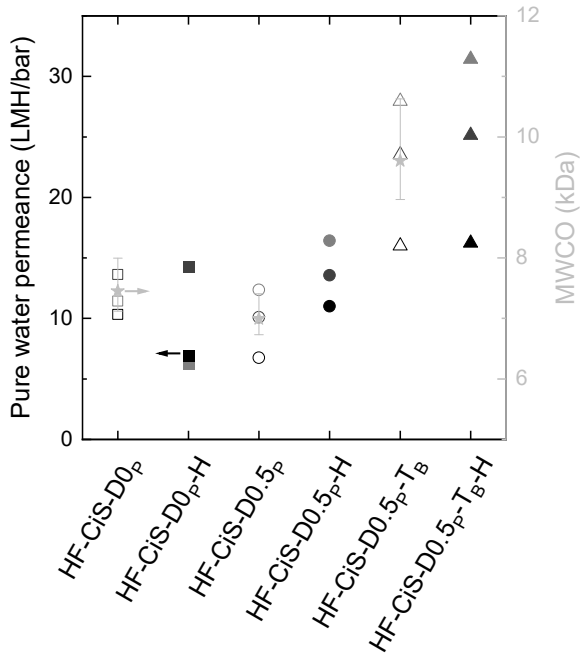

Figure 3.14: Pure water permeance (PWP) of three membrane modules of HF-CiS-D0$_P$, HF-CiS-D0.5$_P$ and HF-CiS-D0.5$_P$-T$_B$ fibers with and without immobilized heparin. Averaged molecular weight cut-off of HF-CiS-D0$_P$, HF-CiS-D0.5$_P$ and HF-CiS-D0.5$_P$-T$_B$.

might be less continuous, which results in a lower influence on PWP.

Overall, the PWP and MWCO of the presented membrane batches are significantly lower compared to the commercial hollow fiber dialysis membranes (cf. Figure 3.7). These characteristics can be tuned by adjusting the polymer solution formulation and spinning parameters during membrane fabrication. To sum up, the in-situ modification with polydopamine represents a promising approach for eliminating costly and time-consuming post-treatment processes in membrane fabrication. Further work needs to focus on the amount of polydopamine in the polymer solution, tuning the membrane transport properties, and the stability of polydopamine and heparin in the membrane structure. A stable heparin functionalized membrane is essential for use as a dialysis membrane.

3.4 Conclusion

By using the chemistry-in-a-spinneret approach, polydopamine functionalized membranes are produced in a single step during membrane fabrication. By adding dopamine into the polymer solution and coagulating it in alkaline conditions, the modified membranes evolved and offered to be heparinized subsequently.

As a reference system, commercial dialysis hollow fiber membranes are post-modified with polydopamine. The effective post-modification of dialysis membrane modules with polydopamine and heparin is proven and analyzed by determining zeta potential, pure water permeance, and sieving coefficients of albumin and myoglobin measurements. To be highlighted is that the coated commercial dialysis hollow fiber membranes maintain their selectivities for proteins present in human blood while the pure water permeance increases. However, the post-modification procedure involves multiple steps that need to be conducted on the hollow fibers potted in membrane modules.

To simplify and accelerate the fabrication of polydopamine functionalized membranes, the chemistry-in-a-spinneret technique superimposes cross-linking of polydopamine and the phase inversion process. Therefore, dopamine is blended into the polymer solution. The cross-linking of dopamine is induced by contacting the polymer solution with an aqueous tris buffer solution at a pH of 8.5. Alkaline conditions are essential for the successful detection of cross-linked polydopamine on the membrane surface. The polydopamine polymer solution shows an intensive discoloration. The resulting flat sheet membranes contain a significant amount of nitrogen indicating the presence of polydopamine. The flat sheet membrane formation conditions are further transferred to the fabrication of in-situ modified hollow fiber membranes via inducing alkaline conditions through the bore solution. Polydopamine functionalized hollow fiber membranes subsequently coated with heparin exhibit a lower zeta potential proving the successful heparin immobilization.

The in-situ polydopamine-functionalized hollow fiber membranes show

highly promising characteristics for an application in the field of hemodialysis. For further development towards dialysis membranes, formulation and spinning parameters need to be tuned to accomplish typical dialysis hollow fiber membrane characteristics regarding permeance and molecular weight cut-off. Additionally, heparin immobilization will be studied in detail with blood tests in the future. Once again, the chemistry-in-a-spinneret approach proves to be a universally applicable technology base for unique novel flat sheet or hollow fiber membrane structures.

4 A Dopamine Alternative to Immobilize Heparin

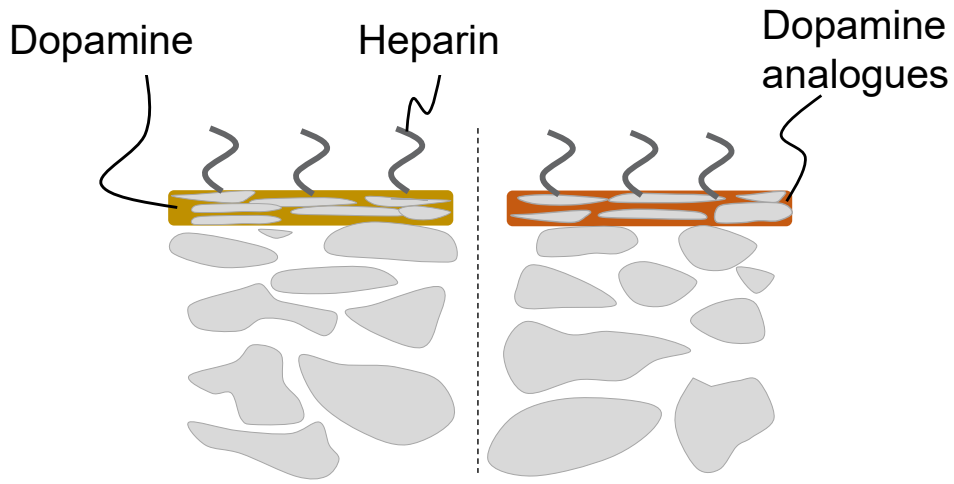

Parts of this chapter are in preparation for publication:
I.I. Rose, M. Kather, H. Roth, J. Hommes, M. Wessling, "A Dopamine Alternative to Immobilize Heparin", *Journal of Membrane Science*

4.1 Introduction

This chapter investigates a cheaper alternative to dopamine, respectively self-polymerized polydopamine, for heparin immobilization on polyethersulfone membranes. As mentioned in Chapter 3, dopamine is an all-around talent that can be used in various applications for surface modification of almost any surface. Furthermore, its simple synthesis by polymerization of dopamine and its impressive coating and adhesive properties have led to its widespread use, for example, in energy, environmental, and medical engineering [Gao2014]. Especially, the possibility to immobilize heparin on polydopamine functionalized surfaces opens the use in hemodialysis [Gao2014]; [Jian2010]; [Kale2021]. However, in view of the large amounts of dialyzers to be coated, coating with dopamine is cost-intensive. Therefore, cost-effective alternatives for dopamine surface modification are needed. There are already alternatives allowing large-scale application, for example, the dopamine analogues catechol and polyamine or catechol and propylamine [Wang2014a]; [Hu2016]; [Sile2013]. Their amine and catechol groups are important for surface modification. Lee et al. [Lee2007] showed that amine and catechol groups are responsible for the oxidative polymerization of dopamine to form strong adhesion. Their research shows that molecules with amine and catechol groups might have a similar adhesive ability as dopamine and can thus be used as dopamine analogues. [Lee2007]; [Wang2014a]

Furthermore, dopamine analogues improve the surface properties, such as hydrophilicity. Wang et al. [Wang2014a] used catechol and polyamine as dopamine analogues to hydrophilizing a polypropylene separator without changing the pore structure and mechanical properties of this separator. Hu et al. [Hu2016] also polymerized catechol and amine groups under similar conditions to that of dopamine polymerization. As dopamine analogues they used catechol and propylamine. Figure 4.1 shows the possible reaction of catechol and propylamine under alkaline conditions, which is similar to that of dopamine (cf. Figure 3.1). The resulting polymerized dopamine analogues exhibit good coating and adhesive properties. [Hu2016]

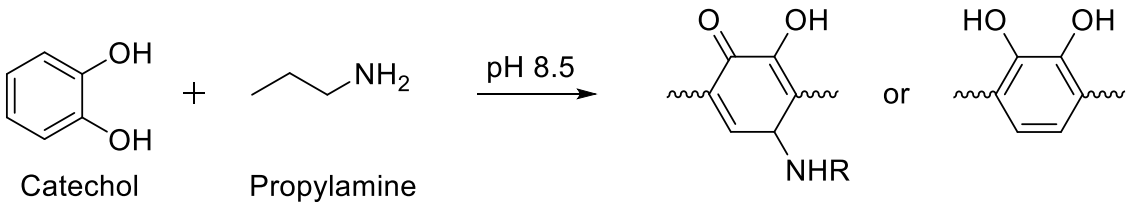

Figure 4.1: Reaction of catechol and propylamine at pH 8.5 (adapted from Hu et al. [Hu2016]).

Moreover, and as discussed in Chapter 3, polydopamine allows the heparin immobilization of the surface. Chapter 4 aims to clarify whether the dopamine analogues, catechol and propylamine, change membrane properties similarly to dopamine. Furthermore, it is investigated whether this functionalization allows subsequent heparin immobilization and, thus, use in hemodialysis. First, the toxicity of both the dopamine and dopamine analogues coated on microtiter plates for cell cultivation are presented in order to avoid a toxic effect on the blood during subsequent use. Then, the dopamine analogues are coated onto a porous flat sheet membrane and compared with equimolar dopamine coated membranes. Subsequently, both membranes are functionalized with heparin and characterized. Finally, the coating procedures are transferred onto hollow fiber membranes.

4.2 Experimental

4.2.1 Materials

In addition to the materials described in Section 2.1, the following materials are used.

For coating, catechol and propylamine with a purity above 99 % are purchased from Sigma Aldrich. The cell culture tests are prepared with L929 mouse-derived fibroblasts (ATCC®; USA), RPMI 1640+ (L)-glutamine medium (Gibco; USA) supplemented with a 10 % fetal bovine serum (Biowest; France), XTT assay kit (ATCC®; USA), and phosphate buffered saline (PBS) (6MB014, Lonza; Switzerland). For factor Xa measurements, the heparin test kit COATEST®Heparin is purchased from Chromogenix. For FeSEM images,

three four-end mini-modules of Revaclear membranes from Baxter International Inc. containing 355 PES/PVP fibers are used.

4.2.2 Membrane Fabrication

Flat sheet and hollow fiber membranes are fabricated to investigate post-modification with dopamine and dopamine analogues. Table 4.1 and 4.2 show the compositions of the polymer solutions for flat sheet and hollow fiber membrane fabrication, respectively. The polymer preparation follows the same technique as described in Section 2.2.1.

Table 4.1: Compositions of polymer solutions for flat sheet casting.

	PES [wt.%]	PVP k30 [wt.%]	PVP k85 [wt.%]	DI water [wt.%]	NMP [wt.%]
FS-PES	14	-	-	3	83

Table 4.2: Compositions of polymer solution for hollow fiber membrane spinning.

	PES [wt.%]	PVP k30 [wt.%]	PVP k85 [wt.%]	DI water [wt.%]	NMP [wt.%]
HF-PES	14	5	2	3	76

For flat sheet membranes, the FS-PES polymer solution is cast as stated in Section 2.2.2. Before further membrane treatment or characterization, membranes are boiled at 80 °C for 2 h in DI water to remove any NMP residues.

The polymer solution HF-PES is used for hollow fiber membrane fabrication by applying the spinning parameters summarized in Table 4.3. The bore solution consists of 80 wt.% DI water and 20 wt.% NMP and prepared at least 2 h before spinning. A double orifice spinneret with a diameter of 1.12 mm for the polymer solution and 0.4 mm for the bore solution is used. The fibers are spun as stated in Section 2.2.4.

Table 4.3: Overview of spinning parameters of hollow fiber membrane HF-PES.

Parameter	Unit	Value
Polymer solution flow rate	g/min	6.8
Polymer solution temperature	°C	60
Bore solution flow rate	mL/min	5.5
Pulling speed	m/min	10.3
Air gap	cm	2
Coagulation bath temperature	°C	60

4.2.3 Preparation of Coating Solutions

Four different solutions (CS1-4) are used as coating solution for surface functionalization (cf. Table 4.4). The solutions are prepared shortly before starting the coating procedure to synchronize the polymerization of dopamine and dopamine analogues, and the coating of the membrane surface. The tris buffer solution (CS-2) contains 10 mM tris buffer adjusted to a pH of 8.5 with HCl. CS-3 is based on CS-2 with the addition of 0.5 mg/mL dopamine. CS-4 is also based on the solution CS-2 with the addition of 0.29 mg/mL catechol and 0.16 mg/mL propylamine.

Table 4.4: Compositions of the coating solutions CS-1 to CS-4.

	DI water	Tris buffer (pH 8.5)	Dopamine [mg/mL]	Catechol [mg/mL]	Propylamine [mg/mL]
CS-1	x	-	-	-	-
CS-2	-	x	-	-	-
CS-3	-	x	0.50	-	-
CS-4	-	x	-	0.29	0.16

4.3 Surface Coatings

Three different surfaces are coated with varying solutions of coating. Some surfaces are subsequently coated with heparin as explained in Section 2.3.

Coating of Microtiter Plates

For toxicity tests, cell culture measurements are prepared on a 96-well plate system. Four wells each are filled with a coating solution. The coating solution used is DI water (CS-1), tris buffer (CS-2), dopamine (CS-3), and dopamine analogues (CS-4) (cf. Table 4.4). Each well is filled with 100 μL of the respective coating solution and stored for 24 h at room temperature. Then, the coating solution is removed and washed with 200 μL PBS.

Coating of Flat Sheet Membranes

For surface characterization such as fouling behavior, flat sheet membranes (FS-PES) are coated with different coating solutions (CS-1, CS-3, and CS-4) as listed in Table 4.5. Flat sheet membrane pieces are immersed in the coating solution for 24 h (see Figure 4.2) and rinsed three times with DI water afterward. Finally, the membrane pieces are dried at room temperature.

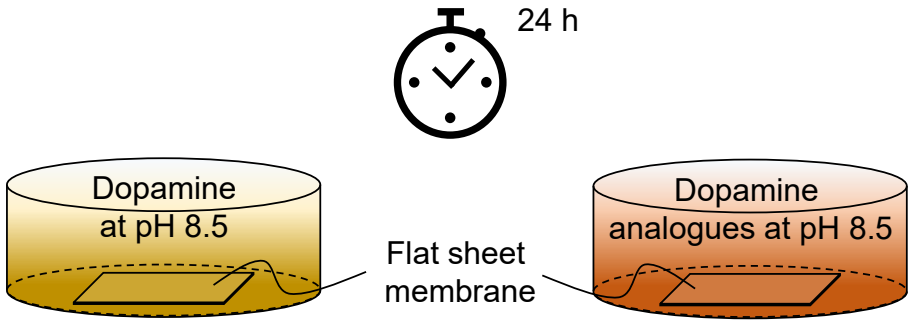

Figure 4.2: Coating procedure of the flat sheet membrane FS-PES with dopamine (left) or with dopamine analogues (right) via alkaline polymerization carried out for 24 h.

Coating of Hollow Fiber Membranes

For further membrane characterization such as permeability or selectivity, membrane modules containing spun hollow fiber membrane (HF-PES) are functionalized with dopamine and dopamine analogues by coating the lumen side of the hollow fibers. The coating procedure of hollow fiber membranes happens in module configuration. HF-PES is filled on the shell and

the lumen side with DI water. For both other membranes (HF-D and HF-DA), first, the shell side of the module is filled with tris buffer at pH 8.5 (see Figure 4.3). Subsequently, the coating solution rinses through the lumen of the fibers. Then, all ports of the module are closed, and the polymerization of dopamine or dopamine analogues is carried out for 24 h in the filled membrane module. Finally, the lumen and the shell side are flushed three times with DI water.

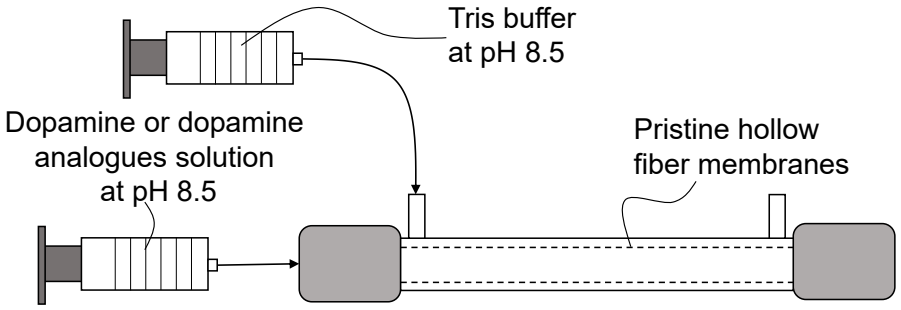

(a) Filling of buffer solution in shell side and dopamine or dopamine analogues solution in lumen channel with syringes.

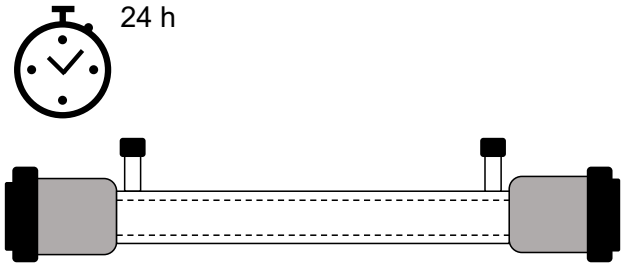

(b) Polymerization carried out for 24 h in closed membrane module.

Figure 4.3: Coating procedure of hollow fiber membrane (HF-PES) modules with dopamine or dopamine analogues on the lumen of the hollow fibers via alkaline polymerization carried out for 24 h.

4.3.1 Surface Characterization

In addition to the characterization methods described in Section 2.4, further characterization methods relevant for this chapter are described below.

Table 4.5: Membrane types and coatings.

Sample	Membrane type	Coating solution
Blank	-	CS-1
Tris	-	CS-2
D	-	CS-3
DA	-	CS-4
FS-PES	Flat sheet	CS-1
FS-D	Flat sheet	CS-3
FS-DA	Flat sheet	CS-4
HF-PES	Hollow fiber	CS-1
HF-D	Hollow fiber	CS-3
HF-DA	Hollow fiber	CS-4

Cell Culture Measurements as Toxicity Tests

L929 mouse cells with a concentration of 10^5 cells/mL are cultivated in RPMI 1640 medium with 10 % fetal bovine serum (FBS) at 37 °C and 5 % CO_2 saturation for two days each coating. The microtiter plate is placed on an Axiovert 100A microskope of Carl Zeiss AG to verify the cultivation of the cells. With an 2,3-Bis-(2-Methoxy-4-Nitro-5-Sulfophenyl)-2H-Tetrazolium-5-Carboxanilide (XTT) assay kit, the cell proliferation are measured. Therefore, 50 μL of the activated XTT solution (0.1 mL activation reagent and 5.0 mL XTT reagent) is added to each well. The plate is returned to the incubator for 2 h and afterward shaken for 1 min at 30 rpm before the color changes are measured using a plate reader (Synergy HT, BioTek Instruments; USA). The measurement is performed at 475 nm and 630 nm. The specific absorbance is calculated according to equation 4.1.

$$\text{Specific Absorbance} = A_{475nm}(\text{sample}) - A_{475nm}(\text{blank}) - A_{660nm}(\text{sample}) \tag{4.1}$$

To determine the cell concentration, a concentration line is required. Therefore, cells were prepared as described in Figure 4.4 in a 96-well plate. In the first well 200 μL of cell suspension with a concentration of 10^4 cells/cm^2 is added. Subsequently, 100 μL is transferred to the next well where 100 μL medium was represented. By this, the cells are diluted at a factor of 2 .

In another well, the medium is added as a blank. The whole approach is performed in triplicates for statistical reasons.

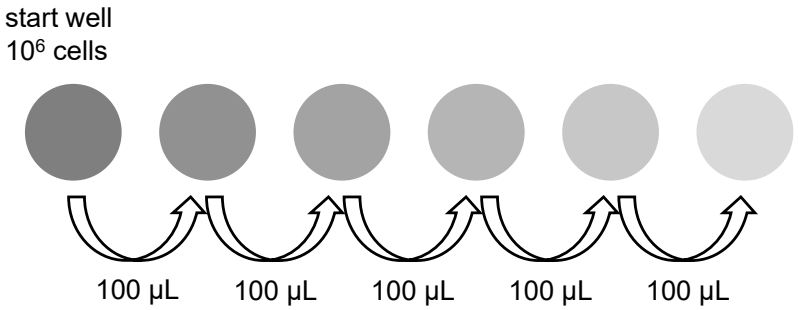

Figure 4.4: Serial dilution of cell suspension in a 96-well plate.

Detection of Immobilized Heparin

To detect immobilized heparin onto flat sheet membranes, a factor Xa test is used. The factor Xa test is performed for the photometric determination of heparin in plasma by using a heparin test kit. First, the supplied reagents are prepared. S-2222 is dissolved in 20 mL DI water to obtain a 1 mM solution. Both factor Xa and anti-thrombin are diluted in 10 mL DI water each. Normal human plasma is dissolved in 1 mL. In addition, the stock solution of the test kit is diluted from 1 to 9 to form the buffer working solution. Furthermore, a 0.9 % NaCl solution, a test plasma consisting of 100 μL test plasma solution, 100 μL anti-thrombin solution, 800 μL buffer working solution, and a heparin standard solution with 10 IU/mL are prepared.

For the calibration curve, 0.1 IU/mL, 0.3 IU/mL, 0.5 IU/mL and 0.7 IU/mL heparin solution are measured.

The measurement is carried out in 24-well plates. Flat sheet membrane samples with a diameter of 1 cm and different coatings are placed in one well each. The reagents in Table 4.6 are added to the well in the order shown, and maintained until the corresponding incubation time is over (cf. Figure 4.5). Next, acetic acid is added to stop the reaction. The samples are then immediately measured in a UV-Vis spectrometer at 405 nm.

Table 4.6: Test procedure for the factor Xa measurement.

Substance	Amount for each sample [μL]	Amount for the blank [μL]
Test plasma	200	200
Factor Xa	100	-
S-222	200	-
Acetic acid	300	-
DI water	-	300

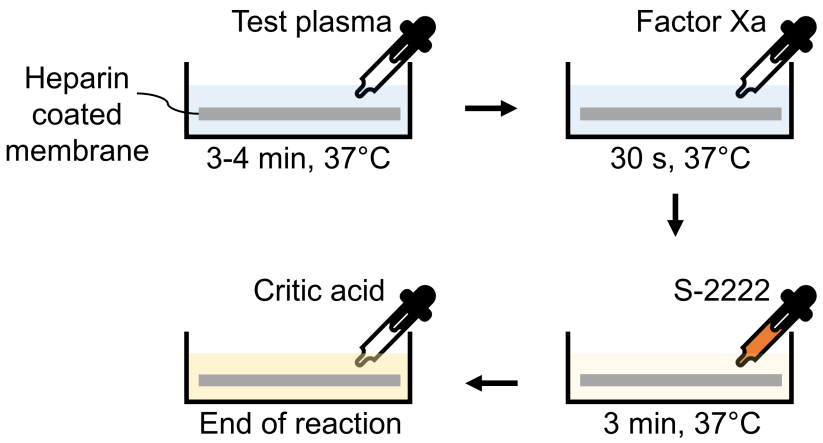

Figure 4.5: Preparation procedure to measure the heparin concentration on the membrane surface during factor Xa measurements.

4.4 Results and Discussion

Particularly with regard to medical applications, it is important, among other things, that coatings are not toxic. Therefore, cell culture tests on microtiter plates are carried out to provide information about possible toxicity of dopamine or dopamine analogues. Afterwards, flat sheet membranes are coated with both dopamine and dopamine analogues to characterize the influences of each coating on the membrane properties compared to untreated membranes. Further, a subsequent heparinization to the functionalized surfaces is investigated. To realize the application in hemodialysis, hollow fiber modules are finally coated with dopamine or dopamine analogues and analyzed.

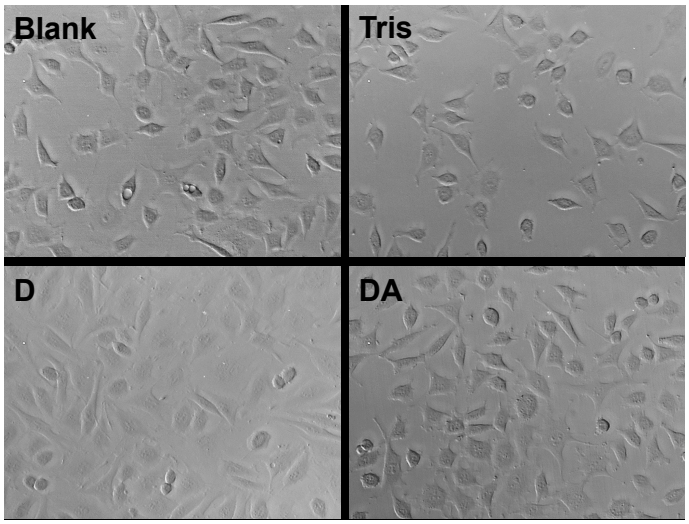

Figure 4.6: Microscope images of cell cultivation of L929 mouse cells on microtiter plates with different coating: DI water (Blank), tris buffer (Tris), dopamine in tris buffer (D) and dopamine analogues in tris buffer (DA).

4.4.1 Toxicity Tests

For toxicity tests, L929 cells are seeded on variously coated microtiter plates. Microtiter plates offer a good basis for the proliferation of cells without any coating and are therefore often used as a positive control, here also as blank. Figure 4.6 shows the results of cell growth on microtiter plates with four different coatings: DI water (Blank), tris buffer (Tris), dopamine in tris buffer (D), and dopamine analogues in tris buffer (DA). As expected, the cells grow well on the DI water-treated microtiter surface (Blank), whereas the cells grow weaker on the tris treated surface (Tris). Compared to the blank, growth with dopamine or dopamine analogues appear stronger.

When plotting the cell number per square centimeter over different coatings, the increase in cells is even more visible (cf. Figure 4.7). The Blank as positive control has around 140.000 cells/cm^2 whereas DA has more than 200.000 cells/cm^2. After a subsequent heparin coating, the cell number increases from around 130.000 cells/cm^2 to around 150.000 cells/cm^2 (D-H) or at least stays constant (DA-H). Thus, the coatings are not toxic and even provide preferential growth on the coated microtiter plates.

Concluding, both the dopamine and the dopamine analogues coatings with and without heparin (-H) exhibit cell compatibility characteristics. The

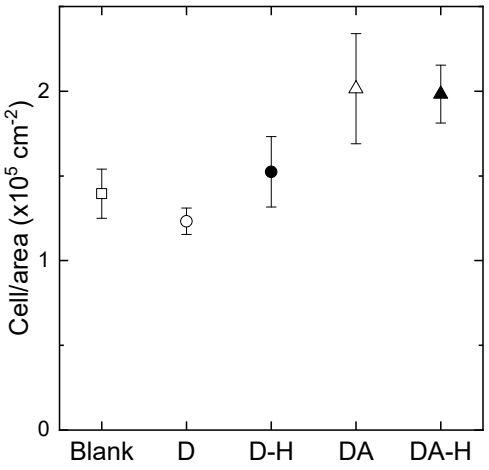

Figure 4.7: XTT measurement of cell growth on untreated (Blank, □) or functionalized microtiter plate surfaces coated with dopamine (D, ○) or dopamine analogues (DA, Δ) with and without a subsequent heparin coating (-H). The error bars correspond to the deviation of three measured wells.

cell growth even increases compared to the positive control. In the following, the promising results are transferred onto porous flat sheet membranes to measure changes in membrane surface properties due to the coatings.

4.4.2 Coating of Flat Sheet Membranes

Since the coatings appear to be non-toxic, they are now used to functionalize porous structures. Flat sheet membranes (FS-PES) consisting of pure PES are coated to measure the influence of each coating to the membrane properties. Therefore, XPS and the fouling behavior of the flat sheet membranes are compared to the untreated membrane. Furthermore, the subsequent possible heparin immobilization due to the coating with dopamine or dopamine analogues is discussed.

The flat sheet membranes FS-PES, FS-D and FS-DA are measured by XPS to detect the elemental composition of the membrane surfaces. Table 4.7 lists the XPS results, the percentage of each element in the membrane surface for FS-PES, FS-D, and FS-DA. Since no PVP is present in the polymer solution, the detection of nitrogen proves the presence of polydopamine or polymerized dopamine analogues on the membrane surface.

The pure PES membrane (FS-PES) is free of nitrogen. After coating with dopamine (FS-D), 8.1 % nitrogen appears on the membrane surface, which indicates the deposition of polydopamine. The nitrogen to carbon signal ratio of FS-D is 0.12 , which further proves the successful deposition of polydopamine on the porous flat sheet membrane [Lee2007].

Table 4.7: Elemental composition on flat sheet membrane surfaces with (FS-D) and without (FS-PES) dopamine or dopamine analogues (FS-DA) coating measured with XPS.

Element or ratio	Unit	FS-PES	FS-D	FS-DA
O	%	21.8	22.2	21.4
N	%	-	8.1	3.9
C	%	64.6	69.7	66.5
S	%	13.6	-	8.2
N/C	-	-	0.12	0.06

On the other hand, the flat sheet membrane coated with dopamine analogues (FS-DA) shows a nitrogen content of 3.9 %. This nitrogen amount indicates the deposition of polymerized dopamine analogues on the membrane surface. Hu et al. [Hu2016] also showed lower nitrogen contents of membranes with polymerized catechol and polylamine compared to those with polydopamine.

In the next step, FITC-BSA adsorption experiments are performed to analyze the antifouling properties of the membrane surfaces. The FITC-BSA protein shines bright green under the fluorescence microscope. Figure 4.8 shows the fluoresence microscopy images of the FITC-BSA adsorption experiments.

The pure PES membrane (FS-PES) surface appears bright green as a high amount of FITC-BSA is adsorbed on it. The surfaces display significantly less prominent coloration when coated with dopamine (FS-D) or dopamine analogues (FS-DA). As expected, this discoloration shows that polymerized dopamine or dopamine analogues reduce the fouling tendency. In addition, the dopamine coating seems slightly stronger regarding the antifouling properties compared to dopamine analogues. After heparinization (FS-D-H and FS-DA-H), the colorization of both coatings changes

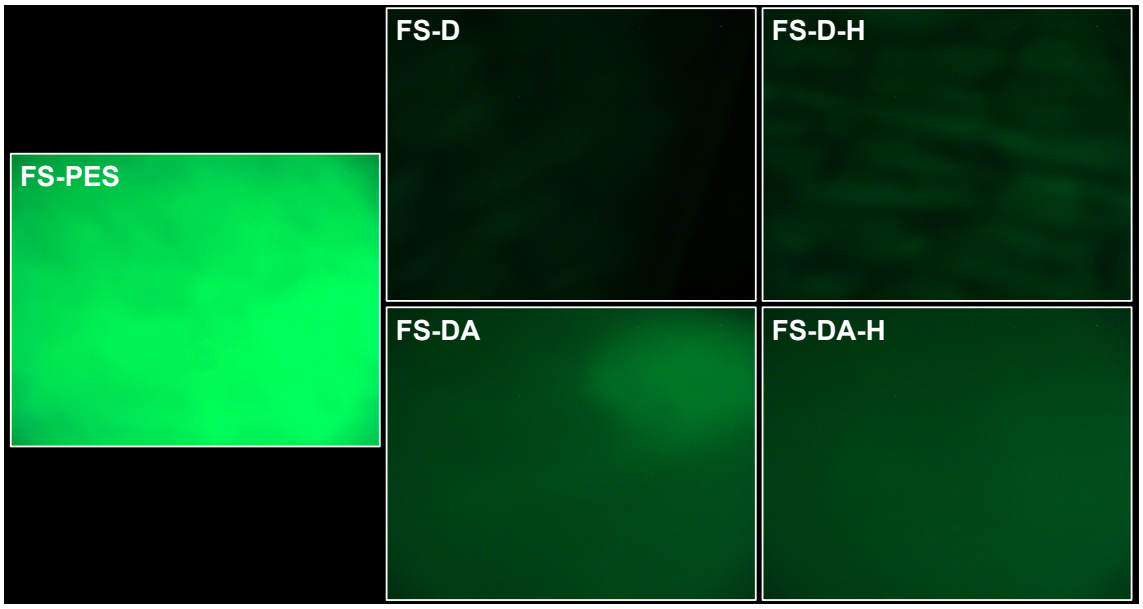

Figure 4.8: Fuorescence microscopy images of pure PES membrane surfaces with (FS-D) and without (FS-PES) dopamine or dopamine analogues (FS-DA) and a subsequent heparin coating (-H) after static adsorption of FITC-BSA.

slightly, but still, the fouling behavior is strongly reduced compared to the FS-PES surface.

The heparin concentrations shown in Figure 4.9 are determined using the factor Xa assay (cf. Section 4.3.1). The membranes without a subsequent heparin coating have heparin concentrations less than 0.1 IU/cm^2, which are negligible. This apparent heparin immobilization is measured due to the non-specific adsorbtion of the factor Xa assay substances on the porous membrane surface. This unspecific binding occurs both on the pure PES membrane (FS-PES) surface and on the surface coated with dopamine (FS-D) or dopamine analogues (FS-DA).

As expected, the heparin-coated membranes show a significant increase in heparin concentration on the membrane surface. FS-D-H shows an increase of about 0.30 IU/cm^2 compared to FS-D. For membranes coated with dopamine analogues (FS-DA and FS-DA-H), the increase in heparin concentration is slightly lower with 0.24 IU/cm^2. Based on this evidence, heparin is successfully immobilized on the membrane surface with both coatings, dopamine and dopamine analogues, and this immobilized heparin is still able to inhibit factor Xa actively.

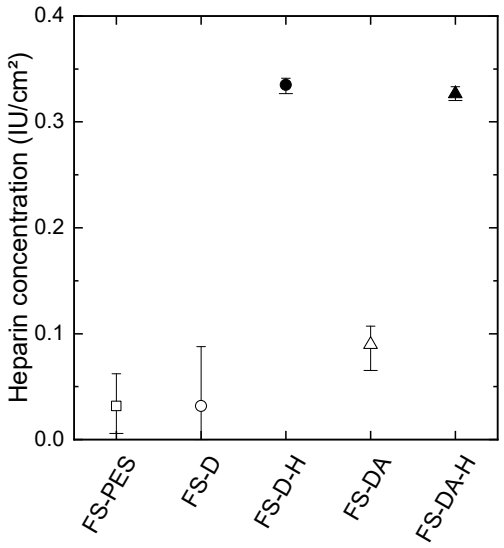

Figure 4.9: Heparin concentration on membrane surfaces of PES (FS-PES, □), dopamine coated PES (FS-D, ○) and dopamine analogues coated PES (FS-DA, Δ) with and without subsequent heparin coating (-H) measured with the factor Xa assay. The error bars correspond to the deviation of three measured surfaces.

Summing up, the results of flat sheet membranes, the XPS analysis, the visible antifouling effect, and the factor Xa results prove the successful immobilization of dopamine or dopamine analogues, and a successful subsequent heparinization. In the following, the coatings are transferred into hollow fiber membranes to prove a transfer to hollow fiber membranes.

4.4.3 Coating of Hollow Fiber Membranes

To study the coatings similar to the end use, hemodialysis, hollow fiber membranes modules are coated with dopamine or the dopamine analogue. For field emission scanning electron microscopy (FeSEM) images, commercial dialysis hollow fiber membranes are coated with dopamine and dopamine analogues. Figure 4.10 shows the FeSEM images of commercial dialysis hollow fiber membranes without a coating, with a dopamine and dopamine analogues coating. All fibers exhibits a band of macrovoids in the center of the hollow fiber wall (cf. Figure 4.10 a) - b)) and a selective layer on the lumen channel (cf. Figure 4.10 d) - f)). The coatings are invisible through microscope images on the selective layer. Hence, no

adverse effects arise from dopamine or dopamine analogues on the membrane morphology.

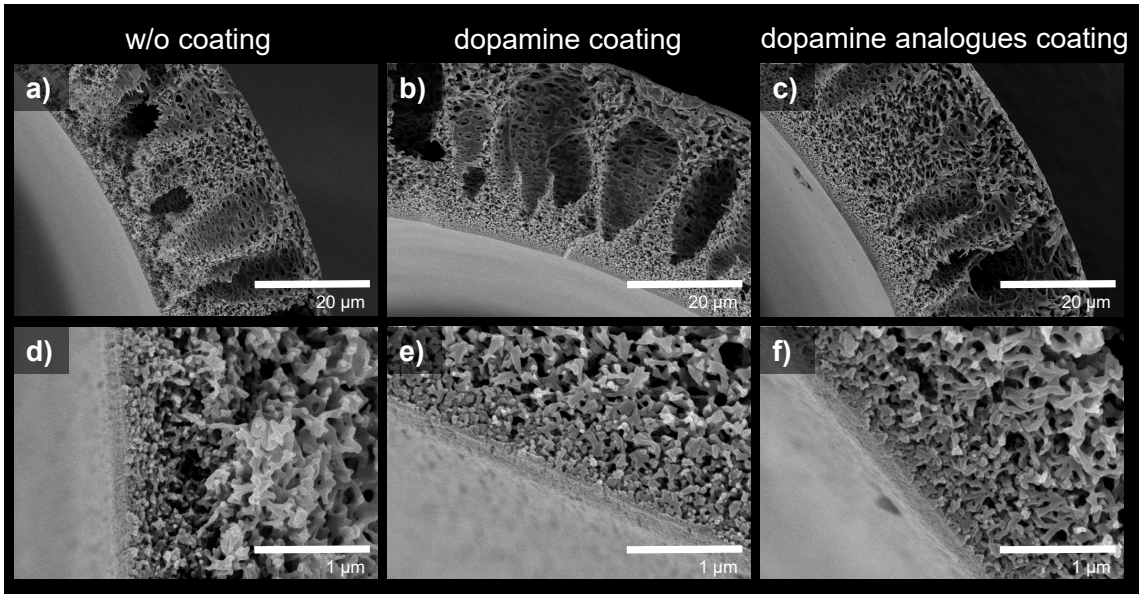

Figure 4.10: Morphology of commercial dialysis hollow fiber membranes without a coating, with dopamine and dopamine analogues coating: a)-c) Cross-section; d)-f) enlarged cross-section of the lumen channel.

For the subsequent hollow fiber membrane characterizations self-made hollow fiber membranes in membrane modules are used. Theses spun fibers have a diameter of around 900 μm and a lumen channel with a diameter of around 710 μm. Figure 4.11 illustrates the results of pure water permeance (PWP) and molecular weight cut-off (MWCO) measurements of HF-PES, HF-D, and HF-DA fibers, each with and without immobilized heparin (-H). The presented membranes have a PWP in a range of around 5 to 15 LMH/bar. Coating with dopamine or dopamine analogues only slightly alters the fluxes of these membranes (HF-D 7.6 LMH/bar and HF-DA 8.6 LMH/bar), whereas the PWP increases with heparin coating for HF-D-H to 12 LMH/bar and for HF-DA-H to around 11 LMH/bar. The additional coating with heparin hydrophilizes the coated membrane surface and thus, results in an increased PWP [Ma2014]. This increase in PWP is also seen in Section 3.3.1. The increase in PWP after heparin coating indicates a successful immobilization.

The MWCO results of the spun fibers are in a range of around 5 to

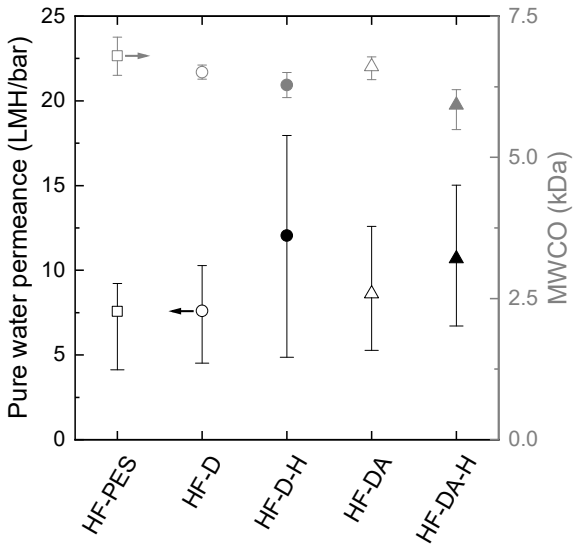

Figure 4.11: Pure water permeance (PWP) and molecular weight cut-off (MWCO) of three membrane modules of HF-PES (□), HF-D (○) and HF-DA (Δ) fibers with and without immobilized heparin (-H). The error bars correspond to the deviation of three measured membrane modules.

8 kDa. The respective coatings induces only a slight change in MWCO compared to the uncoated membrane (HF-PES). However, if the respective membranes are coated with heparin, the MWCO decreases, opposite the PWP.

Overall, the presented membranes' PWP and MWCO are significantly lower than the commercial dialysis hollow fiber membranes since a self-made membrane was used. However, the coating procedure is designed to be easily transferable to commercial dialysis hollow fiber membranes.

To sum up, both coatings, dopamine and dopamine analogues, present promising results for surface heparinization. Especially concerning the amount required for coating dialyzers, the low-cost dopamine analogues have an advantage over dopamine.

4.5 Conclusion

Access to special cost-intensive heparinized membranes in dialysis is only available for high-risk patients. Therefore, cost-effective alternatives are needed that are accessible to all dialysis patients. In this chapter, the

dopamine analogues, catechol and propylamine, are immobilized as heparin anchors on polyethersulfone (PES) membrane surfaces. These dopamine analogues allow subsequent heparin-binding on the respective surface. Furthermore, the dopamine analogues coating is compared to an equimolar dopamine coating. Dopamine has similar groups as the dopamine analogues and is also a heparin anchor.

First, the toxicity of the coating was studied on microtiter plates. Cell cultivation and XTT measurements of L929 cells showed cell growth on the coated surfaces and thus, no toxic behavior of the coatings. Especially the coating with dopamine analogues increases the cell growth.

The transfer of the coatings to porous structures, in this case, PES flat sheet membranes, is promising. XPS measurements and fouling tests revealed significant differences compared to the uncoated PES membrane and the dopamine coated membrane. For the detection of heparin on the coated surfaces, factor Xa tests were performed to measure the concentration of heparin on the membrane surface. Dopamine and dopamine analogues coated membranes exhibit significant amounts of immobilized active heparin. Thus, the dopamine analogues have similar ability to immobilize heparin as dopamine.

Dopamine analogues coated on hollow fiber membranes are promising for application in dialysis hollow fiber membranes. The coating does not significantly influence the permeance and the molecular weight cut-off of the fibers, which is similar to dopamine coated hollow fiber membranes. The subsequent heparinization increases the permeance, while the molecular weight cut-off slightly decreases. Furthermore, the membrane morphology is not visibly changed due to the coating with dopamine analogues and heparin.

Overall, the dopamine analogues coating allows heparinization without adversely affecting the membrane properties. Compared to a dopamine coating, coating with dopamine analogues is a cost-effective option for large-scale applications such as coating a large number of dialyzers. However, further work needs to be done to verify the stability of the dopamine analogues and heparin coating and to ensure that it will withstand the en-

tire treatment time. A stable coating is essential for surfaces in medical applications.

5 Chitosan-Blending Increases Hemocompatibility

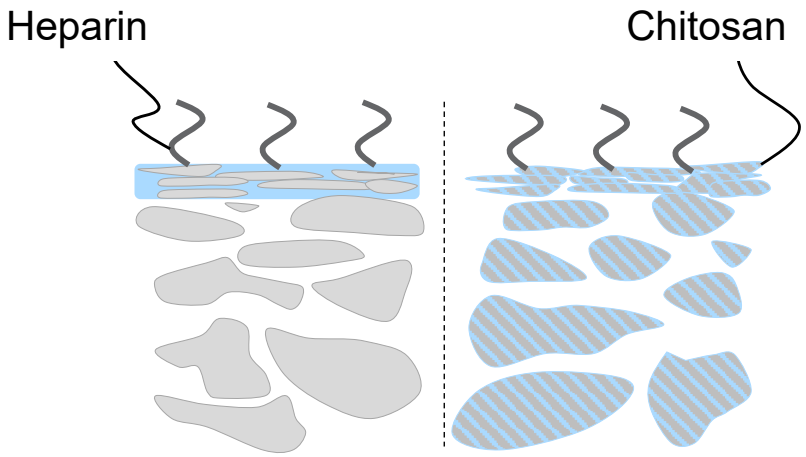

Parts of this chapter have been published and submitted as patent in:
[Rose2022b]: I.I. Rose, M. Kather, H. Roth, H. Dünkelberg, L. Rein, S.N. Klimosch, M. Schmolz, M. Wessling, "Single-step chitosan functionalized membranes for heparinization", *Journal of Membrane Science, 2022, DOI: 10.1016/j .memsci.2022.120567*

M. Wessling, M. Alders, I.I. Rose, M. Kather, R. Menda, B. Krause, M. Storr, M. Rempfer, V.S. Kurbel, "Membrane with immobilized anticoagulant and process for producing same", International patent application Nr. PCT/EP2021/077211

5.1 Introduction

Hollow fiber dialyzers were developed in the 1960s and have become indispensable in the modern dialysis treatment of kidney failure. However, dialysis treatment is a life-prolonging measure, not a cure. The success of this treatment is restrained by the limited hemocompatibility of membrane materials and the insufficient clearance of uremic toxins through the hollow fiber membranes. To prevent blood clotting during dialysis, patients are currently either medicated with the anticoagulant heparin or, in special cases, treated with commercially available heparinized dialyzers. Treatment with a heparinized dialyzer requires significantly reduced amounts of heparin medication for the patient. The Evodial dialyzer of the company Baxter International, for example, consists of acrylonitrile/sodium methallyl sulfonate membranes containing polyethylenimine (PEI). In a further step, heparin is grafted to the PEI functionalized membrane surface, thus enabling heparin-reduced or even heparin-free dialysis treatment. [Kess2013]; [Lavi2014]; [Thom2011] However, such special dialyzers are only used to treat high-risk patients. Consequently, a cost-effective heparinized dialyzer based on polyethersulfone (PES) accessible to any dialysis patient is still missing.

In the last years, many approaches have been studied to increase the biocompatibility and hemocompatibility of commercial dialysis membranes using surface modification. The approaches include the immobilization of heparin or synthetic heparin-like structures on the membrane surface. For example, both the blending of heparin-like polymers into the membrane material [Wang2013]; [Tang2012]; [Ran2012] or the coating of membranes with a layer prone to bind heparin [Shan2020]; [Gao2014]; [Lin2004b]; [Li2020] improve the blood compatibility of the membrane surface. However, heparin-like structures have not yet been used in medical applications. Therefore, research focuses on the immobilization of heparin, which is already well known in medicine.

Heparin has the highest negative charge density of all known biological macromolecules due to its high content of negatively charged sulfonate and carboxylate groups [Capi2002]; [Bhal2015]. Due to this high negative

charge of heparin, especially positively charged additives such as bovine serum albumin (BSA), polyethylenimine (PEI), or chitosan serve as heparin anchors for ionic bonding. Sperling et al. [Sper2006] coated BSA-heparin multilayer onto polyethersulfone (PES) membranes by using the layer-by-layer technique. Platelet activation measured through platelet factor 4 (PF4), thrombin-antithrombin complex (TAT), and complement activation measurements show an improvement compared to the non-treated PES surface. [Sper2006] On the other hand, Dong et al. [Dong2010] coated PEI/heparin on a nickel-titanium (NiTi) alloy using the layer-by-layer technique. Hemolysis and platelet adhesion tests proved the biocompatibility of these heparinized surfaces. Furthermore, Dong et al. showed that additionally to PEI, also chitosan functions as a heparin anchor. [Dong2010]

The amino groups of chitosan bind to the sulfate groups of heparin (cf. Figure 5.1), enabling the heparinization of chitosan-functionalized surfaces [Kweo2003]. Bhalerao et al. [Bhal2015] used a chitosan-heparin complex which gives the layer-by-layer self-assembled thin films a biocompatible behavior. In addition to their biocompatibility, chitosan-heparin complexes achieved distinguishable hemocompatibility [Bala2014]; [Meng2009]. Furthermore, Lin et al. [Lin2004b] used chitosan/heparin polyelectrolyte complexes to increase the hemocompatibility of poly(acrylonitrile) membrane surfaces. Platelet adhesion, protein adsorption and thrombus formation decline due to heparin immobilization. [Lin2004b]

In addition to chitosan functioning as a heparin anchor, chitosan's antibacterial properties, charge density, non-toxicity, and hydrophilic, antifouling and non-allergic effects make it particularly advantageous in medical applications [Koch2012]; [Bala2014]; [Akba2015]; [Kuri1992]. Consequently, chitosan has been extensively researched as a material base for biomedical applications because of its excellent biocompatibility [Jafa2016], but it is also utilized in membrane synthesis due to its hydrophilic and antifouling effects [Akba2015]; [Zhao2015]. For chitosan functionalization, Akbari et al. [Akba2015] immersed polyamide (PA) membranes into a chitosan solution, thus achieving a higher water flux and better antifouling properties [Akba2015]. Zhao et al. [Zhao2015], on the other hand, discovered

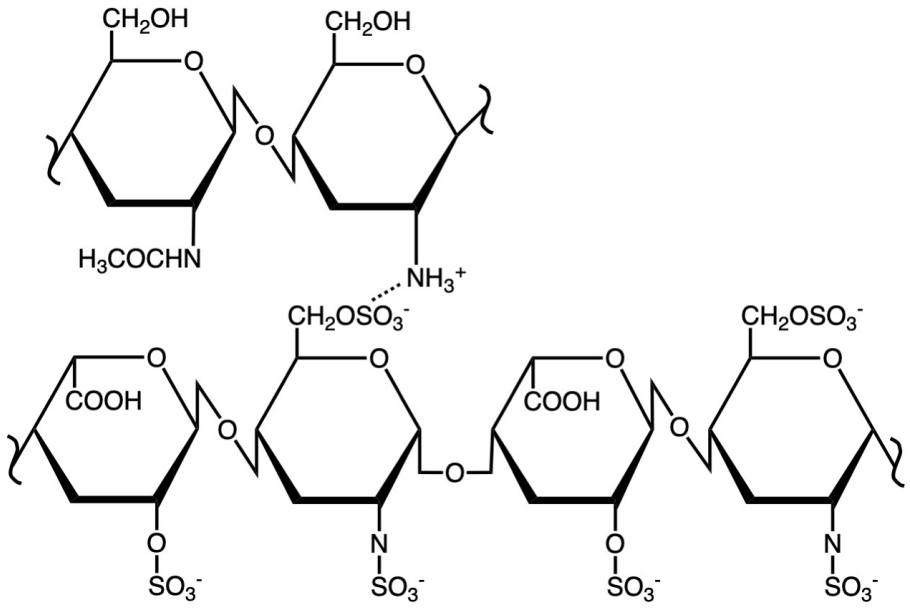

Figure 5.1: Binding of chitosan and heparin [Kweo2003].

a significant improvement in antifouling behavior for polyvinylidene fluoride (PVDF) ultrafiltration membranes anchored with chitosan and sodium alginate [Zhao2015]. Furthermore, Kochan et al. [Koch2012] coated polyelectrolytes, chitosan among others, containing silver nanoparticles onto membrane surfaces to achieve antibacterial effects [Koch2012].

To omit time-consuming post-treatment steps, blending functional additives into the polymer solution offers a direct integration. Gherasim et al. [Gher2016], Roth et al. [Roth2018]; [Roth2019] as well as Emonds et al. [Emon2020] blended polyelectrolytes directly into polymer solutions. Combined with oppositely charged polyelectrolytes or crosslinkers from the lumen fluid hollow fiber membranes with nanofiltration characteristics form [Gher2016]; [Emon2020].

Susanto et al. [Susa2020] report the blending of chitosan into a polyethersulfone (PES) polymer solution by using the surfactant tween 80. The resulting ultrafiltration flat sheet membranes show a low fouling behavior. However, the fabrication of these membranes needs additional additives typically not used in dialysis membrane fabrication. Further functionalization of the membranes with heparin or other functional molecules has not been studied. Furthermore, a chitosan-blended polymer solution has not

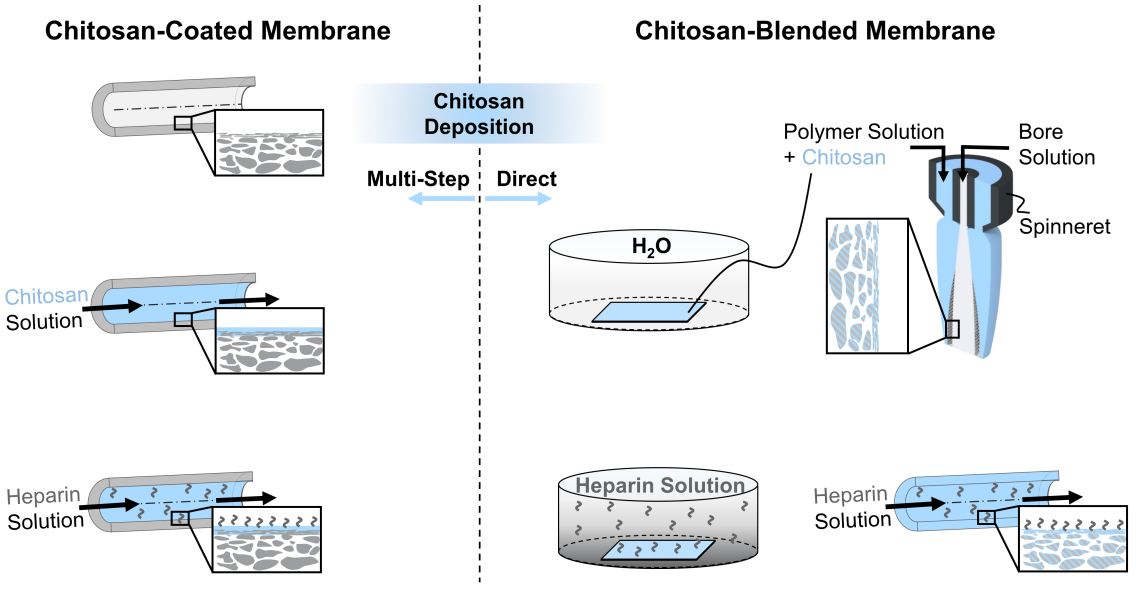

Figure 5.2: Scheme of chitosan coating of commercial membranes and chitosan blending lab-made membranes in this chapter.

yet been transformed into hollow fiber membranes.

Despite many promising characteristics, to date, material systems with chitosan and heparin have not been transferred into medical devices due to the limited availability of additional materials next to chitosan and heparin or elaborate multi-step processes. Therefore, no simple and cost-effective methods are yet available to heparinize surfaces, especially dialysis membranes.

This chapter evaluates the usage of the widely available favorable biopolymer chitosan as a coating for standard commercial PES dialysis membranes (cf. Figure 5.2 left). Additionally, chitosan blends into PES polymer solutions without requiring additional surfactants and hollow fiber membranes evolve from this formulation (cf. Figure 5.2 right). In both cases, chitosan may function as an anchor for a subsequent heparin binding. Hemocompatibility tests serve to validate our hypothesis. The simple chitosan blending turns an elaborate multi-step procedure into a single-step functionalization of hollow fiber membranes.

5.2 Experimental

5.2.1 Materials

In addition to the materials described in Section 2.1, the following materials are used. For the functionalization, chitosan with a MW of 50 - 190 kDa (Sigma Aldrich, Germany) and citric acid granulate ($\geq$99 %, Sigma Aldrich, Germany) are used.

For blood tests, active complement component 3 (C3a) assay (HK354-02, Hycult Bio.), platelet factor 4 (PF4) assay (DY795, R&D), and thrombin-antithrombin complex (TAT) assay (OWMG15, Siemens) are used.

Four-end membrane modules containing Revaclear hollow fiber membranes are prepared by Baxter International Inc. and provided for chitosan post-treatment.

5.2.2 Chitosan-Coated Hollow Fiber Membranes

For coating, a chitosan solution is prepared. 1 mg/mL chitosan is added to 1450 mg/mL citric acid granules in DI water and stirred until a homogeneous solution is formed. The chitosan solution is flushed through the lumen side of commercial hollow fibers (Com-HF) in a membrane module (cf. Figure 5.2 left), and the shell side is filled with citric acid. The membrane module is stored for 24 hours at 6 °C. Then, the lumen side is thoroughly flushed with DI water (pH 7). Chitosan precipitates on the membrane surface due to the pH change. Subsequently, some membrane modules are functionalized with heparin as described in Section 2.3.

Table 5.1: Overview of commercial hollow fiber membranes (Com-HF) functionalized with chitosan (Com-HF-C).

	Chitosan concentration [mg/mL]	Citric acid in DI water [mg/mL]	Coating time [h]
Com-HF	-	-	-
Com-HF-C	1	1450	24

Table 5.2: Composition of the polymer solutions P5.1 - P5.4 and the resulting membranes.

Polymer solution	Membrane batch	PES [wt.%]	PVP k90 [wt.%]	NMP [wt.%]	Chitosan [wt.%]	Citric acid in DI water [wt.%]
P5.1	FS	14	2	84.00	-	-
P5.2	FS-C1	14	2	79.95	0.05	4
P5.3	FS-C2, HF-C	14	2	79.90	0.10	4
P5.4	FS-C3	14	2	79.80	0.20	4

5.2.3 Chitosan-Blended Membranes

By blending the chitosan into the polymer solution, the membrane functionalization with chitosan occurs in a single step. Chitosan is added in different concentrations into the polymer solution. Each polymer solution is transformed in flat sheet and hollow fiber membranes, as described in the following subsections.

Preparation of Chitosan-Blended Polymer Solution

Citric acid granulate (5.8 mg) is dissolved in 4 mL DI water. After complete homogenization, chitosan is added and the solution is stirred for 24 h until homogeneous. Following, NMP is added to the chitosan/citric acid solution and stirred for 24 h. The amount of NMP varies with the amount of chitosan in the chitosan/citric acid/NMP solution. Finally, 14 wt.% PES and 2 wt.% PVP are added to the chitosan/citric acid/NMP solution and stirred with a KPG stirrer at room temperature for at least 24 h. To avoid defects in the membrane structure, the homogeneous polymer solution is left for degassing overnight and subsequently transformed into membranes, as described in the following section.

Flat Sheet Membrane Casting

The fabrication of flat sheet membranes occurs in a casting process as stated in Section 2.2.2 (cf. Figure 5.2 middle). Flat sheet membranes out of four different polymer solutions are fabricated (cf. Table 5.2 P5.1 - 5.4).

Spinning of Hollow Fiber Membranes

The polymer solution P5.3 (cf. Table 5.2) is used for the hollow fiber membrane fabrication (cf. Figure 5.2 right). The used spinning parameters are summarized in Table 5.3. Hollow fiber membranes are spun as stated in Section 2.2.4. During spinning, the polymer solution and the bore solution are coextruded through a single orifice spinneret with a bore needle diameter of 0.4 mm and a polymer orifice diameter of 1.12 mm.

For membrane characterization, the hollow fiber membranes are glued into membrane modules as stated in Section 2.4.6.

Table 5.3: Overview of spinning parameters of hollow fiber membrane fabrication.

	Polymer solution flow rate [g/min]	Bore solution flow rate [mL/min]	Pulling speed [m/min]	Air gap [cm]
Spinning parameter	6.6	3.0	10.3	2.0

5.2.4 Membrane Characterization

In addition to the characterization methods described in Section 2.4, further characterization methods relevant for this chapter are described below.

Hemocompatibility

A testing platform based on the proprietary TruCulture® system (an established in-vitro system for immuno-monitoring of pharmaceuticals using whole human blood) is used to assess the hemocompatibility of flat sheet membranes. The blood is collected from three different human donors. TruCulture® tubes (HOT Screen GmbH, Reutlingen, Germany) are loaded with 10x25 mm^2 membrane pieces before adding 3 mL human whole blood. The blood is obtained by venipuncture, using heparinized syringes (0.75 IU/mL) and 19G butterfly needles. To prevent any loss of cell activity or non-specific activation, the whole blood cultures are initiated within 60 min after blood draw and incubated for 1.5 hours at 37 °C. The tubes are inverted

periodically to prevent sedimentation of cells. Afterward, measurements, such as activation of the complement cascade (active complement component 3: C3a), platelets (platelet factor 4: PF4), and blood coagulation (thrombin-antithrombin complex: TAT) are performed.

5.3 Results and Discussion

The following section is divided into two main parts: chitosan-coated hollow fiber membranes and chitosan-blended membranes (cf. Figure 5.2). In the first part, the results of commercial hollow fiber dialysis membranes from Baxter International Inc. coated with chitosan and subsequent immobilization of heparin are presented and discussed. Afterward, the investigation on chitosan-blended flat sheet and hollow fiber membranes are presented. For chitosan-blended flat sheet membranes, a single-step fabrication method to create chitosan immobilized flat sheet membranes is used and subsequently heparinization. Their properties are compared to the multi-step chitosan coating procedure. Finally, the most promising polymer compositions of the flat sheet membranes are transferred to hollow fiber membranes and described in the section chitosan blended hollow fiber membranes.

5.3.1 Chitosan-Coated Hollow Fiber Membranes

Commercial hollow fiber dialysis membranes from Baxter International Inc. are coated with chitosan dissolved in citric acid to immobilize chitosan on the lumen side of the membrane (cf. Section 5.2.2). Afterward, some of the membrane modules are coated with heparin according to Section 2.3.

Figure 5.3 shows the zeta potential over the pH values of untreated commercial dialysis membranes (Com-HF) that were subsequently coated with chitosan (Com-HF-C) and in a second step coated with heparin (Com-HF-C-H). The zeta potential of Com-HF shows a negative potential between pH 3 and 6. This course is typical for membranes fabricated out of a polymer solution containing PES and PVP. As expected, the chitosan-coated mem-

brane surface induces a shift to a positive charge between pH 3 and 6 (cf. Com-HF-C) due to its high amount of amino groups [Zhao2003]. Zhao et al. showed similar charge changes in zeta potential due to the immobilization of chitosan on PES membrane surface [Zhao2003].

The subsequent heparin-coated membrane (cf. Com-HF-C-H) shows the opposite, a shift into the negative range between pH 3 and 6. The negatively charged sulfate groups in the carbohydrate moiety of heparin induce the negative zeta potential [Chan2003]. The negative surface charge generated by the immobilization of heparin is widely discussed in the literature [Shan2020]; [Li2020]. Thus, this change in surface charge proves the successful immobilization of heparin on the chitosan-coated membrane [Li2020].

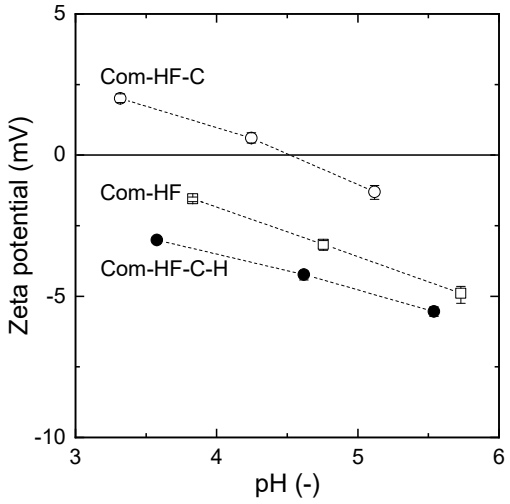

Figure 5.3: Surface charge of the commercial dialysis membrane (Com-HF, □), the chitosan-coated commercial dialysis membrane (Com-HF-C, ○), and the heparinized chitosan-coated commercial membrane (Com-HF-C-H, ●).

The coatings influence the pure water permeance (PWP) of the membranes (cf. Table 5.4). The commercial membrane Com-HF has a PWP of 72 LMH/bar. After chitosan coating, the PWP decreases to 43 LMH/bar. Although chitosan has a high hydrophilicity [Akba2015]; [Mach2019], the membrane coating reduces the PWP, implying that the coating also reduces the pore size. Musale et al. [Musa1999] demonstrated similar results of chitosan-coated poly(acrylonitrile) membranes, which show a decreased

flux after chitosan coating due to pore size reduction. In literature, chitosan coatings are reported in combination with an increase in water flux with increasing chitosan concentration [Akba2015]; [Mach2019]. Presumably, for the coatings fabricated with a 1 mg/mL chitosan coating solution, the pore size reduction already outweighs the effect of increased hydrophilicity.

In comparison, the heparin-coated chitosan fiber (Com-HF-C-H) features a high PWP of 213 LMH/bar. This significant increase is due to the hydrophilic property of heparin. This assumption is in accordance with the literature. Lin et al. [Lin2004b] showed an increase in the water permeance of chitosan-modified polyacrylonitrile membranes due to a heparin immobilization.

Table 5.4: Pure water permeance of the Com-HF, Com-HF-C, and Com-HF-C-H membranes.

Membranes	Pure water permeance [LMH/bar]
Com-HF	72 $\pm$3.6
Com-HF-C	43 $\pm$2.2
Com-HF-C-H	213 $\pm$10.6

Summing up, the presented chitosan coating provides an effective anchor for the subsequent heparinization of commercial hollow fiber dialysis modules. However, despite the successful proof, a multi-step coating is a time-consuming process.

5.3.2 Chitosan-Blended Membranes

Following the promising results of chitosan post-modification of commercial PES dialysis membranes, the fabrication of chitosan functionalized membranes in a single step is presented in the following sections. This single-step fabrication is significantly less time-consuming and therefore more cost-effective than a multi-step coating process. In a subsequent coating step, heparin is immobilized on the membrane surface.

Chitosan-Blended Flat Sheet Membranes

Unlike other additives, chitosan cannot be dissolved in organic solvents or water and thus cannot be used directly as an additive in the polymer solution. However, by first dissolving chitosan in a citric acid solution, adding the organic solvent NMP subsequently and finally, the polymers, it is possible to achieve a homogeneous polymer solution. In the following, a reference flat sheet membrane (FS) is compared to flat sheet membranes evolved from polymer solutions with different chitosan concentrations (FS-C1, FS-C2, and FS-C3, cf. Table 5.2).

Figure 5.4 summarizes the zeta potential over the pH value of the untreated membrane (FS) and the chitosan-blended membrane (FS-C2) with and without a subsequent heparin coating, FS-H and FS-C2-H. The zeta potential of FS is negatively charged between pH 3 and 6 and is in a similar range than Com-HF (cf. Figure 5.3). After heparin coating, the charge is even slightly more negative. It seems that small amounts of heparin adsorb non-specific to the membrane surface and thus influence the surface charge.

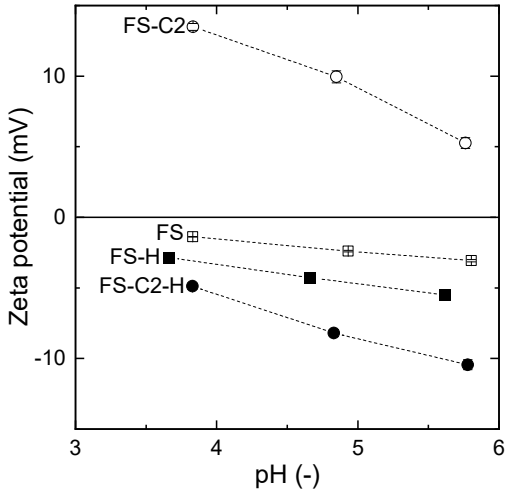

Figure 5.4: Zeta potential of FS (□) and FS-C2 (○) membrane with (-H, filled symbols) and without a subsequent heparin coating.

Comparing the zeta potential of FS to the chitosan-blended membrane FS-C2, a clear influence of the positively charged chitosan is observed. Between pH 3 and 6 , the membrane surface has a zeta potential of above

5 mV. It is assumed that the amino groups of the blended chitosan are located at the surface, which causes the charge difference between FS and FS-C2. These amino groups enable the ionic binding of heparin to the membrane surface. The zeta potential of FS-C2-H reflects the ionically bound heparin, as the charge difference between FS-C2 and FS-C2-H is above 15 mV.

Compared to the chitosan-coated membranes (cf. Section 5.3.1), the charge differences between the chitosan-functionalized membrane and the reference membrane are significantly higher for the chitosan-blended membranes. Significant charge differences between the reference membrane and chitosan-functionalized membranes indicate a higher amount of amino groups on the membrane surface. This higher amount of amino groups provides more binding opportunities for heparin.

Furthermore, the fouling properties of the chitosan-blended membranes are investigated. Figure 5.5 shows the fluorescence microscope images of the reference flat sheet membrane (FS) and chitosan-blended membranes (FS-C1, FS-C2, and FS-C3) with and without heparin after contact with fluorescently labeled bovine serum albumin (BSA). FS appears bright green, which is the color of the fluorescein-labeled BSA (cf. Figure 5.5). The presence of chitosan strongly reduces the fouling behavior of the membranes FS-C1, FS-C2, and FS-C3. This influence suggests that the antifouling effect of chitosan also works with blended chitosan in the polymer solution. FS-C1 and FS-C2 exhibit excellent protein repelling properties. No fluorescent staining of the membrane surface is observable despite the exposure of 2000 ms. Since the increase from 0.05 wt.% to 0.1 wt.% chitosan induces no change in antifouling behavior, already low weight percentages of chitosan are sufficient.

In contrast, FS-C3 contains small crystalline structures visible due to fluorescent staining. A possible explanation for this is the agglomeration of chitosan at higher concentrations, leading to an inhomogeneous polymer solution.

Subsequent heparin coating slightly deteriorates the antifouling properties of all membranes (FS-C1-H, FS-C2-H, and FS-C3-H), except the ref-

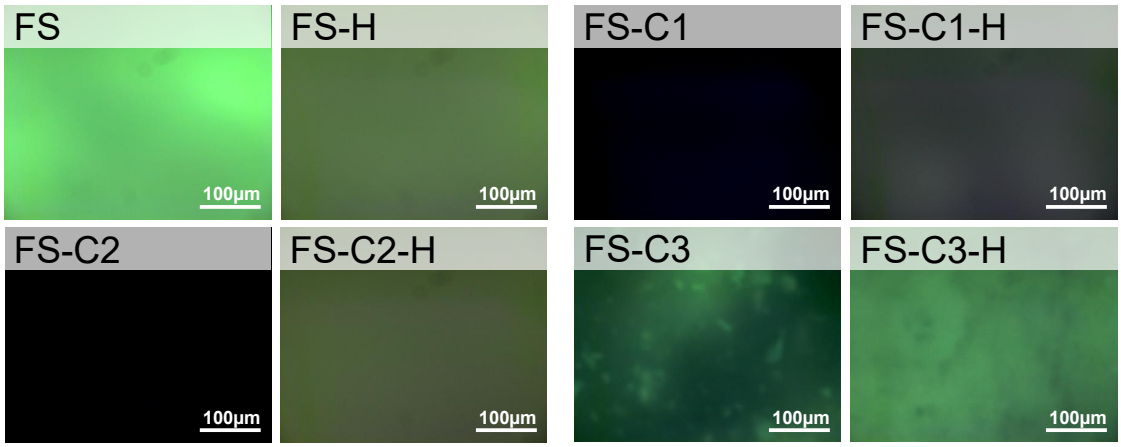

Figure 5.5: Fouling studies using fluorescent BSA of reference (FS) and the chitosan-blended membranes FS-C1 (0.05 wt.%), FS-C2 (0.1 wt.%), and FS-C3 (0.2 wt.%), subsequently coated with heparin (-H).

erence. Therefore, it seems that the antifouling effect of heparin is not as strong as that of chitosan.

Thrombin-antithrombin complex (TAT), complement activation (active complement component 3 (C3a)) and platelet activation (platelet factor 4 (PF4)) give insights into the hemocompatibility of the functionalized surfaces. Figure 5.6 summarizes the results of the hemocompatibility tests. Specifically, the reference membrane (FS) and the chitosan-blended membranes (FS-C1, FS-C2, and FS-C3), with (-H, filled symbols) and without heparin (unfilled symbols) coating undergo hemocompatibility tests. To show the influence of heparinization and guide the eye, dashed lines connect results of membrane samples from the same polymer formulation without and with heparin coating when contacted with the same donor blood.

Two further samples serve as control: the blood sample (0 h) immediately after blood draw, and a Blank as no-sample control (tube without membrane sample). Overall, the measurements of the Blank show that the blood of donor 3 creates a more substantial rash when contacted with a surface than the other two blood samples of donors 1 and 2. This is observed in all conducted measurements.

In Figure 5.6 (a), the thrombin-antithrombin complex (TAT) concentration decreases significantly for nearly all samples with heparin coating. For samples contacted with blood from donor 1, the heparin coating reduces

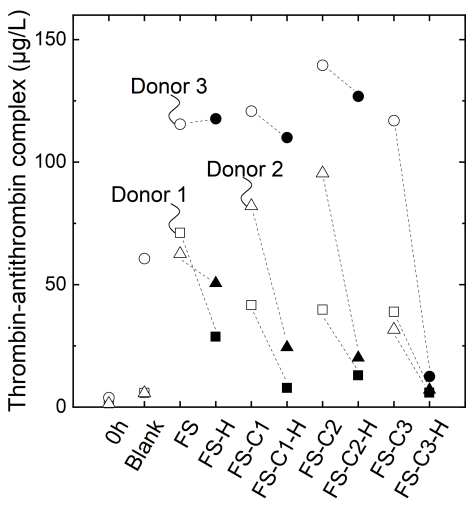

(a) Thrombin-antithrombin complex

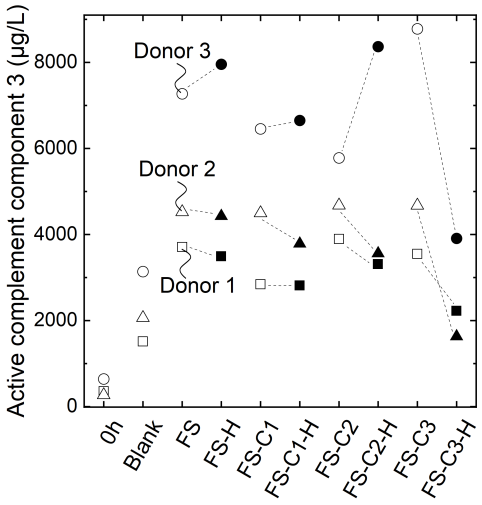

(b) Active complement component 3

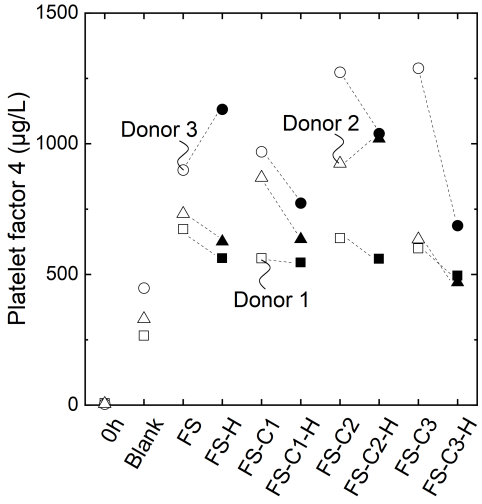

(c) Platelet factor 4

Figure 5.6: Hemocompatibility studies of chitosan-blended flat sheet membranes with (filled symbols) and without heparin (unfilled symbols). Thrombin-antithrombin complex concentration (TAT) (a), active complement component 3 (C3a) (b) and platelet factor 4 (PF4) concentration (c) using blood of three donors □: donor 1; Δ: donor 2; ○: donor 3. Samples are: 0 h: time of blood collection; Blank: blood in tube without membrane piece; all others: membrane samples as indicated.

the TAT complex concentration close to the same level as the Blank (around 6 μg/L). Decreasing TAT concentration reflects a decrease in thrombin generation in the human blood [Sper2006] and a lower probability for blood clot formation.

On the other hand, the presence of chitosan shows no clear influence on

the TAT complex concentration. For blood from donor 2 and 3, TAT complex concentration increases with increasing chitosan concentration from 0 wt.% to 0.1 wt.% chitosan (FS - FS-C2). The membrane FS-C3 with 0.2 wt.% chitosan results in lower TAT complex concentration. The most promising results are achieved with FS-C3-H, for which blood from all donors shows low TAT complex concentrations of 6 μg/L to 10 μg/L. Furthermore, these TAT values are similar to the measured TAT values of the Blank. This shows successful heparinization of the membrane surface and mitigation of TAT activity. Sperling et al. [Sper2006] showed a decrease in TAT after heparinization of PES surfaces via an albumin-coating. Compared to their results [Sper2006], the heparinized chitosan-blended membranes FS-C1-H, FS-C2-H and FS-C3-H induce significantly lower TAT complex concentrations. Considering these promising results from the TAT data, it seems that chitosan-blended membranes function as an excellent anchor for heparin. The resulting membrane shows extraordinary properties regarding its TAT complex mitigation.

Compared to the TAT complex concentration, C3a concentration (cf. Figure 5.6 (b)) and PF4 concentration measurements (cf. Figure 5.6 (c)) provide a similar trend. Figure 5.6 (b) shows the complement activation results, present as the amount of active complement component 3 (C3a). No significant effect on the complement activation is visible for FS and the blended-chitosan membranes (FS-C1, FS-C2, and FS-C3). Again, nearly all samples show an influence of immobilized heparin, as decreasing the amounts of C3a concentration indicates. The lowest C3a concentrations are achieved for the membranes with higher chitosan concentrations (compare, for example, FS-C1-H with FS-C3-H). This indicates that the immobilized heparin amount increases with higher chitosan concentrations in the membrane matrix. This confirms the trend already observed in the TAT complex concentration measurements (cf. Figure 5.6 (a)).

Figure 5.6 (c) shows results of the platelet activation, here by measuring the activation of platelet factor 4 (PF4). PF4 activation concentrations increase for the membrane samples compared to the Blank. However, the chitosan in the blended membranes does not significantly influence platelet

activation. The influence of the blood donor is more pronounced than the sample type. After heparin immobilization, the membrane samples induce significantly less PF4 concentrations, cf. FS-H, FS-C1-H, FS-C2-H, and FS-C3-H. Like for the TAT complex and C3a concentration, the decrease is stronger for higher chitosan concentrations in the membranes. Similar behavior was demonstrated by Sperling et al. [Sper2006] with their heparinized albumin-coated membranes. The authors also showed a significant decrease in platelet activation due to the heparinization of membrane surfaces [Sper2006].

These measurements indicate an excellent improvement in hemocompatibility by heparinizing the chitosan-blended membranes. Even though FS-4-H shows the lowest activation with all blood samples and, therefore, might have the highest amount of immobilized heparin at the surface, the not homogeneous polymer solution as seen in the BSA fouling measurements (cf. Figure 5.5), the polymer solution formulation containing 0.2 wt.% chitosan is not further considered. Instead, the formulation containing 0.1 wt.% chitosan in the polymer solution is transferred to hollow fiber membrane fabrication, which is discussed in the next section.

Chitosan-Blended Hollow Fiber Membranes

HF-C evolves from the polymer solution (P5.3) containing 0.1 wt.% chitosan. Figure 5.7 shows the field emission scanning electron microscopy (FeSEM) images of the hollow fiber HF-C. It has a diameter of around 510 μm and a lumen channel with a diameter of around 330 μm. The hollow fiber membrane exhibits a band of macrovoids in the center of the hollow fiber wall (cf. Figure 5.7 a) and b)), has an open pore structure (cf. Figure 5.7 c)) and a selective layer on the lumen channel (cf. Figure 5.7). Similar morphologies are known from hollow fibers fabricated out of PES/PVP blends. The blending of chitosan into the polymer solution using citric acid shows no formation of crystals or defects in the membrane structure. Hence, no negative effects arise from using chitosan as an additive in the polymer solution during spinning or on the resulting membrane

morphology.

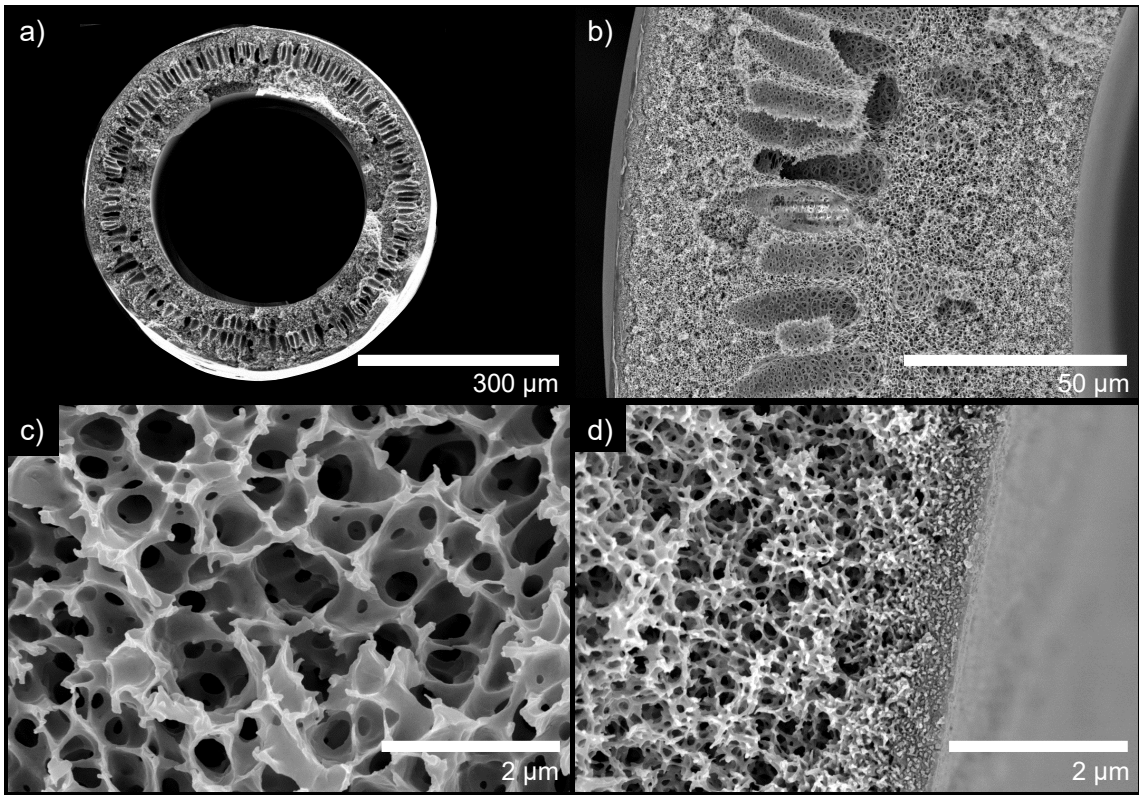

Figure 5.7: Morphology of the hollow fiber membrane HF-C: a)+b) Cross-section; c) enlarged cross-section of the pore structure; d) enlarged cross-section of the lumen channel.

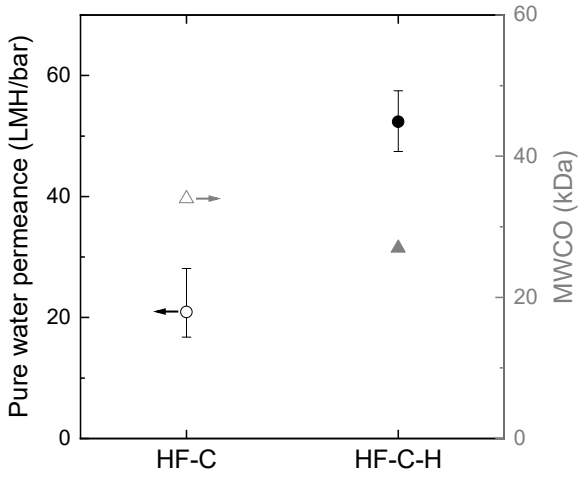

Figure 5.8: Pure water permeance (PWP) and molecular weight cut-off (MWCO) of the fibers HF-C and HF-C-H.

Figure 5.8 presents the pure water permeance (PWP) and the molec-

ular weight cut-off (MWCO) results of the chitosan-blended hollow fiber membrane (HF-C) and the hollow fiber membrane subsequently coated with heparin (HF-C-H). The HF-C fiber has a PWP of 21 LMH/bar and a MWCO of 34 kDa. By tuning the polymer formulation and spinning parameters e.g. temperatures, the PWP and MWCO of the resulting hollow fiber membranes can be further fine tuned.

As shown for the chitosan-coated commercial dialysis hollow fiber membranes (cf. Section 5.3.1), heparin influences the permeance of the membrane, which is also observed here. Coated with heparin, the PWP of HF-C-H rices to 52 LMH/bar while the MWCO decreases to 26 kDa. Although the cut-off decreases, presumably because of the additional layer of heparin, the PWP increases because of the hydrophilic property of heparin [Gao2014].

To conclude, the chitosan-blended membranes show promising results and the blending enables a single-step fabrication of functionalized membranes. These membranes have excellent antifouling properties due to uniform chitosan functionalization and are suitable for heparin immobilization. The heparinization demonstrates a significant improvement in hemocompatibility, and the fabrication of hollow fiber membranes allows their use in dialysis systems.

5.4 Conclusion

Broadly available heparinized dialysis hollow fiber membranes are still missing. This chapter reports facil methods to incorporate chitosan onto and into membrane structures which serves as an anchor for subsequent heparin coating. By coating commercial dialysis membranes with chitosan and by blending chitosan into the polymer solution before membrane formation, functionalized membrane surfaces evolve, allowing the successful binding of heparin.

Changes in surface charge prove the chitosan coating and the subsequent heparin immobilization onto commercial dialysis membranes. After chitosan coating and heparinization, the dialysis hollow fiber membrane

modules exhibit increased permeance.

To mitigate time-consuming coating procedures, chitosan blends into the polymer solution. By adding citric acid, a homogeneous polymer solution with PES, PVP, NMP and up to 0.1 wt.% chitosan forms. Charge differences and excellent antifouling properties of the resulting functionalized flat sheet membranes suggest successful chitosan incorporation and heparinization. In particular, the excellent hemocompatibility of the chitosan and heparin functionalized membranes, which thrombin-antithrombin complex, active complement component 3, and platelet factor 4 concentration measurements showed, are highlighted. Furthermore, hollow fiber membranes formed from the same polymer solution formulation show increased pure water permeance after heparinization.

Overall, the presented chitosan and heparin functionalized membranes are highly hemocompatible while providing promising separation characteristics. A great potential for these hollow fiber membranes in the field of dialysis is in the simple and inexpensive functionalization method. Beyond dialysis, medical devices that require hemocompatible surfaces and membranes in aqueous operations benefit enormously from a reduced fouling tendency.

6 Glutaraldehyde Cross-Linked Amine Sources for Heparinization

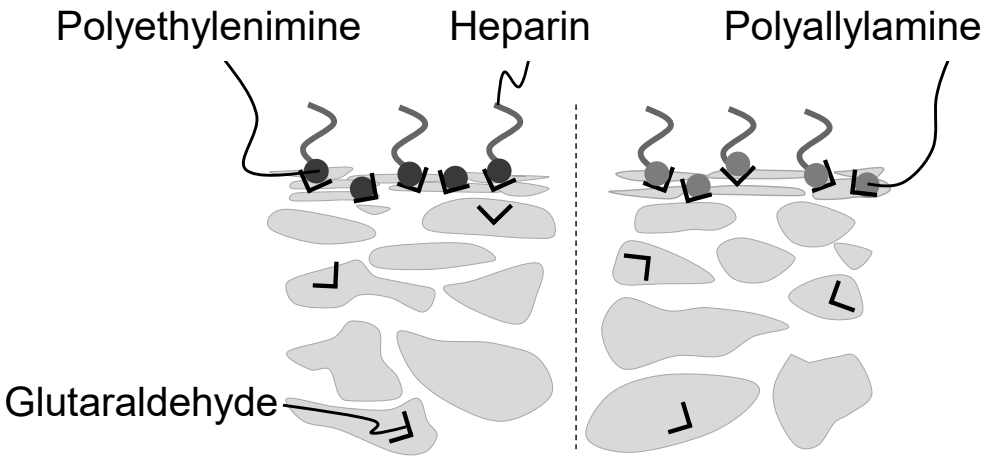

Parts of this chapter are in preparation for publication:
I.I. Rose, H. Roth, L. Rein, M. Wessling, "Glutaraldehyde Cross-Linked Amine Sources for Heparinization", *Journal of Membrane Science*

6.1 Introduction

A widely used cross-linker for membrane functionalization is glutaraldehyde (GA). The variety of reaction mechanisms allows applications in many different areas, for example, to immobilize proteins or enzymes [Joch2011]; [Sigu2018]. Furthermore, GA is used to immobilize polyelectrolytes by the layer-by-layer coating procedure of membrane surfaces [Menn2016a]; [Cho2015]; [Virg2019]; [Kamp2021]. Kamp et al. [Kamp2021] coated ceramic micro- and ultrafiltration membranes with polystyrene sulfonate sodium salt (PSS) and polyallylamine hydrochloride (PAH) to achieve nanofiltration characteristics. To ensure a stable bond, they cross-linked the amino groups of the PAH with GA [Kamp2021].

In addition, the chemistry-in-a-spinneret technique allows the preparation of nanofiltration membranes in a single-step process by cross-linking polyelectrolytes with GA [Roth2018]; [Roth2019]; [Emon2020]. Roth et al. [Roth2018], for example, prepared nanofiltration membranes by cross-linking GA from the bore solution with polyethylenimine (PEI) from the polymer solution. They demonstrated that the high reactivity of GA allows PEI to be cross-linked from the polymer solution during membrane fabrication and thereby creating a positively charged selective layer [Roth2018]. However, high amounts of GA and PEI are used to reach nanofiltration characteristics, creating a dense, cross-linked layer. Figure 6.1 shows the cross-linking reactions of GA with PEI and GA with PAH [Kamp2021].

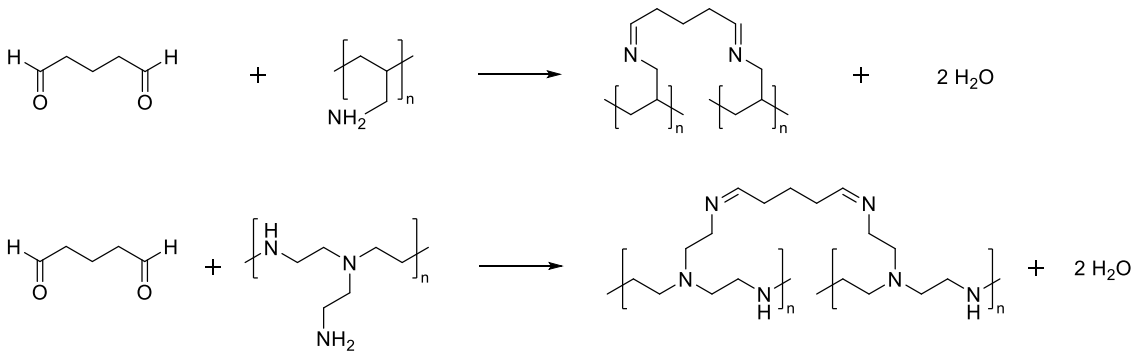

Figure 6.1: Cross-linking reaction with top: PAH amino groups with GA (adapted from Kamp et al. [Kamp2021]) and bottom: PEI amino groups with GA (adapted from Roth et al. [Roth2018]).

In literature, a dense, stable layer with a positive charge is cross-linked in a single step to achieve nanofiltration properties. However, nanofiltration properties are not suitable for dialysis. This chapter aims to achieve a stable, positive layer on the lumen side in a single-step process using GA and an amine source without significant changes in membrane properties for later use in the fabrication of dialysis membranes. Therefore, a low concentration of 0.5 wt.% of the cross-linker GA is added to the polyethersulfone-based polymer solution (cf. Figure 6.2). The coagulation bath for flat sheet membrane or the bore solution for hollow fiber membrane contains an amine source, PEI or PAH, to be cross-linked. Using the chemistry-in-a-spinneret technique, the cross-linking reaction between the amine source and the GA occurs in parallel to the phase inversion process.

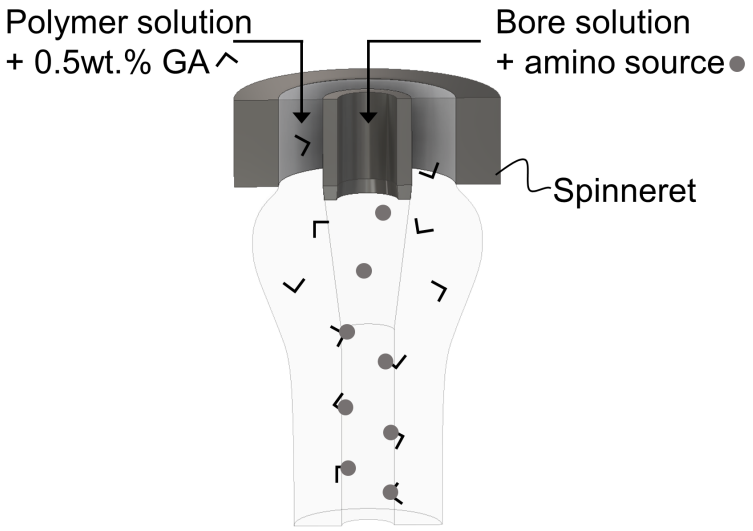

Figure 6.2: Scheme of the chemistry-in-a-spinneret technique with GA in the polymer solution and an amine source in the bore solution.

Compared to previous work, the amounts of amine sources and cross-linker GA are significantly lower (0.5 wt.%). Therefore, the membrane properties such as permeability and selectivity are only slightly affected. For the first time, the chemistry-in-a-spinneret approach is carried out with GA in the polymer solution. A positively charged and stable layer on the membrane surface is formed due to the presence of amine groups in the bore solution.

The created positively charged surface of the membrane lumen chan-

nel enables subsequent ionic binding of the strongly negatively charged heparin. Heparinized surfaces increase the hemocompatibility of the membrane surface and enable the use in blood contact, for example, in hemodialysis.

6.2 Experimental

First, the fabrication of the polymer solution is presented. Then, different coagulation bath or bore solutions with amine sources, such as polyethylenimine (PEI) or polyallylamine hydrochloride (PAH), are listed.

6.2.1 Materials

In addition to the materials described in Section 2.1, the following materials are used. Glutaraldehyde (GA) with grade II as 25 wt.% solution in water at pH 3 is purchased at Sigma Aldrich. Branched PEI with an average MW of 60 kDa and PAH with an average MW of 17 kDa are obtained from Sigma Aldrich.

6.2.2 Preparation of Solutions

Polymer Solution

The components of the used polymer solution are summarized in Table 6.1. The GA solution is directly stirred with the other polymer solution components. The further preparation of the polymer solution is performed as described in Section 2.2.1.

Table 6.1: Composition of the glutaraldehyde polymer solutions P6.1

Polymer solution	PES [wt. %]	NMP [wt. %]	PVP K30 [wt. %]	PVP K85 [wt. %]	DI water [wt. %]	GA [wt. %]
P6.1	14	76.0	5	2	3	0.5

Bore Solutions

Table 6.2 lists the composition of the bore solutions. These bore solutions are prepared as stated in Section 2.2.3. For the bore solutions P6.2 and P6.3, PEI is first dissolved in NMP. Then, DI water is added and stirred until a homogeneous solution is formed. For the bore solutions P6.4 and P6.5, PAH is dissolved in DI water. Then, NMP is added and stirred until the solution is homogeneous.

Table 6.2: Composition of bore solutions B6.1 - B6.5.

Bore solution	DI water [wt. %]	NMP [wt. %]	PEI [wt. %]	PAH [wt. %]
B6.1	50	50	-	-
B6.2	48.875	48.875	0.25	-
B6.3	49.75	49.75	0.5	-
B6.4	48.875	48.875	-	0.25
B6.5	49.75	49.75	-	0.5

6.2.3 Flat Sheet Membrane Fabrication

Flat sheet membranes are cast as stated in Section 2.2.2. Different amine sources are dissolved in the coagulation bath as described in Sections 6.2.5 and 6.2.6. The membranes differ only in the composition of the coagulation bath (cf. Tables 6.4 and 6.6). In some cases, heparin immobilization is subsequently carried out as described in Section 2.3 and the resulting samples are marked with a "-H". After flat sheet membrane fabrication or after heparinization, the membranes are boiled at 80 °C for 2 h in DI water to remove any NMP residues and check the stability of the immobilization. Subsequently, the membrane samples are air-dried at room temperature before measuring.

6.2.4 Hollow Fiber Membrane Fabrication

The fabrication of hollow fiber membranes is conducted as stated in Section 2.2.4. Table 6.3 lists the spinning parameters, which are similar for all

spun membranes. A single orifice spinneret with a bore needle diameter of 0.4 mm and a polymer orifice diameter of 1.12 mm is used.

Table 6.3: Overview of spinning parameters of hollow fiber membrane fabrication.

Parameter	Unit	Value
Polymer solution flow rate	g/min	7.5
Polymer solution temperature	°C	60
Bore solution flow rate	mL/min	5.5
Pulling speed	m/min	11.9
Air gap	cm	2
Coagulation bath temperature	°C	60

6.2.5 Glutaraldehyde Cross-Linked Polyethylenimine

The first amine source used is PEI. PEI is added to the coagulation bath during flat membrane fabrication and to the bore solution for hollow fiber membrane fabrication (see Tables 6.4 and 6.5). Two different concentrations are used: 0.25 wt.% and 0.5 wt.% PEI.

Table 6.4: Overview of GA/PEI flat sheet membranes and subsequent heparin functionalization.

Membrane type	Polymer solution	Coagulation bath		Heparin immobilization	
		DI water [wt.%]	PEI [wt.%]	Concentration [mg/mL]	Time [h]
FS-GA	P6.1	100.00	-	-	
FS-GA-0.25PEI	P6.1	99.75	0.25	-	-
FS-GA-0.25PEI-H	P6.1	99.75	0.25	1	24
FS-GA-0.5PEI	P6.1	99.50	0.50	-	-
FS-GA-0.5PEI-H	P6.1	99.50	0.50	1	24

Table 6.5: Overview of GA/PEI hollow fiber membranes and subsequent heparin functionalization.

Membrane type	Polymer solution	Bore solution	Heparin immobilization Concentration [mg/mL]	Time [h]
HF-GA	P6.1	B6.1	-	
HF-GA-0.25PEI	P6.1	B6.2	-	-
HF-GA-0.25PEI-H	P6.1	B6.2	1	24
HF-GA-0.5PEI	P6.1	B6.3	-	-
HF-GA-0.5PEI-H	P6.1	B6.3	1	24

6.2.6 Glutaraldehyde Cross-Linked Polyallylamine

For comparison with PEI and as a further amine source, PAH is used. As PEI, PAH is added to the coagulation bath during flat membrane fabrication and to the bore solution for hollow fiber membrane fabrication (see Tables 6.6, and 6.7). Two different PAH concentrations are used: 0.25 wt.% and 0.5 wt.% PAH.

Table 6.6: Overview of GA/PAH flat sheet membranes and subsequent heparin functionalization.

Membrane type	Polymer solution	Coagulation bath DI water [wt.%]	PAH [wt.%]	Heparin immobilization Concentration [mg/mL]	Time [h]
FS-GA-0.25PAH	P6.1	99.75	0.25	-	-
FS-GA-0.25PAH-H	P6.1	99.75	0.25	1	24
FS-GA-0.5PAH	P6.1	99.50	0.50	-	-
FS-GA-0.5PAH-H	P6.1	99.50	0.50	1	24

The membranes are analyzed using the characterization methods described in the previous chapters.

Table 6.7: Overview of GA/PAH hollow fiber membranes and subsequent heparin functionalization.

Membrane type	Polymer solution	Bore solution	Heparin immobilization Concentration [mg/mL]	Time [h]
HF-GA	P6.1	B6.1	-	
HF-GA-0.25PAH	P6.1	B6.4	-	-
HF-GA-0.25PAH-H	P6.1	B6.4	1	24
HF-GA-0.5PAH	P6.1	B6.5	-	-
HF-GA-0.5PAH-H	P6.1	B6.5	1	24

6.3 Results and Discussion

The following sections present the results of glutaraldehyde (GA) cross-linking strategies with the two different amine sources, polyethylenimine (PEI) and polyallylamine hydrochloride (PAH), during membrane fabrication. The amine sources immobilized on the membrane surface serve for subsequent binding of heparin. First, PEI is investigated as an amine source in both flat sheet and hollow fiber membranes, followed by PAH as an amine source.

6.3.1 Glutaraldehyde Cross-Linked Polyethylenimine

Flat Sheet Membranes

In the following, a reference membrane FS-GA is compared to flat sheet membranes functionalized with PEI from the coagulation bath and cross-linked with GA from the polymer solution. Figure 6.3 summarizes the zeta potential over the pH values of the reference membrane FS-GA and the PEI functionalized membranes FS-GA-0.25PEI and FS-GA-0.5PEI with and without a subsequent heparin coating (-H). The zeta potential of FS-GA is negatively charged between pH 2 and 10. This surface charge is typical for polyethersulfone membranes [Ma2014]. As assumed, the GA in the polymer solution does not influence the surface charge of the membrane surface. Due to the size of the GA, it will be flushed out of the membrane

during membrane formation if it does not react with an amine group. Compared to this membrane, the PEI cross-linked fibers, FS-GA-0.25PEI and FS-GA-0.5PEI, have a higher surface charge due to the number of amine groups of the PEI located on the membrane surface. Roth et al. [Roth2018] showed similar results after cross-linking GA and PEI using the chemistry-in-a-spinneret approach. This increased surface charge of FS-GA-0.25PEI and FS-GA.0.5PEI enables the ionic binding of heparin. The difference in the zeta potential of the membranes with and without heparin is up to 10 mV at pH 9. These results presume that heparin is ionically bound to the surface. Furthermore, there is no significant difference in charge between the two membranes, FS-GA-0.25PEI and FS-GA-0.5PEI, even though there is twice as much PEI in FS-GA-0.5PEI compared to FS-GA-0.25PEI. Similarly, there are no significant charge differences in the heparinized membranes (FS-GA-0.25PEI-H and FS-GA-0.5PEI-H). Therefore, these charge differences lead to the assumption that 0.25 wt.% PEI provides already sufficient binding opportunities for heparin.

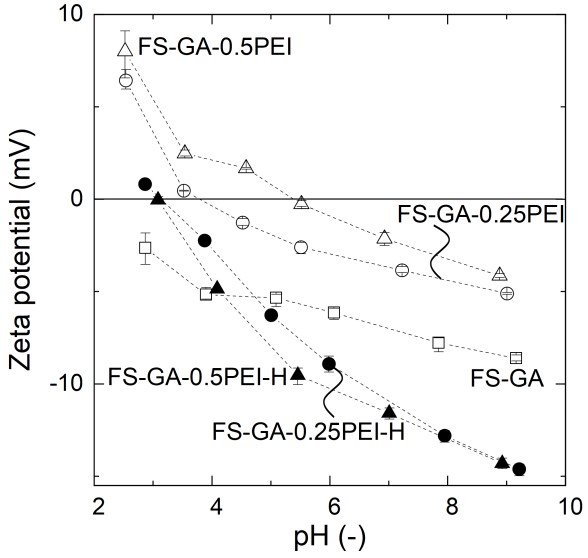

Figure 6.3: Surface charge measurements of FS-GA (□), FS-GA-0.25PEI (○), and FS-GA-0.5PEI (△) with and without subsequent heparinization (-H, filled symbols).

A factor Xa assay (cf. Section 4.3.1) is performed to confirm the assumption of heparinization and is used to determine the heparin concentration on the membrane surfaces. Figure 6.4 shows the results of the

measured heparin concentrations of FS-GA, FS-GA-0.25PEI, and FS-GA-0.5PEI with and without heparin. The heparin concentration is less than 0.1 IU/cm^2 on the membranes FS-GA, FS-GA-0.25PEI, and FS-GA-0.5PEI. This measured heparin concentration is considered as background noise of the measurement. On the other hand, heparin-coated membranes prove to have a significantly increased heparin concentration on the membrane surface. Both membranes, FS-GA-0.25PEI-H and FS-GA-0.5PEI-H, exhibit a heparin concentration of 0.37 IU/cm^2. Based on this evidence, heparin is successfully immobilized on the membrane surface of FS-GA-0.25PEI-H and FS-GA-0.5PEI-H. Furthermore, the immobilized heparin can still inhibit factor Xa. Moreover, the concentration of 0.25 wt.% PEI in the precipitating solution appears to be sufficiently high to immobilize a similar amount of heparin on the membrane surface as 0.5 wt.% PEI.

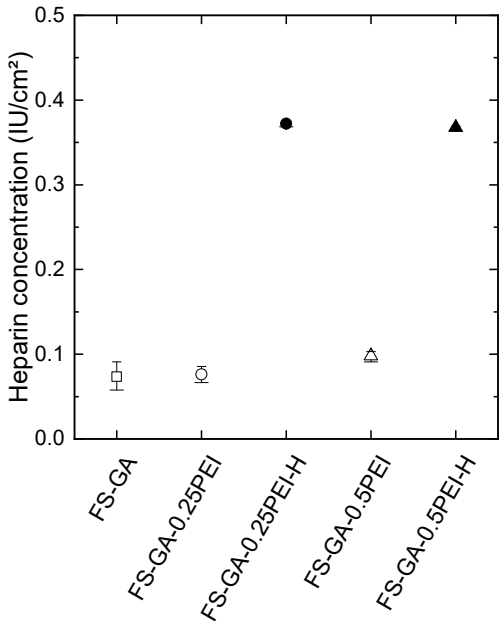

Figure 6.4: Heparin concentration on membrane surfaces of FS-GA (□), FS-GA-0.25PEI (○), and FS-GA-0.5PEI (△) with and without subsequent heparin coating (-H, filled symbols).

Static fouling measurements with fluorescence-labeled BSA (cf. Section 2.4.3) evaluate the fouling tendency of the membrane sample surfaces. The evaluation is based on images of the membrane samples taken with a fluorescent microscope. Figure 6.5 images all membrane samples in

green color, the color of the fluorescence-labeled BSA. Compared to the reference membrane (FS-GA) without PEI, the samples FS-GA-0.25PEI and FS-GA-0.5PEI show significantly less prominent coloration. However, the membranes appear similar to the FS-GA after heparinization, and no significant antifouling effect is observable. Thus, the immobilized heparin attenuates the antifouling effect of the cross-linked PEI on the membrane surface.

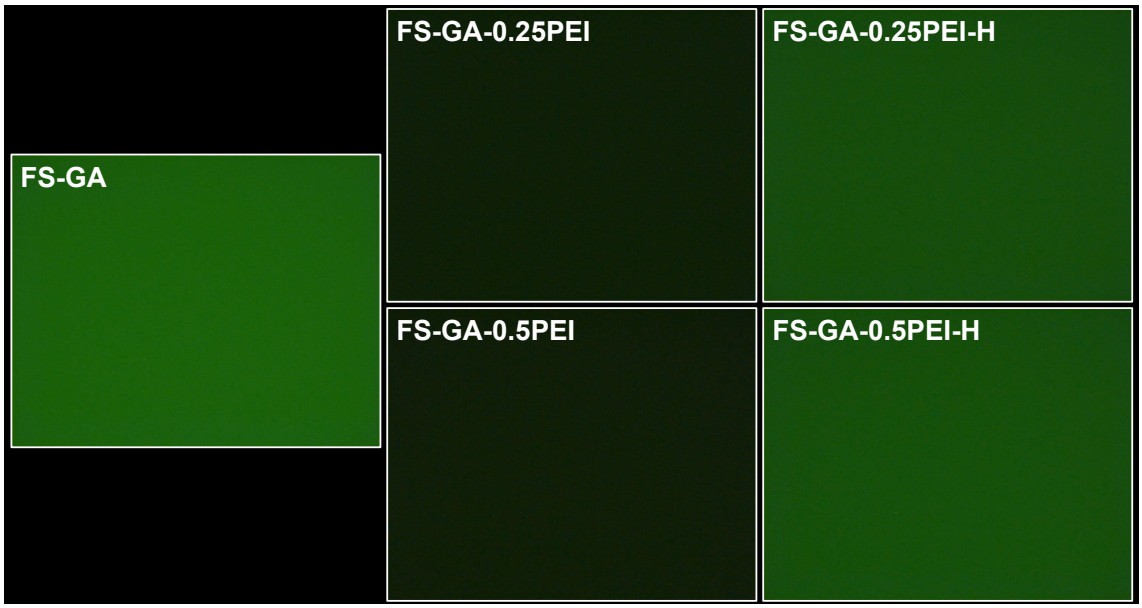

Figure 6.5: Fluorescence microscopy images the surface of FS-GA, FS-GA-0.25PEI and FS-GA-0.5PEI with and without a subsequent heparin coating after static adsorption of FITC-BSA.

Summing up, the surface charge and BSA fouling measurements prove the successful cross-linked functionalization with PEI. Furthermore, the charge differences and the factor Xa assay of the heparinized PEI surfaces show a successful immobilization of heparin with both PEI concentrations (0.25 wt.% and 0.5 wt.%). There are no significant differences between the two PEI concentrations in the immobilized heparin and antifouling properties. In the following, the promising results of the flat sheet membrane characterization are transferred to hollow fiber membranes.

Hollow Fiber Membrane

In addition to the cross-linking reaction during membrane fabrication, the spinning parameters influence the membrane properties during hollow fiber membrane fabrication. Therefore, the spinning parameters are kept the same for all spun fibers. These fibers have an inner diameter of around 730 μm, a wall thickness of around 200 μm, and a burst pressure of around 8 bar.

Figure 6.6 images the morphology of the hollow fiber membranes HF-GA, HF-GA-0.25PEI and HF-GA-0.5PEI. The walls of the three membranes are open porous, and all lumen sides show a skin (cf. Figure 6.5). All membrane morphologies show similar structures. This was to be expected since the membranes differ only in the composition of the bore solution. The bore solutions consist of a low concentration of PEI that cross-links with the GA in the polymer solution. While cross-linking does occur, it does not significantly affect the membrane morphology.

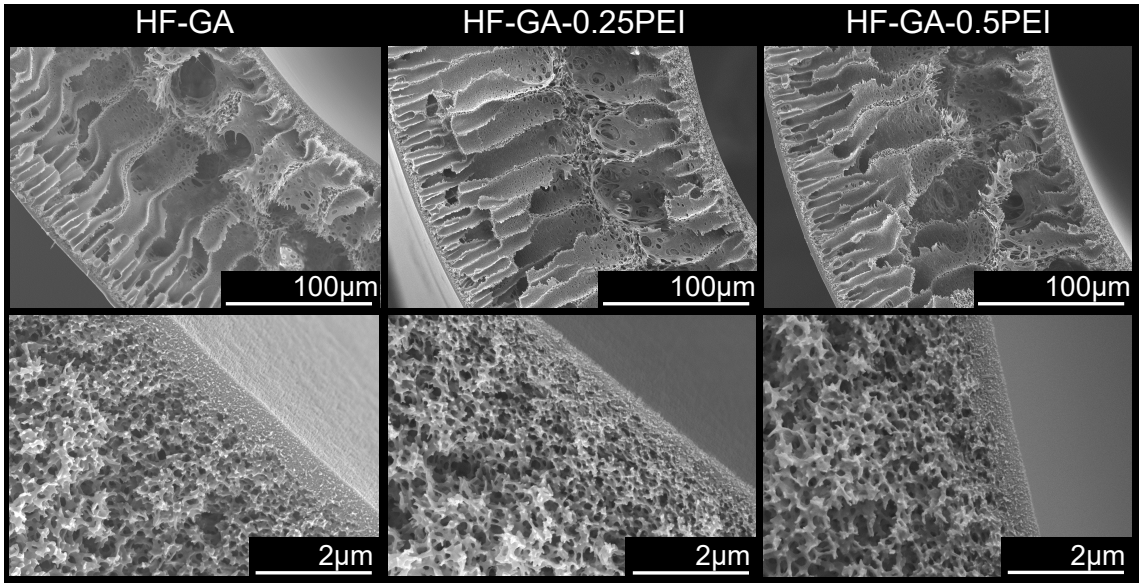

Figure 6.6: Morphology of the hollow fiber membranes HF-GA, HF-GA-0.25PEI, and HF-GA-0.5PEI. First row: cross-section; second row: enlarged cross-section of the lumen channel.

Cross-linking of GA and PEI can have an additional influence on the permeability and the selectivity of the membrane [Roth2018]. These effects do not occur at low concentrations such as 0.5 wt.% GA and 0.25 - 0.5 wt.%

PEI as shown in Figure 6.7. This figure shows the pure water permeance (PWP) and molecular weight cut-off (MWCO) results of the fibers HF-GA, HF-GA-0.25PEI and HF-GA-0.5PEI with and without a subsequent heparin coating (-H). Despite the cross-linking of the GA/PEI membranes, the permeances are with around 6 - 9 LMH/bar in almost the same range as for the reference membrane (HF-GA) with around 8 LMH/bar. Therefore, there is no evidence of a significant change in permeance due to the cross-linking. The same is true for the MWCO of HF-GA, HF-GA-0.25PEI and HF-GA-0.5PEI with and without a heparin coating. Compared to HF-GA with a MWCO of around 17 kDa, the MWCOs of HF-GA.0.25PEI and HF-GA-0.25PEI-H are in a range of around 15 - 16 kDa. Using a higher concentration of PEI in the bore solution (HF-GA-0.5PEI), the cut-offs of the membranes are slightly reduced up to a range of 11 - 12 kDa. The cross-linking reaction makes the membrane denser, resulting in a lower MWCO [Roth2018].

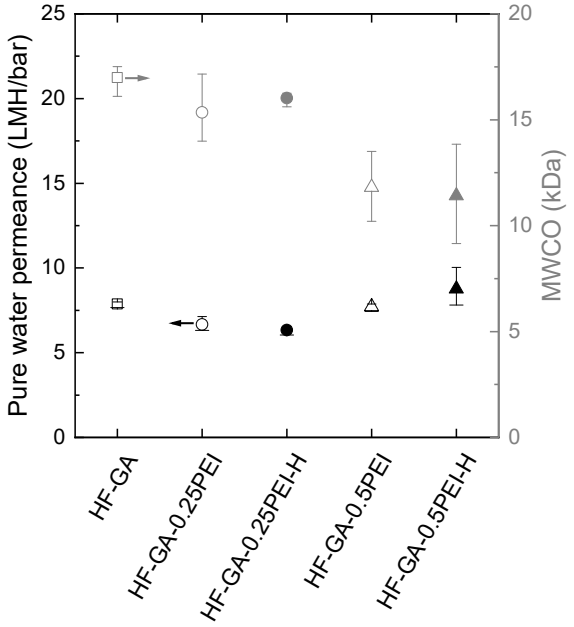

Figure 6.7: Pure water permeance (PWP, black) and molecular weight cut-off (MWCO, gray) of three membrane modules of HF-GA (□), HF-GA-0.25PEI (○), and HF-GA-0.5PEI (△) fibers with and without immobilized heparin (-H, filled symbols).

In summary, small amounts of PEI cross-linked with GA are sufficient to successfully immobilize heparin on the membrane surface and improve

fouling properties. Furthermore, the PWP and MWCO results showed that cross-linking with 0.25PEI almost does not change the permeances and molecular weight cut-offs. Therefore, the chemistry-in-a-spinneret approach allows the formation of a stable, positively charged surface for a successful subsequent heparinization without adversely affecting the membrane properties.

6.3.2 Glutaraldehyde Cross-Linked Polyallylamine

Flat Sheet Membranes

The same reference membrane FS-GA of section 6.3.1 is compared with flat sheet membranes functionalized with polyallylamine hydrochloride (PAH) from the coagulation bath, cross-linked during membrane formation with glutaraldehyde (GA) from the polymer solution. Figure 6.8 summarizes the surface charge measurements of FS-GA, FS-GA-0.25PAH, and FS-GA-0.5PAH with and without a subsequent heparinization (-H). As explained in the previous section, FS-GA has a typical surface charge of polyethersulfone membranes. Compared to this membrane, the zeta potential of both FS-GA-0.25PAH and FS-GA-0.5PAH slightly increased due to the functionalization with PAH cross-linked with GA. However, these increases in zeta potential are lower compared to the membranes functionalized with PEI and GA (cf. Figure 6.3). After heparinization, the zeta potential decreases significantly, indicating a successful heparin immobilization. To confirm this, the heparin concentration on the membrane surface of both membranes is measured using a factor Xa assay.

Figure 6.9 demonstrates the results of the determined heparin concentration of FS-GA, FS-GA-0.25PAH, and FS-GA-0.5PEI with and without further heparinization. The background noise of FS-GA differs compared to that in Figure 6.4. The factor Xa assay is highly sensitive and susceptible. Therefore, a reference membrane is tested with each measurement, which can slightly differ from other factor Xa measurements with the same membrane. The membranes FS-GA, FS-GA-0.25PAH, and FS-GA-0.5PAH, have a heparin concentration set to 0 IU/cm^2, as the measured

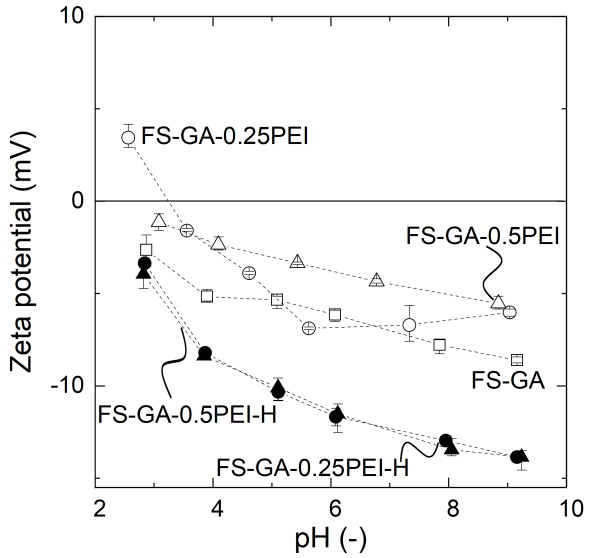

Figure 6.8: Surface charge measurements of FS-GA (□), FS-GA-0.25PAH (○), and FS-GA-0.5PAH (Δ) with and without subsequent heparin immobilization (-H, filled symbols).

heparin concentrations are measured below 0 IU/cm^2.

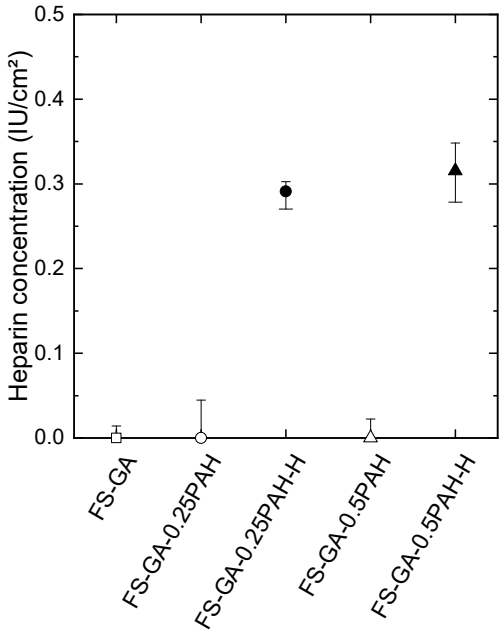

Figure 6.9: Heparin concentration on membrane surfaces of FS-GA (□), FS-GA-0.25PAH (○), and FS-GA-0.5PAH (Δ) with and without subsequent heparin coating (-H, filled symbols).

The results of the heparinized membranes confirm the results of the zeta potential measurements and are similar to the heparin concentration of

the PEI functionalized membrane in Figure 6.4. Both membranes, FS-GA-0.25PAH-H and FS-GA-0.5PAH-H, immobilized around 0.3 IU/cm^2 heparin. As for the functionalization with PEI, there is no significant difference between the used PAH concentrations. A PAH concentration of 0.25 wt.% seems to be sufficient for successful heparinization. However, these factor Xa measurements show successful immobilization with heparin.

In a further step, these PAH functionalized membranes are examined regarding their fouling tendency. Figure 6.10 images the results of the BSA labeled membrane surfaces taken with a fluorescent microscope. Again, compared to the PEI functionalized membranes, all membranes shine greenish, the color of the labeled BSA.

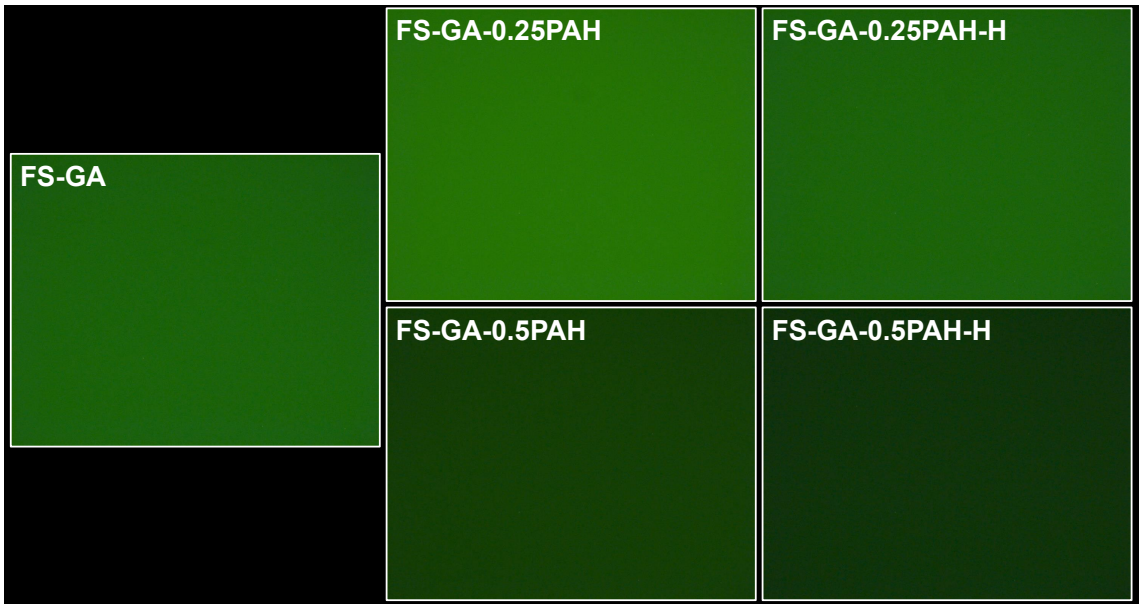

Figure 6.10: Fluorescence microscopy images the surface of FS-GA, FS-GA-0.25PAH and FS-GA-0.5PAH with and without a subsequent heparin coating (-H) after static adsorption of FITC-BSA.

The FS-GA, as well as the membranes FS-GA-0.25PAH and FS-GA-0.25PAH-H, shine green. There is no visual difference between these membranes, which indicates no effect of the immobilized PAH or heparin on the fouling behavior of these membranes. However, if the PAH concentration in the coagulation bath is doubled to 0.5 wt.% PAH, the membrane shows less prominent coloration. Furthermore, the fouling property of the membrane surface is not negatively affected by the immobilized heparin, either.

Summing up, the zeta potential and the heparin concentration measurements prove the successful immobilization of heparin on the PAH cross-linked surfaces. Cross-linking 0.25 wt.% PAH with GA provides sufficient binding spots for heparinization without affecting the fouling behavior of the membrane surfaces. This occurs with twice the amount of PAH. In the following, both material systems are transferred to hollow fiber membranes.

Hollow Fiber Membranes

PAH is added to the bore solution and cross-linked with the GA present in the polymer solution during hollow fiber membrane fabrication. The resulting spun hollow fibers have an inner diameter of around 700 μm and a burst pressure of around 8.5 bar.

Figure 6.11 images the morphology of HF-GA, HF-GA-0.25PAH, and HF-GA-0.5PAH taken with an electron microscope. The cross-linking reaction between GA from the polymer solution and PAH from the bore solution occurs at the lumen side of the membrane during membrane formation. Therefore, especially the selective layer on the lumen side is considered. The selective layer of the HF-GA membrane seems slightly rough. Compared to HF-GA-0.25PAH, no obvious differences in the layer are visible. However, when twice the amount of PAH is used, HF-GA-0.5PAH, the selective layer appears to become denser. More PAH present provides more cross-linking with GA. The more cross-linked, the more visible the cross-linked selective layer on the lumen side becomes[Roth2018].

To measure the influence of the selective layer on permeability and selectivity, PWP and MWCO measurements of these membranes are performed. Figure 6.12 shows the results of PWP and MWCO of HF-GA, HF-GA-0.25PAH, and HF-GA-0.5PAH with and without immobilized heparin (-H). As already discussed in the PWP results of PEI functionalized membranes (cf. Figure 6.7), cross-linking of low amine source concentrations do not have a significant effect on the permeability of the membranes. The PWP of HF-GA is about 7 LMH/bar. The PWP of membranes functionalized with 0.25 wt.% PAH are slightly below with about 6 LMH/bar

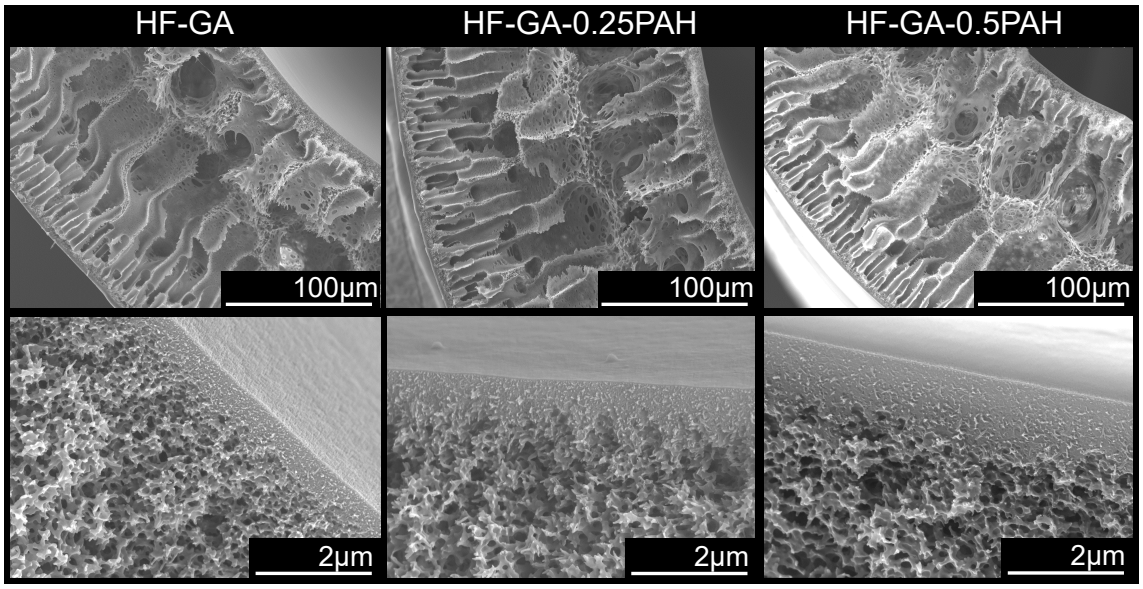

Figure 6.11: Morphology of the hollow fiber membranes HF-GA, HF-GA-0.25PAH, and HF-GA-0.5PAH. First row: Cross-section; second row: enlarged cross-section of the lumen channel.

for HF-GA-0.25PAH and HF-GA-0.25PAH-H. The 0.5 wt.% PAH functionalized membranes, HF-GA-0.5PAH and HF-GA-0.5PAH-H, have PWPs in the same range (between 7 - 8 LMH/bar).

However, comparing the MWCO results of the PAH cross-linked membranes, a significant decrease in selectivity is observed. Compared to the reference membrane HF-GA with an MWCO of 17 kDa, the cross-linked membranes have only an MWCO of about 3.5 kDa. Subsequent heparinization of these membranes does not affect selectivity. The apparently denser cross-linked layer on the lumen side of the membrane surface obviously influences selectivity. The PAH exhibits significantly lower selectivities compared to the PEI cross-linked membranes.

Overall, the permeances and the molecular weight cut-offs of all presented membranes are significantly lower than commercial hollow fiber dialysis membranes. These membrane characteristics can be tuned by varying the spinning parameters during membrane fabrication. Summing up, the chemistry-in-a-spinneret approach with GA and PEI and GA and PAH represents a promising surface modification in a single step for further stable heparinization. In particular, cross-linking with PEI and GA maintains

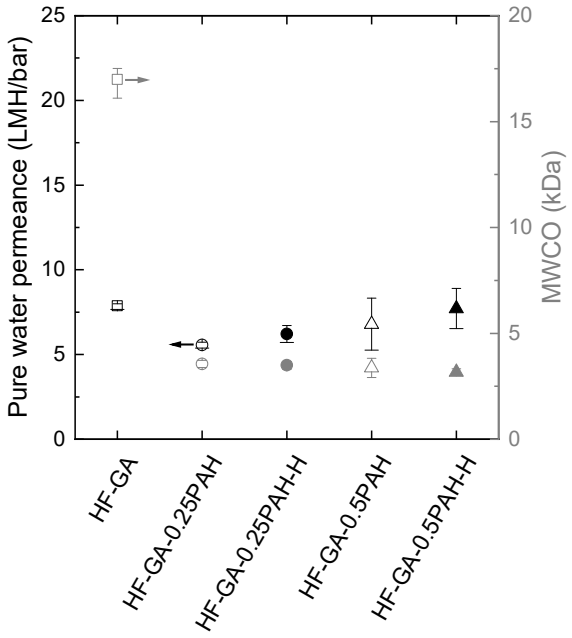

Figure 6.12: Pure water permeance (PWP, black) and molecular weight cut-off (MWCO, gray) of three membrane modules of HF-GA (□), HF-GA-0.25PAH (○), and HF-GA-0.5PAH (△) fibers with and without immobilized heparin (-H, filled symbols).

almost the same membrane properties, such as permeability and selectivity.

6.4 Conclusion

Simple heparin immobilization methods that are not time-consuming and/or that can be scalable produced are still missing for application on dialysis membranes. This chapter reports two material systems to fabricate positively charged surfaces. The chemistry-in-a-spinneret approach produces functionalized flat sheet and hollow fiber membranes within a single step. Positively charged surfaces serve to subsequently ionically bind heparin.

First, polyethylenimine (PEI) is used as an amine source and is cross-linked with glutaraldehyde (GA). Slight changes in surface charge and increased anti-fouling properties of the resulting membrane suggest successful PEI functionalization. The factor Xa measurements are highlighted, which prove excellent heparin concentration on the membrane surfaces

even after 2 h thermal treatment. Furthermore, hollow fiber membranes spun with the same polymer solutions show similar permeability and cut-off compared to the unmodified reference membrane.

For the second material system, polyallylamine hydrochloride (PAH) is used as an amine source to cross-link with GA. Surface charge and anti-fouling properties show slight differences and suggest a better PAH functionalization by using 0.5 wt.% PAH in the coagulation bath. Nevertheless, factor Xa measurements show similar results for immobilized heparin concentrations on 0.25 wt.% and 0.5 wt.% PAH. Afterward, hollow fiber membranes are spun with both PAH concentrations in the bore solution. As well as with the PEI functionalized membranes, the hollow fibers do not significantly differ in membrane morphology and permeability. The MWCO, on the other hand, decreases significantly due to cross-linking. A cross-linked surface functionalization without affecting membrane morphology, permeability, and the MWCO is an excellent approach for simple transferability to existing fiber fabrication processes, such as, for dialysis fiber fabrication. Therefore, the material system with PEI and GA is more suitable for this application.

Overall, both material systems show high amounts of stable, immobilized heparin on the functionalized membrane surfaces. The cross-linking of the amine sources, and thus the functionalization of the membrane, occurs during the hollow fiber membrane fabrication. This eliminates the need for time-consuming membrane functionalization steps for later heparinization.

7 Conclusion and Future Work

7.1 Conclusion

The present work investigated the fabrication routes and functionalization methods of a cost-effective heparinized dialyzer, which is based on polyethersulfone (PES). A local heparinization of artificial surfaces is required to prevent blood coagulation during blood treatment. However, the state of the art is to inject heparin into the patient's bloodstream, which can lead to long-term damage. Nevertheless, there are already products on the market that allow treatment without injecting heparin. Unfortunately, these products are available only to high-risk patients due to their complex handling and high production costs compared with commercial PES dialyzers. One way to reduce the costs of the functionalization of membrane surfaces for dialyzers is to reduce the number of functionalization steps.

Polydopamine was used with the goal of immobilizing heparin onto PES/PVP membranes (cf. Chapter 3). Post-modified polydopamine and, subsequently, heparinized commercial dialysis hollow fiber membranes retained their selectivity for proteins present in human blood while improving the pure water permeance. To reduce the polydopamine post-modification steps, the chemistry-in-a-spinneret approach can be applied. This approach combines the cross-linking of dopamine and the porous precipitation of PES/PVP within the phase inversion process. It could be concluded that alkaline conditions promote the cross-linking of dopamine. Tris buffer with a pH of 8.5 in the coagulation bath for flat sheet membranes or in the bore solution for hollow fiber membranes is essential for the detection of the cross-linked polydopamine on the membrane surface. Changes in surface charge proved the successful subsequent heparin immobilization.

With the goal of reducing the fabrication costs of functionalized membranes for dialysis, an alternative to dopamine was investigated and compared with dopamine functionalized membranes (cf. Chapter 4). Catechol and propylamine were used as dopamine analogues. Like dopamine, these dopamine analogues have amine and catechol groups, which, according to the literature, are responsible for the strong adhesion of dopamine. Cell growth on coated microtiter plates showed no toxic effect of the dopamine

analogues coating. PES flat sheet membranes coated with dopamine analogues showed improved fouling behavior of the membrane surface. Subsequent heparinization was successfully detected by a factor Xa assay. Transferred to hollow fiber membranes, the dopamine analogues functionalization had no significant effect on the pure water permeance and selectivity. The subsequent heparinization increased the pure water permeance while selectivity decreased slightly. Overall, the dopamine analogues allowed heparin immobilization, with no significant difference in membrane performance compared with the dopamine coating.

To improve the sustainability of the membrane functionalization, chitosan is a promising alternative to dopamine analogues (cf. Chapter 5). Therefore, chitosan was used to immobilize heparin on PES membrane surfaces. The strong positive charge of chitosan allows ionic binding to the strong negatively charged heparin. The charge differences and permeability of chitosan-coated commercial dialysis hollow fiber membranes confirmed the successful functionalization with chitosan and the subsequent heparinization. To reduce the coating steps, the chitosan was blended into the polymer solution. Strongly improved fouling behavior and charge differences of the functionalized membrane surfaces demonstrated a successful one-step functionalization with chitosan. In addition to the charge differences of the surfaces, human blood measurements underline both the successful immobilization and the hemocompatible influences of heparin onto the chitosan-blended membranes. These measurements included the thrombin-antithrombin complex, the active complement component 3, and the platelet factor 4 measurements. Furthermore, heparinized chitosan-blended hollow fiber membranes increased the pure water permeance, while the molecular weight cut-off decreased slightly.

An additional dopamine substitute is the use of the cross-linker glutaraldehyde (GA) and two different amine sources, polyethylenimine (PEI) and polyallylamine hydrochloride (PAH) (cf. Chapter 6). An amount of 0.5 wt.% GA was dissolved in the polymer solution, cross-linked with the amine source from the coagulation bath for flat sheet and in the bore solution for hollow fiber membrane fabrication. During PES precipitation, the cross-

linking process takes place on the lumen surface. Surface charge differences and heparin concentration measurements confirmed a successful and stable subsequent heparin immobilization on all formed and positively charged selective layers. The hollow fiber membranes prepared through this chemistry-in-a-spinneret approach showed no significant variation in burst pressures and permeances due to the small amounts of the amine sources and cross-linker used. Only the selectivity of the membranes decreased during cross-linking of PAH and GA.

Concluding, this work presented four different surface functionalizations that enable the immobilization of heparin on PES surfaces, while reducing the number of coating steps.

7.2 Future Work

Based on the results and findings of this work, the four different surface functionalizations offer multiple starting points for future research and developments. The targeted dosage of reactive additives in material systems results in differences in geometry, permeability, and cut-off, inspiring future work in different areas. Furthermore, the membrane fouling measurements of the functionalized membranes in this work showed a significant improvement in fouling behavior. Therefore, the use of these functionalized membranes in, for example, wastewater treatment is also worth considering.

The functionalization methods of this work can be adjusted for use on any surface, including membranes, in various applications. The separation properties of the membranes can be tuned by adjusting the spinning parameters. Especially for the application of dialysis membrane, the permeance and the cut-off have to be adapted. In particular, the chemistry-in-a-spinneret approaches need to be studied carefully during the adaptation of the hollow fiber membranes, as the changed spinning parameters could strongly impact the cross-linking.

There are various DIN standards to which a medical device should conform. Accordingly, there are many tests, especially plasma and whole blood tests, which future medical devices must pass. Due to the functionaliza-

tion of PES membranes, the basic surface, i.e., the base material PES, can already be found in commercially available medical devices. However, the behavior of the functionalization under dynamic conditions in extended blood tests is still unknown. Furthermore, the leaching of the functionalization needs to investigated in detail to exclude possible harmful effects on the patients.

This work has focused exclusively on the immobilization of heparin. However, alternatives to heparin, heparin-like polymers, can also be found in the literature. These heparin-like polymers have similar functional groups to heparin and are able to improve hemocompatibility on surfaces significantly. These can be incorporated into the membrane structure by blending (as in Chapter 5), for example, and spun to hollow fiber membranes.

Furthermore, the functionalizations used in this work can not only be applied to PES materials. A possible transferability to other material systems is quite conceivable. This opens up a broad spectrum of medical products that can also prevent blood coagulation due to the heparinized surfaces.

The functionalisation routes presented in this work offer with some further research and development to be translated into real medical membrane devices in the near future.

Bibliography

[Akba2015] A. Akbari, Z. Derikvandi, and S. M. M. Rostami. “Influence of chitosan coating on the separation performance, morphology and antifouling properties of the polyamide nanofiltration membranes”. *Journal of Industrial and Engineering Chemistry* 28 (2015). DOI: 10.1016/j.jiec.2015.03.002 (cit. on pp. 91, 98, 99).

[Akso2008] A. E. Aksoy, V. Hasirci, and N. Hasirci. “Surface modification of polyurethanes with covalent immobilization of heparin”. In*Macromolecular Symposia*. Vol. 269. 1. Wiley Online Library. 2008, pp. 145–153. DOI: 10.1002/masy.200850918 (cit. on p. 22).

[Azar2012] S. Azari and L. Zou. “Using zwitterionic amino acid l-DOPA to modify the surface of thin film composite polyamide reverse osmosis membranes to increase their fouling resistance”. *Journal of Membrane Science* 401 (2012). DOI: 10.1016/j.memsci.2012.01.041 (cit. on pp. 54, 63).

[Bake2012] R. W. Baker. *Membrane technology and applications*. John Wiley & Sons, 2012 (cit. on pp. 2–5, 7, 8).

[Bala2014] V. Balan and L. Verestiuc. “Strategies to improve chitosan hemocompatibility: A review”. *European Polymer Journal* 53 (2014). DOI: 10.1016/j.eurpolymj.2014.01.033 (cit. on p. 91).

[Bhal2015] U. M. Bhalerao et al. “Controlled release studies of antimalarial 1, 3, 5-trisubstituted-2-pyrazolines from biocompatible chitosan-heparin Layer-by-Layer (LbL) self assembled thin films”. *Colloids and Surfaces B: Biointerfaces* 125 (2015). DOI: 10.1016/j.colsurfb.2014.11.016 (cit. on pp. 21, 90, 91).

[Brin1939] K. Brinkhous et al. “The inhibition of blood clotting: an unidentified substance which acts in conjunction with heparin to prevent

the conversion of prothrombin into thrombin". *American Journal of Physiology-Legacy Content* 125.4 (1939). (Cit. on p. 20).

[Buch2017] T. Bucher et al. "Colour-value based method for polydopamine coating-stability characterization on polyethersulfone membranes". *Membranes* 7.4 (2017). DOI: 10.3390/membranes7040070 (cit. on pp. 57, 60).

[Bulw2012] M. Bulwan et al. "Chitosan-based ultrathin films as antifouling, anticoagulant and antibacterial protective coatings". *Journal of Biomaterials Science, Polymer Edition* 23.15 (2012). DOI: 10.1163/092050611X601711 (cit. on p. 11).

[Capi2002] I. Capila and R. J. Linhardt. "Heparin–protein interactions". *Angewandte Chemie International Edition* 41.3 (2002). DOI: 10.1002/1521-3773(20020201)41:3<390::AID-ANIE390>3.0.CO;2-B (cit. on pp. 21, 90).

[Chan2003] J. Chanard et al. "New insights in dialysis membrane biocompatibility: relevance of adsorption properties and heparin binding". *Nephrology Dialysis Transplantation* 18.2 (2003). DOI: 10.1093/ndt/18.2.252 (cit. on pp. 54, 98).

[Cho2015] K. L. Cho et al. "Chlorine resistant glutaraldehyde crosslinked polyelectrolyte multilayer membranes for desalination". *Advanced Materials* 27.17 (2015). DOI: 10.1002/adma.201405783 (cit. on p. 110).

[Chou2020] S.-F. Chou et al. "Inhibition of platelet adhesion from surface modified polyurethane membranes". *Biomedical journal of scientific & technical research* 32.3 (2020). DOI: 10.26717/BJSTR.2020.32.005247 (cit. on p. 21).

[Chun2021] T. Chung and Y. Feng. *Hollow Fiber Membranes: Fabrication and Applications*. Elsevier Science, 2021 (cit. on p. 8).

[Colm2006] R. W. Colman. *Hemostasis and thrombosis: basic principles and clinical practice*. Lippincott Williams & Wilkins, 2006 (cit. on pp. 19, 20).

[Dech1997] G. Decher. "Fuzzy nanoassemblies: toward layered polymeric multicomposites". *science* 277.5330 (1997). DOI: 10.1126/science.277.5330.1232 (cit. on p. 11).

[Dong2010] P. Dong et al. “Comparison study of corrosion behavior and biocompatibility of polyethyleneimine (PEI)/heparin and chitosan/heparin coatings on NiTi alloy”. *Journal of Materials Science & Technology* 26.11 (2010). DOI: 10.1016/S1005-0302(10)60169-7 (cit. on pp. 11, 22, 91).

[Droz2022] N. N. Drozd et al. “Chitosan/heparin layer-by-layer coatings for improving thromboresistance of polyurethane”. *Surfaces and Interfaces* 28 (2022). DOI: 10.1016/j.surfin.2021.101674 (cit. on p. 22).

[Dutc2012] S. Dutczak et al. ““Chemistry in a spinneret” to fabricate hollow fibers for organic solvent filtration”. *Separation and purification technology* 86 (2012). DOI: 10.1016/j.seppur.2011.11.003 (cit. on pp. 12, 13).

[Emon2020] S. Emonds, H. Roth, and M. Wessling. “Chemistry in a spinneret–Formation of hollow fiber membranes with a cross-linked polyelectrolyte separation layer”. *Journal of Membrane Science* 612 (2020). DOI: 10.1016/j.memsci.2020.118325 (cit. on pp. 12, 13, 92, 110).

[Emon2022] S. Emonds et al. “Open and dense hollow fiber nanofiltration membranes through a streamlined polyelectrolyte-based spinning process”. *Journal of Membrane Science* 644 (2022). DOI: 10.1016/j.memsci.2021.120100 (cit. on pp. 12, 13).

[Fish2021] C. Fisher, H. Shao, and C.-H. Ho. “Improved hemocompatibility of polysulfone hemodialyzers with Endexo® surface modifying molecules”. *Journal of Biomedical Materials Research Part B: Applied Biomaterials* (2021). DOI: 10.1002/jbm.b.35003 (cit. on p. 21).

[Gao2014] A. Gao, F. Liu, and L. Xue. “Preparation and evaluation of heparin-immobilized poly (lactic acid) (PLA) membrane for hemodialysis”. *Journal of Membrane Science* 452 (2014). DOI: 10.1016/j.memsci.2013.10.016 (cit. on pp. 22, 40–42, 70, 90, 107).

[Gao2020] J. Gao, K. Y. Wang, and T.-S. Chung. “Design of nanofiltration (NF) hollow fiber membranes made from functionalized bore fluids containing polyethyleneimine (PEI) for heavy metal removal”. *Journal of Membrane Science* 603 (2020). DOI: 10.1016/j.memsci.2020.118022 (cit. on pp. 12, 13).

[Gher2016] C. V. Gherasim et al. “Dual-charged hollow fiber membranes for low-pressure nanofiltration based on polyelectrolyte complexes: one-step fabrication with tailored functionalities”. *ACS applied materials & interfaces* 8.29 (2016). DOI: 10.1021/acsami.6b05706 (cit. on pp. 12, 13, 92).

[Gott1963] V. L. Gott, J. D. Whiffen, and R. C. Dutton. “Heparin bonding on colloidal graphite surfaces”. *Science* 142.3597 (1963). DOI: 10.1126/science.142.3597.1297 (cit. on p. 21).

[Guil2011] G. R. Guillen et al. “Preparation and characterization of membranes formed by nonsolvent induced phase separation: a review”. *Industrial & Engineering Chemistry Research* 50.7 (2011). DOI: 10.1021/ie101928r (cit. on p. 6).

[Hail2020] R. H. Hailemariam et al. “Reverse osmosis membrane fabrication and modification technologies and future trends: A review”. *Advances in Colloid and Interface Science* 276 (2020). DOI: 10.1016/j.cis.2019.102100 (cit. on p. 5).

[He2019] C. He et al. “Heparin-based and heparin-inspired hydrogels: size-effect, gelation and biomedical applications”. *Journal of Materials Chemistry B* 7.8 (2019). DOI: 10.1039/C8TB02671H (cit. on p. 20).

[He2021] T. He et al. “Modification strategies to improve the membrane hemocompatibility in extracorporeal membrane oxygenator (ECMO)”. *Advanced Composites and Hybrid Materials* (2021). DOI: 10.1007/s42114-021-00244-x (cit. on p. 21).

[Hetz2005] G. R. Hetzel and C. Sucker. “The heparins: all a nephrologist should know”. *Nephrology Dialysis Transplantation* 20.10 (2005). DOI: 10.1093/ndt/gfi004 (cit. on p. 19).

[Hirs2001] J. Hirsh et al. “Heparin and low-molecular-weight heparin mechanisms of action, pharmacokinetics, dosing, monitoring, efficacy, and safety”. *Chest* 119.1 (2001). DOI: 10.1378/chest.119.1_suppl.64S (cit. on pp. 19, 20).

[Ho2014] C. C. Ho and S. J. Ding. “Structure, properties and applications of mussel-inspired polydopamine”. *Journal of Biomedical Nanotechnology* 10.10 (2014). DOI: 10.1166/jbn.2014.1888 (cit. on p. 40).

[Hou2008] C. Hou et al. “Investigation on clotting and hemolysis characteristics of heparin-immobilized polyether sulfones biomembrane”. *Journal of Biomedical Materials Research Part A: An Official Journal of The Society for Biomaterials, The Japanese Society for Biomaterials, and The Australian Society for Biomaterials and the Korean Society for Biomaterials* 85.3 (2008). DOI: 10.1002/jbm.a.31502 (cit. on p. 22).

[Hu2016] H. Hu et al. “Investigation of dopamine analogues: Synthesis, mechanistic understanding, and structure–property relationship”. *Langmuir* 32.38 (2016). DOI: 10.1021/acs.langmuir.6b02141 (cit. on pp. 70, 71, 81).

[Huan2018] Y. Huang et al. “Layer-by-layer self-assembled chitosan/PAA nanofiltration membranes”. *Separation and Purification Technology* 207 (2018). DOI: 10.1016/j.seppur.2018.06.032 (cit. on pp. 10, 11).

[Jafa2016] A. Jafari Sanjari and M. Asghari. “A review on chitosan utilization in membrane synthesis”. *ChemBioEng Reviews* 3.3 (2016). DOI: 10.1002/cben.201500020 (cit. on p. 91).

[Jian2010] J.-H. Jiang et al. “Surface modification of PE porous membranes based on the strong adhesion of polydopamine and covalent immobilization of heparin”. *Journal of Membrane Science* 364.1-2 (2010). DOI: 10.1016/j.memsci.2010.08.017 (cit. on pp. 22, 40–42, 70).

[Jin2020] Y. Jin et al. “A facile heparin/carboxymethyl chitosan coating mediated by polydopamine on implants for hemocompatibility and antibacterial properties”. *Applied Surface Science* 528 (2020). DOI: 10.1016/j.apsusc.2020.146539 (cit. on p. 41).

[Joch2011] P. Jochems et al. “Enzyme immobilization on/in polymeric membranes: status, challenges and perspectives in biocatalytic membrane reactors (BMRs)”. *Green chemistry* 13.7 (2011). DOI: 10.1039/C1GC15178A (cit. on p. 110).

[Jung2016] F. Jung and S. Braune. “Thrombogenicity and hemocompatibility of biomaterials”. *Biointerphases* 11.2 (2016). DOI: 10.1116/1.4938557 (cit. on pp. 18, 21).

[Kale2021] N. J. Kaleekkal. “Heparin immobilized graphene oxide in polyetherimide membranes for hemodialysis with enhanced hemocompatibility and removal of uremic toxins”. *Journal of Membrane Science* 623 (2021). DOI: 10.1016/j.memsci.2021.119068 (cit. on pp. 22, 40, 70).

[Kamp2021] J. Kamp, S. Emonds, and M. Wessling. “Designing tubular composite membranes of polyelectrolyte multilayer on ceramic supports with nanofiltration and reverse osmosis transport properties”. *Journal of Membrane Science* 620 (2021). DOI: 10.1016/j.memsci.2020.118851 (cit. on pp. 11, 110).

[Kess2013] M. Kessler et al. “Heparin-grafted dialysis membrane allows minimal systemic anticoagulation in regular hemodialysis patients: A prospective proof-of-concept study”. *Hemodialysis International* 17.2 (2013). DOI: 10.1111/j.1542-4758.2012.00733.x (cit. on pp. 23, 90).

[Khad2016] A. Khademhosseini and R. Langer. “A decade of progress in tissue engineering”. *Nature protocols* 11.10 (2016). DOI: 10.1038/nprot.2016.123 (cit. on p. 15).

[Koch2012] J. Kochan et al. “Characterization of antibacterial polyethersulfone membranes using the respiration activity monitoring system (RAMOS)”. *Water research* 46.16 (2012). DOI: 10.1016/j.watres.2012.07.019 (cit. on pp. 11, 91, 92).

[Kope2011a] K. K. Kopeć. “Charged porous membrane structures for separation of biomolecules”. (2011). DOI: 10.3990/1.9789036531467 (cit. on p. 10).

[Kope2011b] K. Kopeć et al. “Chemistry in a spinneret—On the interplay of crosslinking and phase inversion during spinning of novel hollow fiber membranes”. *Journal of membrane science* 369.1-2 (2011). DOI: 10.1016/j.memsci.2010.12.010 (cit. on pp. 12, 13).

[Kope2011c] K. Kopeć et al. “Tailoring the surface charge of an ultrafiltration hollow fiber by addition of a polyanion to the coagulation bore liquid”. *Journal of membrane science* 369.1-2 (2011). DOI: 10.1016/j.memsci.2010.11.060 (cit. on pp. 12, 13).

[Krau2006] B. Krause, H. Göhl, and F. Wiese. “Medizintechnik”. *Membranen: Grundlagen, Verfahren und industrielle Anwendungen* (2006). DOI: 10.1002/3527609008.ch6 (cit. on pp. 16, 17, 21).

[Kuri1992] K. Kurita et al. “Preparation of tosylchitins as precursors for facile chemical modifications of chitin”. *Macromolecules* 25.14 (1992). DOI: 10.1021/ma00040a026 (cit. on p. 91).

[Kweo2003] D.-K. Kweon, S.-B. Song, and Y.-Y. Park. “Preparation of water-soluble chitosan/heparin complex and its application as wound healing accelerator”. *Biomaterials* 24.9 (2003). DOI: 10.1016/S0142-9612(02)00566-5 (cit. on pp. 91, 92).

[Lang1994] L. J. Langsdorf and A. L. Zydney. “Diffusive and convective solute transport through hemodialysis membranes: a hydrodynamic analysis”. *Journal of biomedical materials research* 28.5 (1994). DOI: 10.1002/jbm.820280507 (cit. on p. 17).

[Lanz2020] R. Lanza et al. *Principles of tissue engineering*. Academic press, 2020 (cit. on p. 15).

[Lavi2014] M. Laville et al. “Results of the HepZero study comparing heparin-grafted membrane and standard care show that heparin-grafted dialyzer is safe and easy to use for heparin-free dialysis”. *Kidney international* 86.6 (2014). DOI: 10.1038/ki.2014.225 (cit. on pp. 22, 23, 41, 42, 90).

[Lee2006] H. Lee, N. F. Scherer, and P. B. Messersmith. “Single-molecule mechanics of mussel adhesion”. *Proceedings of the National Academy of Sciences* 103.35 (2006). DOI: 10.1073/pnas.0605552103 (cit. on pp. 40, 41).

[Lee2007] H. Lee et al. “Mussel-inspired surface chemistry for multifunctional coatings”. *science* 318.5849 (2007). DOI: 10.1126/science.1147241 (cit. on pp. 22, 40, 41, 61, 70, 81).

[Li2012] X. L. Li et al. “Hydrophilic nanofiltration membranes with self-polymerized and strongly-adhered polydopamine as separating layer”. *Chinese Journal of Polymer Science (English Edition)* 30.2 (2012). DOI: 10.1007/s10118-012-1107-5 (cit. on p. 54).

[Li2014] Y. Li et al. “Antifouling, high-flux nanofiltration membranes enabled by dual functional polydopamine”. *ACS Applied Materials and Interfaces* 6.8 (2014). DOI: 10.1021/am405990g (cit. on p. 60).

[Li2020] L. Li et al. “LBL deposition of chitosan/heparin bilayers for improving biological ability and reducing infection of nanofibers”. *International journal of biological macromolecules* 154 (2020). DOI: 10.1016/j.ijbiomac.2020.03.152 (cit. on pp. 10, 11, 22, 90, 98).

[Lieb2013] J. Liebscher et al. “Structure of polydopamine: A never-ending story?” *Langmuir* 29.33 (2013). DOI: 10.1021/la4020288 (cit. on p. 40).

[Lin2004a] D.-J. Lin et al. “Immobilization of heparin on PVDF membranes with microporous structures”. *Journal of membrane science* 245.1-2 (2004). DOI: 10.1016/j.memsci.2004.07.028 (cit. on p. 22).

[Lin2004b] P. H. Lin et al. “Small-caliber heparin-coated ePTFE grafts reduce platelet deposition and neointimal hyperplasia in a baboon model”. *Journal of vascular surgery* 39.6 (2004). DOI: 10.1016/j.jvs.2004.01.046 (cit. on pp. 41, 90, 91, 99).

[Lin2004c] W.-C. Lin, T.-Y. Liu, and M.-C. Yang. “Hemocompatibility of polyacrylonitrile dialysis membrane immobilized with chitosan and heparin conjugate”. *Biomaterials* 25.10 (2004). DOI: 10.1016/j.biomaterials.2003.08.027 (cit. on p. 22).

[Liu2013] X. Liu et al. “Mussel-inspired polydopamine: a biocompatible and ultrastable coating for nanoparticles in vivo”. *ACS nano* 7.10 (2013). DOI: 10.1021/nn404117j (cit. on p. 41).

[Loeb1962] S. Loeb and S. Sourirajan. “Sea water demineralization by means of an osmotic membrane”. In. ACS Publications, 1962. (Cit. on p. 6).

[Luxb2012] T. Luxbacher. “Assessment of Surface Charge for Polymer Hollow Fibre Membranes”. *Procedia Engineering* 44 (2012). DOI: 10.1016/j.proeng.2012.08.820 (cit. on p. 54).

[Ma2014] L. Ma et al. “Mussel-inspired self-coating at macro-interface with improved biocompatibility and bioactivity via dopamine grafted heparin-like polymers and heparin”. *Journal of Materials Chemistry B* 2 (2014). DOI: 10.1039/C3TB21388A (cit. on pp. 42, 53–55, 84, 116).

[Mach2019] M. J. Machodi and M. O. Daramola. “Synthesis and performance evaluation of PES/chitosan membranes coated with polyamide for acid mine drainage treatment”. *Scientific reports* 9.1 (2019). DOI: 10.1038/s41598-019-53512-8 (cit. on pp. 98, 99).

[Mahl2013] F. Y. Mahlicli and S. A. Altinkaya. “Surface modification of polysulfone based hemodialysis membranes with layer by layer self assembly of polyethyleneimine/alginate-heparin: A simple polyelectrolyte blend approach for heparin immobilization”. *Journal of Materials Science: Materials in Medicine* 24.2 (2013). DOI: 10.1007/s10856-012-4804-2 (cit. on p. 22).

[Mala2017] B. Malard et al. “Adsorption as a contributor for inflammatory mediators removal by different hemofiltration membranes: a pilot study”. *Artificial organs* 41.6 (2017). DOI: 10.1111/aor.12785 (cit. on p. 42).

[Mass2005] T. Massa et al. “Fibrinogen surface distribution correlates to platelet adhesion pattern on fluorinated surface-modified polyetherurethane”. *Biomaterials* 26.35 (2005). DOI: 10.1016/j.biomaterials.2005.05.063 (cit. on p. 21).

[McKe1997] S. A. McKelvey, D. T. Clausi, and W. J. Koros. “A guide to establishing hollow fiber macroscopic properties for membrane applications”. *Journal of membrane science* 124.2 (1997). DOI: 10.1016/S0376-7388(96)00249-9 (cit. on pp. 8, 9).

[Meli2007] T. Melin and R. Rautenbach. *Membranverfahren: Grundlagen der Modul-und Anlagenauslegung*. Springer-Verlag, 2007 (cit. on pp. 2–6).

[Meng2009] S. Meng et al. “The effect of a layer-by-layer chitosan–heparin coating on the endothelialization and coagulation properties of a coronary stent system”. *Biomaterials* 30.12 (2009). DOI: 10.1016/j.biomaterials.2008.12.075 (cit. on p. 91).

[Menn2016a] D. Menne et al. “Precise tuning of salt retention of backwashable polyelectrolyte multilayer hollow fiber nanofiltration membranes”. *Journal of membrane science* 499 (2016). DOI: 10.1016/j.memsci.2015.10.058 (cit. on pp. 11, 110).

[Menn2016b] D. Menne et al. “Regenerable polymer/ceramic hybrid nanofiltration membrane based on polyelectrolyte assembly by layer-by-layer technique”. *Journal of Membrane Science* 520 (2016). DOI: 10.1016/j.memsci.2016.08.048 (cit. on pp. 10, 11).

[Mill2017] D. Miller et al. “Surface Modification of Water Purification Membranes”. *Angewandte Chemie - International Edition* 56 (2017). DOI: 10.1002/anie.201601509 (cit. on p. 55).

[Moha2015] A. W. Mohammad et al. “Nanofiltration membranes review: Recent advances and future prospects”. *Desalination* 356 (2015). DOI: 10.1016/j.desal.2014.10.043 (cit. on p. 5).

[Moha2021] M. Mohammadifakhr et al. “Single-step synthesis of a polyelectrolyte complex hollow-fiber membrane for forward osmosis”. *Separation and Purification Technology* 264 (2021). DOI: 10.1016/j.seppur.2021.118430 (cit. on pp. 12, 13).

[Muld1996] M. Mulder. *Basic Principles of Membrane Technology*. Springer science & business media, 1996 (cit. on pp. 2, 3, 5, 7).

[Musa1999] D. Musale, A. Kumar, and G. Pleizier. “Formation and characterization of poly(acrylonitrile)/Chitosan composite ultrafiltration membranes”. *Journal of Membrane Science* 154.2 (1999). DOI: 10.1016/S0376-7388(98)00265-8 (cit. on p. 98).

[Phil2018] S. J. Phillips and J. A. Stenken. “In situ inner lumen attachment of heparin to poly (ether sulfone) hollow fiber membranes used for microdialysis sampling”. *Analytical chemistry* 90.8 (2018). DOI: 10.1021/acs.analchem.7b03927 (cit. on p. 22).

[Pinn2000] I. Pinnau and B. Freeman. “Formation and modification of polymeric membranes: overview”. (2000). DOI: 10.1021/bk-2000-0744.ch001 (cit. on p. 10).

[Pino2017] C. J. Pino and H. D. Humes. “Chapter 83 - Renal Replacement Devices”. (2017). DOI: 10.1016/B978-0-12-801734-0.00083-7 (cit. on pp. 4, 5).

[Ran2012] F. Ran et al. “Heparin-like macromolecules for the modification of anticoagulant biomaterials”. *Macromolecular bioscience* 12.1 (2012). DOI: 10.1002/mabi.201100249 (cit. on p. 90).

[Rose2022a] I. I. Rose et al. “Chemistry in a spinneret—Polydopamine functionalized hollow fiber membranes”. *Journal of Membrane Science* (2022). DOI: 10.1016/j.memsci.2022.120324 (cit. on pp. xi, 12, 13, 29, 39).

[Rose2022b] I. I. Rose et al. “Single-step chitosan functionalized membranes for heparinization”. *Journal of Membrane Science* (2022). DOI: 10.1016/j.memsci.2022.120567 (cit. on pp. xi, 29, 89).

[Roth2018] H. Roth et al. “Chemistry in a spinneret–composite hollow fiber membranes in a single step process”. *Journal of Membrane Science* 554 (2018). DOI: 10.1016/j.memsci.2018.02.051 (cit. on pp. 12, 13, 92, 110, 117, 120, 121, 125).

[Roth2019] H. Roth et al. “Chemistry in a spinneret—Sinusoidal-shaped composite hollow fiber membranes”. *Journal of Membrane Science* 585 (2019). DOI: 10.1016/j.memsci.2019.05.029 (cit. on pp. 12, 13, 92, 110).

[Roth2022] H. Roth. “Fabrication of Functionalized Hollow Fiber Membranes through Chemistry in a Spinneret”. (2022). DOI: 10.18154/RWTH-2022-01738 (cit. on p. 13).

[Sagl2009] A. C. Sagle et al. “PEG-coated reverse osmosis membranes: desalination properties and fouling resistance”. *Journal of Membrane Science* 340.1-2 (2009). DOI: 10.1016/j.memsci.2009.05.013 (cit. on p. 63).

[Sala2016] P. Salazar, M. Martín, and J. González-Mora. “Polydopamine-modified surfaces in biosensor applications”. *Polymer science: research advances, pratical applications and educational aspects* 1.July (2016). (Cit. on p. 40).

[Sali2016] E. Salimi et al. “Current Approaches in Improving Hemocompatibility of Polymeric Membranes for Biomedical Application”. *Macromolecular Materials and Engineering* 301.7 (2016). DOI: 10.1002/mame.201600014 (cit. on p. 10).

[Seft2020] M. V. Sefton and M. B. Gorbet. “Nonthrombogenic treatments and strategies”. *Biomaterials science* (2020). DOI: 10.1016/B978-0-12-816137-1.00035-0 (cit. on pp. 19, 21).

[Shah2021] V. Shah, N. Prasetya, and K. Li. “Polydopamine modification of high-performance PVDF ultrafiltration membranes prepared by the combined crystallisation and diffusion (CCD) method”. *Journal of Membrane Science* (2021). DOI: 10.1016/j.memsci.2021.119538 (cit. on p. 40).

[Shan2016] E. Shantsila and G. Y. Lip. “Introduction”. In. *Non-Vitamin K Antagonist Oral Anticoagulants: A Concise Guide*. Cham: Springer International Publishing, 2016, pp. 1–6. DOI: 10.1007/978-3-319-25460-9_1 (cit. on p. 18).

[Shan2020] L. Shan et al. “Recent advances in heparinization of polymeric membranes for enhanced continuous blood purification”. *Journal of Materials Chemistry B* 8.5 (2020). DOI: 10.1039/C9TB02515D (cit. on pp. 10, 21, 22, 90, 98).

[Sigu2018] S. B. Sigurdardóttir et al. “Enzyme immobilization on inorganic surfaces for membrane reactor applications: mass transfer challenges, enzyme leakage and reuse of materials”. *Advanced Synthesis & Catalysis* 360.14 (2018). DOI: 10.1002/adsc.201800307 (cit. on p. 110).

[Sile2013] T. S. Sileika et al. “Colorless multifunctional coatings inspired by polyphenols found in tea, chocolate, and wine”. *Angewandte Chemie* 125.41 (2013). DOI: 10.1002/ange.201304922 (cit. on p. 70).

[Sper2006] C. Sperling et al. “In vitro hemocompatibility of albumin–heparin multilayer coatings on polyethersulfone prepared by the layer-by-layer technique”. *Journal of Biomedical Materials Research Part A: An Official Journal of The Society for Biomaterials, The Japanese Society for Biomaterials, and The Australian Society for Biomaterials and the Korean Society for Biomaterials* 76.4 (2006). DOI: 10.1002/jbm.a.30519 (cit. on pp. 10, 11, 21, 22, 91, 103–105).

[Stam2008] D. F. Stamatialis et al. “Medical applications of membranes: Drug delivery, artificial organs and tissue engineering”. *Journal of Membrane Science* 308.1-2 (2008). DOI: 10.1016/j.memsci.2007.09.059 (cit. on pp. 14–17).

[Stra1971] H. Strathmann, P. Scheible, and R. Baker. “A rationale for the preparation of Loeb-Sourirajan-type cellulose acetate membranes”. *Journal of Applied Polymer Science* 15.4 (1971). DOI: 10.1002/app.1971.070150404 (cit. on p. 8).

[Sun2003] S. Sun et al. “Protein adsorption on blood-contact membranes”. *Journal of membrane science* 222.1-2 (2003). DOI: 10.1016/S0376-7388(03)00313-2 (cit. on p. 14).

[Susa2020] H. Susanto et al. “Preparation of low-fouling polyethersulfone ultrafiltration membranes by incorporating high-molecular-weight chitosan with the help of a surfactant”. *South African Journal of Chemical Engineering* 33 (2020). DOI: 10.1016/j.sajce.2020.07.003 (cit. on p. 92).

[Tang2012] M. Tang et al. “Heparin-like surface modification of polyethersulfone membrane and its biocompatibility”. *Journal of colloid and interface science* 386.1 (2012). DOI: 10.1016/j.jcis.2012.07.076 (cit. on p. 90).

[Tang2021] Y. Tang et al. “A review on models and simulations of membrane formation via phase inversion processes”. *Journal of Membrane Science* 640 (2021). DOI: 10.1016/j.memsci.2021.119810 (cit. on p. 8).

[Teli2014] L. Teligui et al. “An ex vivo evaluation of blood coagulation and thromboresistance of two extracorporeal circuit coatings with reduced and full heparin dose”. *Interactive cardiovascular and thoracic surgery* 18.6 (2014). DOI: 10.1093/icvts/ivu011 (cit. on p. 23).

[Thom2011] M. Thomas, K. Moriyama, and I. Ledebo. “AN69: evolution of the world’s first high permeability membrane”. *High-performance membrane dialyzers* 173 (2011). DOI: 10.1159/000328961 (cit. on pp. 23, 42, 90).

[Thom2017] M. Thompson et al. *Biological Fluid-Surface Interactions in Detection and Medical Devices*. 8. Royal Society of Chemistry Cambridge, UK: 2017 (cit. on p. 19).

[Tul 2017] S. Tul Muntha, A. Kausar, and M. Siddiq. “Advances in polymeric nanofiltration membrane: A review”. *Polymer-Plastics Technology and Engineering* 56.8 (2017). DOI: 10.1080/03602559.2016.1233562 (cit. on p. 5).

[Van 2009] B. Van der Bruggen. “Chemical modification of polyethersulfone nanofiltration membranes: a review”. *Journal of applied polymer science* 114.1 (2009). DOI: 10.1002/app.30578 (cit. on p. 11).

[Virg2019] E. Virga et al. “Stable polyelectrolyte multilayer-based hollow fiber nanofiltration membranes for produced water treatment”. *ACS Applied Polymer Materials* 1.8 (2019). DOI: 10.1021/acsapm.9b00503 (cit. on p. 110).

[Wang2013] L. Wang et al. “Direct synthesis of heparin-like poly (ether sulfone) polymer and its blood compatibility”. *Acta biomaterialia* 9.11 (2013). DOI: 10.1016/j.actbio.2013.07.010 (cit. on p. 90).

[Wang2014a] H. Wang et al. “Mussel inspired modification of polypropylene separators by catechol/polyamine for Li-ion batteries”. *ACS applied materials & interfaces* 6.8 (2014). DOI: 10.1021/am406052u (cit. on p. 70).

[Wang2014b] L. Wang et al. “Route to hemocompatible polyethersulfone membranes via surface aminolysis and heparinization”. *Journal of colloid and interface science* 422 (2014). DOI: 10.1016/j.jcis.2014.02.005 (cit. on p. 22).

[Wang2017] W. Wang et al. “Hemocompatibility and oxygenation performance of polysulfone membranes grafted with polyethylene glycol and heparin by plasma-induced surface modification”. *Journal of Biomedical Materials Research Part B: Applied Biomaterials* 105.7 (2017). DOI: 10.1002/jbm.b.33709 (cit. on pp. 22, 23).

[Wang2021] C. Wang et al. “In-situ synthesis of PA/PVDF composite hollow fiber membranes with an outer selective structure for efficient fractionation of low-molecular-weight dyes-salts”. *Desalination* 503 (2021). DOI: 10.1016/j.desal.2021.114957 (cit. on pp. 12, 13).

[West2021] H. Westphalen, A. Abdelrasoul, and A. Shoker. “Protein adsorption phenomena in hemodialysis membranes: Mechanisms, influences of clinical practices, modeling, and challenges”. *Colloid and*

Interface Science Communications 40 (2021). DOI: 10.1016/j.colcom.2020.100348 (cit. on p. 21).

[Will2021] A. Willers et al. “New trends, advantages and disadvantages in anticoagulation and coating methods used in extracorporeal life support devices”. *Membranes* 11.8 (2021). DOI: 10.3390/membranes11080617 (cit. on p. 10).

[Xie2016] B. Xie et al. “Decoration of heparin and bovine serum albumin on polysulfone membrane assisted via polydopamine strategy for hemodialysis”. *Journal of Biomaterials science, Polymer edition* 27.9 (2016). DOI: 10.1080/09205063.2016.1169479 (cit. on pp. 22, 40).

[Yang2002] M.-C. Yang and W.-C. Lin. “Surface modification and blood compatibility of polyacrylonitrile membrane with immobilized chitosan–heparin conjugate”. *Journal of Polymer Research* 9.3 (2002). DOI: 10.1023/A:1021347810130 (cit. on p. 22).

[Yang2003] M.-C. Yang and W.-C. Lin. “Protein adsorption and platelet adhesion of polysulfone membrane immobilized with chitosan and heparin conjugate”. *Polymers for advanced technologies* 14.2 (2003). DOI: 10.1002/pat.337 (cit. on p. 22).

[Yang2015] H. C. Yang et al. “Surface engineering of polymer membranes via mussel-inspired chemistry”. *Journal of Membrane Science* 483 (2015). DOI: 10.1016/j.memsci.2015.02.027 (cit. on p. 40).

[You2011] I. You et al. “Enhancement of blood compatibility of poly (urethane) substrates by mussel-inspired adhesive heparin coating”. *Bioconjugate chemistry* 22.7 (2011). DOI: 10.1021/bc2000534 (cit. on pp. 41, 42).

[Zhai2020] W. Zhai et al. “Fouling resistance of 3-[[3-(trimethoxysilane)-propyl] amino] propane-1-sulfonic acid zwitterion modified poly (vinylidene fluoride) membranes”. *Separation and Purification Technology* 239 (2020). DOI: 10.1016/j.seppur.2020.116589 (cit. on p. 10).

[Zhan2018] W. Zhang et al. “Surface and anti-fouling properties of a polyampholyte hydrogel grafted onto a polyethersulfone membrane”. *Journal of colloid and interface science* 517 (2018). DOI: 10.1016/j.jcis.2018.01.106 (cit. on p. 10).

[Zhan2021] M. Zhang et al. “Anti-thrombogenic Surface Coatings for Extracorporeal Membrane Oxygenation: A Narrative Review”. *ACS Biomaterials Science & Engineering* 7.9 (2021). DOI: 10.1021/acsbiomaterials.1c00758 (cit. on p. 22).

[Zhao2003] Z.-P. Zhao, Z. Wang, and S.-C. Wang. “Formation, charged characteristic and BSA adsorption behavior of carboxymethyl chitosan/PES composite MF membrane”. *Journal of Membrane Science* 217.1-2 (2003). DOI: 10.1016/S0376-7388(03)00105-4 (cit. on p. 98).

[Zhao2015] X. Zhao et al. “Tuning the antifouling property of PVDF ultrafiltration membrane with surface anchored polyelectrolyte complexes for sewage treatment”. *RSC advances* 5.78 (2015). DOI: 10.1039/C5RA08041J (cit. on pp. 91, 92).

[Zhen2016] Z. Zheng et al. “Fabrication, characterization, and hemocompatibility investigation of polysulfone grafted with polyethylene glycol and heparin used in membrane oxygenators”. *Artificial organs* 40.11 (2016). DOI: 10.1111/aor.12803 (cit. on p. 22).

[Zhu2009] L. P. Zhu et al. “Surface modification of PVDF porous membranes via poly(DOPA) coating and heparin immobilization”. *Colloids and Surfaces B: Biointerfaces* 69.1 (2009). DOI: 10.1016/j.colsurfb.2008.11.011 (cit. on pp. 22, 40–42).